Use of climate in a simple entomological framework to improve dynamic simulation and forecast of malaria transmission

Israel Uchenna Ukawuba

Submitted in partial fulfillment of the
requirements for the degree of
Doctor of Philosophy
under the Executive Committee
of the Graduate School of Arts and Sciences

COLUMBIA UNIVERSITY

2021

Abstract

Use of climate in a simple entomological framework to improve dynamic simulation and forecast of malaria transmission

Israel Uchenna Ukawuba

Malaria is a serious and life-threatening mosquito-borne disease that every year affects over 200 million individuals and causes 400,00 deaths. An additional 0.5 billion people globally are at risk of malaria infection. The unique role of climate in influencing malaria transmission outcomes across individual communities by acting on multiple dimensions of the malaria vector and parasite ecology has been long recognized. This recognition has led to the development of explicit and implicit climate-driven models of malaria transmission designed to better understand and predict patterns of population vulnerability and uncover potential challenges to malaria control. However, existing implicitly-forced process-based models of malaria have relied on indirectly correlated predictors of malaria transmission, instead of direct relationships among climate, vector entomology and parasite ecology. The lack of biologically-motivated modulation of malaria transmission compromises meaningful interpretation of the ecological role played by climate in malaria transmission. Similarly, the specific influence of climate on vector and parasite dynamics is obscured, limiting the utility of these simple and powerful model forms.

This dissertation focuses on elaborating the direct ecological relationships between climate, the malaria vector and parasite to enhance the ecological utility of lower dimensional mathematical models of malaria transmission.

In the 1st Chapter of this thesis, a climate-driven entomological modeling framework is developed, consisting of a simple dynamic model that explicitly tracks malaria transmission in human populations and implicitly represents the malaria force of infection through climate-regulation of multiple aspects of the Entomological Inoculation Rate (EIR). The EIR-model construct is found to accurately capture seasonal malaria dynamics under free-simulation, when coupled to local rainfall and temperature climatology across multiple local regions in Rwanda. Furthermore, local rainfall modulation of sub-adult survivorship is found to be a more critical driver of seasonal malaria dynamics than other environmentally-regulated components of EIR.

In Chapter 2, the model framework is paired with data assimilation methods to dynamically simulate interannual malaria incidence in Rwanda, infer parameters of malaria transmission and validate the malaria model. Results indicate that the implicitly-forced transmission model is able to reproduce interannual and seasonal malaria incidence at regional and local scales. However, accuracy of model description of malaria incidence is more varied at the more resolved local level. Intensified malaria control efforts during the later years of the study are suspected to increase the discrepancy between the vector and parasite dynamics dictated by climate and the observed widespread decline in malaria activity in the region. Nonetheless, the parameters of transmission identified across populations in Rwanda were comparable to existing estimates of malaria, further validating the transmission model and data assimilation approach.

For the 3rt Chapter, a state-of-the-art Bayesian inference forecasting system for the EIR-model framework is developed, as well as a multi-model forecasting system consisting of weighted-average predictions from the dynamic malaria model and historical expectance predictions. Retrospective forecasts of four years of malaria data from 42 regions in Rwanda indicate that the model-inference forecasting system predicts malaria incidence more accurately than historical expectance alone, particularly for predictions with 1-6 weeks lead times. Although slightly less skillful, the multi-model system was found to substantively enhance forecast reliability of the EIR-model system, bolstering the utility of the malaria model as a robust forecaster of malaria in the region.

The concluding Chapter describes areas for improving the specification of the parsimonious model construct. The need to include malaria control coverage data as exogenous forces of transmission, non-climate drivers and alternate sources of climate exposure that support transmission are highlighted. Future works on forecast calibration needed to improve model performance for real-time prediction are also detailed. In addition, areas for application within information systems for evaluating malaria risk and for advising malaria control efforts, specifically relating to local variability in malaria burden and characterization of entomological drivers of local malaria, are identified and further discussed. The model systems developed in this thesis advance the capabilities of lower dimension dynamic models to connect the ecological drivers of malaria transmission to climate variation. Such process-based formulations could provide better climate-driven descriptions of malaria, while limiting model complexity, without compromising representation of entomological relationships that are potentially valuable for improved understanding and control of malaria transmission.

Table of Contents

List of Tables and Figures ..... **v**

List of Abbreviations ..... **viii**

Acknowledgments ..... **xi**

Introduction **1**

Malaria 1

Malaria parasite life cycle 2

The malaria vector 4

Climate and malaria 6

Malaria immunity 9

Malaria surveillance and diagnosis 10

Malaria prevention and control 11

Mathematical Modeling of Malaria Transmission 13

Thesis Aims 15

Chapter 1: Malaria model development and free-simulation **20**

1.1 Background 20

1.2 Materials and Methods 26

1.2.1 Study region 26

1.2.2 Model description 28

1.2.3.1 Compartmental model 28

1.2.3.2 Force of infection 32

1.2.3.3 Climate regulation of parasite and vector ecology 34

1.2.4 Simulation of malaria incidence 40

1.3 Results 42

1.3.1 Free simulation of malaria 42

1.3.2 Relative benefit of temperature/rainfall regulation on seasonal dynamics 44

1.3.3 Influence of climate conditions on host and vector dynamics 47

1.4 Conclusion 48

1.6 Supplemental text 50

1.6.1 Parameterization of moisture-regulated subadult survivorship 50

1.7 Supplemental figures 52

Chapter 2: Model inference and dynamic simulation 54

2.1 Background 54

2.2 Materials and Methods 56

2.2.1 Simulation of malaria incidence 56

2.2.2 Data and study region 56

2.2.3 Model inference system 57

2.3 Results 60

2.3.1 Model simulation of interannual and seasonal malaria 60

2.3.2 Ento-epidemiological parameters of malaria 63

2.4 Conclusion 68

2.6 Supplemental text 75

2.6.1 Synthetic testing 75

2.6.1.1 Synthetic transmission 75

2.6.1.2 Data assimilation and inference 75

2.6.2 Observation Error Variance (OEV) of malaria data 77

2.6.3 Water temperature (Tw) sensitivity of the malaria model 78

2.7 Supplemental figures 79

2.8 Supplemental tables 83

Chapter 3: A dynamic forecasting system for malaria incidence 88

3.1 Background 88

3.2 Materials and Methods 90

3.2.1 The malaria model 90

3.2.2 Malaria and climate data 92

3.2.3 Model inference 93

3.2.4 Retrospective malaria forecast 94

3.2.5 Historical probability model 95

3.2.6 Multi-model ensemble forecast 96

3.2.7 Forecast Analysis 96

3.3 Results 99

3.4 Conclusion 105

Conclusion 109

Summary of findings 109

Improvements to model accuracy and forecast needed 111

Malaria surveillance and climate data 111
Incorporating anti-malaria control efforts to improve local prediction 113
Impact of remotely sensed climate data on model accuracy 114
Better resolved denominator population 116
Opportunity for multi-model ensemble forecasting 117
Model application for malaria control 119
Planning of anti-malaria products 119
Real-time forecast for ongoing control 120
Characterizing local entomological profile for malaria control 122
Improving evaluation of the impact of malaria interventions 123
Importance to other vector-borne diseases 125
Conclusion 126
References 128

List of Tables and Figures

Tables:

Chapter 1

Table 1: Description and prior ranges of the parameters of the malaria transmission model..... 31

Chapter 2

Table 1: Range of the mean posterior estimates for two epidemiological parameters of malaria 67

Table S1: Description and prior range of the parameters of the malaria transmission model 83

Table S2: Mean and 95% credible interval of posterior ensemble of model parameter estimates 84

Table S3: Mean and 95% confidence interval estimates of k, the common rate of dispersion within the OEV for model-EAKF simulation 86

Chapter 3

Table 1: Proportion of multi-model forecasts with higher logarithmic scores than model-EAKF predictions..... 104

Figures:

Introduction

Figure 1. Global map of malaria case incidence rate (cases per 1000 population at risk) by country, 2018..... 2

Figure 2. Global map of the distribution of major important vectors of malaria. 5

Figure 3. Map of malaria risk based on annual parasite incidence (API) by districts in Ethiopia, 2014..... 7

Figure 4. Monthly rainfall (black) and monthly reported cases of Plasmodium falciparum (red), Kutch, India, 1987-2007..... 7

Chapter 1

Figure 1. Map of rainfall (left panel) and temperature (right panel) climatology (1981-2016) in Rwanda 26

Figure 2. Flow diagram of the malaria transmission model..... 29

Figure 3. Simulations of seasonal malaria incidence from the environmentally-driven malaria transmission model in free simulation. 43
Figure 4. Mean absolute percentage error (MAPE) of the top 10 seasonal models. 44
Figure 5. Distribution of posterior parameters of seasonal malaria simulations. 44
Figure 6. Percent change in error of seasonal malaria, when individual entomological functions are decoupled from climate. 46
Figure 7. Percent change in error of simulated incidence, when the transmission system is decoupled entirely from climate modulation 46
Figure S1. Averaged seasonal dynamics of state variables of the model system 52
Figure S2. Seasonality of weekly climatology of rainfall and temperature (CHIRPS and CHIRTS) 53
Figure S3. Average seasonality of entomological parameters from the top 10 malaria models 53

Chapter 2

Figure 1. Model-EAKF simulated incidence of malaria at the province level from 2016-2019. 61
Figure 2. Fit of model predicted malaria incidence, across all 42 catchment sites, computed over various study periods, during inter-annual (light blue) and intra-annual (yellow) simulations 62
Figure 3. Correlation between malaria incidence and cumulative moisture conditions of the final model 63
Figure 4. Incidence of malaria simulated for individual years by the model-EAKF 64
Figure 5. Model estimated annual average for the daily Entomological Inoculation Rate (EIR). 65
Figure 6. Percent change in MARE of simulated malaria when individual entomological functions are decoupled from climate. 66
Figure S1. Model-EAKF simulated incidence of malaria from 2016-2019 for the 42 catchment sites 79
Figure S2. Mosquito development and estimated survivorship as modulated by temperature and rainfall in model simulations 80
Figure S3. Posterior parameters of the malaria transmission model estimated from the EAKF-model inference system 81
Figure S4. Relative error of mean posterior estimate of true parameters made by the EAKF system during synthetic testing 82

Figure S5. Contour of percent change in RMSE of simulations and mosquito density of the final climate model under various conditions of the water temperature (Tw) model 82

Chapter 3

Figure 1. Flow diagram of the malaria transmission model..... 91

Figure 2. Province-level forecast of malaria incidence (2016-2019) at varied lead times..... 100

Figure 3. Performance of model-EAKF point forecasts over four years for the 42 local sites across Rwanda's five provinces 101

Figure 4. Boxplot of logarithmic score of local malaria forecasts generated by the various forecast systems 102

Figure 5. Relative forecast skill of historical probability and top multi-model compared to model-EAKF forecasts 103

Figure 6. Forecast reliability of the model-EAKF and multi-model forecast systems 105

Conclusion

Figure 1. El Nino and global rainfall anomaly..... 121

Figure 2. Counterfactual effects of climate variability while assessing the impact of concurrent control measures on malaria incidence 124

List of Abbreviations

ACD	Active case detection
ACTs	Artemisinin combination therapies.
AE	Average error
API	Annual parasite incidence
ARIMA	Auto regressive integrated moving average
BPD	Bites per person per day
CHIRPS	University of California, Santa Barbara Climate Hazards Group InfraRed Precipitation with Station products
CHIRTS	University of California, Santa Barbara Climate Hazards Group InfraRed Temperature with Station products
CHW	Community Health Workers
CI	Credible Interval
DDT	Dichlorodiphenyltrichloroethane
DHS	Demographic and Health Survey
EAKF	Ensemble Adjustment Kalman Filter
EIP	Extrinsic Incubation Period
EIR	Entomological Inoculation Rate
ENACTS	Enhancing National Climate Services
ENSO	El Niño Southern Oscillation
HBR	Human Biting Rate
HMIS	Health Management Information Systems

IRS	Indoor Residual Spraying
ITCZ	Inter-Tropical Convergence Zone
ITN	Insecticide-treated bed net
LHS	Latin Hypercube Sampling
LLINs	Long-lasting Insecticidal Nets
LMICs	Lower-Middle Income Countries
LS	Log Score
MAPE	Mean Absolute Percentage Error
MoH	Ministry of Health
NWP	Numerical Weather Prediction
OEV	Observational Error Variance
PCD	Passive Case Detection
PCR	Polymerase Chain Reaction
R_0	Reproductive number
RBC	Rwanda Biomedical Center
RDT	Rapid Diagnostic Tests
RE	Relative Error
SEIRS	Susceptible Exposed Infected Recovered and Susceptible
S.L	Sensu Lato
SMC	Seasonal Malaria Chemoprophylaxis
SR	Source Reduction
SST	Sea Surface Temperature
Tw	Water Temperature

USAID	United States Agency for International Development
VC	Vectorial Capacity
WHO	World Health Organization

Acknowledgments

I foremostly grateful and thankful to Dr. Jeffrey Shaman, whose kind mentorship, immense support and wealth of resources during this doctoral program has been truly invaluable. I am deeply grateful to have you as my advisor and cannot thank you enough for the training and education I have received during the 7 plus years of knowing you. Because of your masterful tutelage, I have gained a better understanding of disease modeling and public health; but over these years, I have gained even more from your incredible capacity, supportive nature, openness and friendly person. For this and much more than words can say, thank you. I could not have achieved this without you!

I am also very grateful and thankful to my thesis committee members for believing in me and for their excellent guidance and keen support, which helped me better navigate the model development, testing, result analysis and improved my write-up of this thesis.

I would also like to thank all the members of the Shaman lab group for the insights and knowledge they provided me over these years. Thank you also to the supportive cohort of EHS doctoral students and administrators, for creating a positive and amiable environment that has made the entire process smooth and rewarding.

Finally, I am very grateful to my family, and to my dear wife and friend, for always being there for me. Their love, support and kindness over these years truly made the whole experience much more fulfilling and enriching.

Introduction

Malaria

Malaria is a serious and life-threatening febrile disease caused by parasites from the *Plasmodium* genus. These parasites are transmitted to human and non-human hosts by infected female *Anopheles* mosquitoes during blood-feeding. Individuals infected with malaria experience fever and flu-like symptoms, including shaking chills, muscle aches, and tiredness. If not properly treated, malaria infection can become severe causing kidney failure, seizures, and death (Trampuz et al. 2003; World Health Organization 2000). Although anyone is at risk of acquiring malaria, people with little or no immunity, including children and pregnant women, are more likely to experience life-threatening malaria outcomes (Baird 1998; Brabin 1983; Duffy and Fried 2005).

Early mention of debilitating fevers, undoubtedly suggestive of malaria, date as far back as 270 BC (Bruce-Chwatt 1988), with records of the feared fever devastating populations during epidemics in 496-322 BC (Sherman 1998). Till now, malaria continues to be of great public health concern, causing epidemics and high endemic transmission worldwide. An estimated 0.5 billion individuals globally are at risk of malaria infection, of which 200 million contract malaria every year, leading to 400,000 malaria-linked deaths (World Health Organization 2019). The heaviest malaria burden is borne by communities in sub-Saharan Africa (Fig. 1), where more than 90% of all global malaria cases and morbidity are recorded (World Health Organization 2019); poor public health infrastructure, favorable climate, highly efficient vectors and high malaria endemicity are major factors contributing to the high malaria burden in the region (World Health Organization 2015b; Dhiman 2019; World Health Organization 2018b). In

addition to the health casualties suffered by communities, malaria imposes huge economic costs stemming from medical expenses and loss of human productivity due to the febrile illness (Institute of Medicine 2004b). Countries with high malaria burden, in particular Lower-Middle Income Countries (LMICs), additionally experience up to 1.3% decreases in economic growth annually as a result of malaria death and disability (Gallup and Sachs 2001).

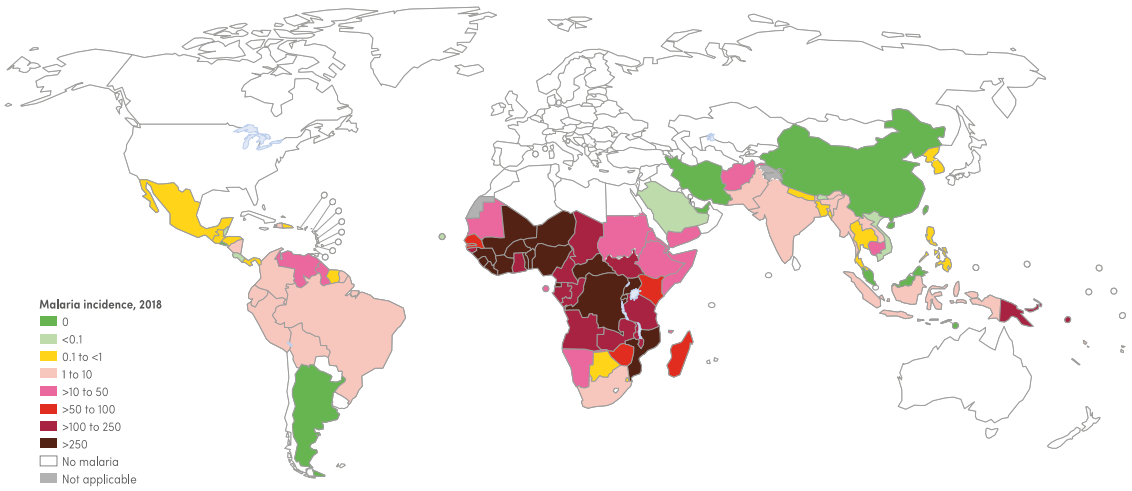

Figure 1: Global map of malaria case incidence rate (cases per 1000 population at risk) by country, 2018. Image credit: World malaria report 2019. Geneva: World Health Organization; 2019. Licence: CC BY-NC-SA 3.0 IGO.

Malaria parasite life cycle

There are over 100 known *Plasmodium* parasites, but only *P. falciparum, P.vivax, P. malariae, P. ovale, and P. knowlesi* are known to cause disease in humans (Vernick et al. 2005). These *Plasmodium* parasites have evolved a complex reproductive lifecycle that requires two different hosts – an arthropod and a vertebrate -- to fully complete and survive. In human hosts, *Plasmodium* parasites begin their lifecycle as sporozoites. Sporozoite transmission mostly occurs during the blood meal, i.e. the bite of an infected female anopheles. However, non-vector transmission can also occur although rarely, through blood transfusion or by vertical

transmission from an infected pregnant mother to child across the placenta. Once sporozoites are in the bloodstream, they are carried to the liver, where they invade liver cells and undergo multiple rounds of nuclear division to form merozoites (Baton and Ranford-Cartwright 2005). In *P. vivax* and *P. ovale*, sporozoites do not immediately undergo replication but enter a dormant stage; and at the end of latency, replication is reactivated leading to relapse in infection weeks, months and even years after sporozoite exposure (Taylor and Agbenyenga 2013; Institute of Medicine 2004c).

Following the period of unabated replication, merozoites escape liver cells and are released into the bloodstream. Here they invade red blood cells and undergo multiple rounds of reproduction, creating both gametocytes and more merozoites, which subsequently rupture the erythrocytes releasing parasites, antigens and inciting host immune response. This clinical pathology accounts for the intermittent bouts of fevers and chills associated with malaria (Taylor and Agbenyenga 2013). Due to lack of immunity and treatment, symptoms could worsen resulting in severe infection, as parasites proliferate unchecked, invading and impeding functions of multiple organs, and invariably causing death (Trampuz et al. 2003). Of the malaria parasites that infect humans, *Plasmodium falciparum* is the most virulent of the species and is responsible for most uncomplicated infections, severe malaria and mortality (World Health Organization 2018b).

In the malaria vector, *Plasmodium* parasites begin the second phase of their heterogynous lifecycle as gametocytes, the stage which is infective to mosquito hosts (Baton and Ranford-Cartwright 2005). Female *Anopheles* mosquitoes become infected with *Plasmodium* gametocytes during a bloodmeal on infected hosts. Following ingestion by the mosquito, gametocytes undergo multiple rounds of nuclear replication, forming macrogametes and flagellated

microgametes. The fusing of macrogametes with flagellated microgametes results in the formation of highly motile and invasive ookinetes, that invade the extracellular space between the epithelial cells of *Anopheles* mosquitoes before terminating as oocysts. Here, the oocysts begin the sporogonic cycle, the asexual reproduction of oocysts into sporozoites, the stage infectious to human hosts; this process of sporogonic reproduction is highly regulated by temperature and can last 10-28 days (Shapiro, Whitehead, and Thomas 2017; Mordecai et al. 2013), producing several thousand sporozoites highly specialized to recognize and invade the salivary glands of *Anopheles* mosquitoes. Once at the salivary gland, the sporozoites cross the surrounding epithelial cells and accumulate within the epithelial lumen. And during mosquito blood-feeding, these *Plasmodium* sporozoites are expelled into the hosts, re-initializing the parasite reproductive cycle.

The malaria vector

Of the near 400 known species of *Anopheles* mosquitoes, about 40 found throughout the globe (Fig. 2) are considered malaria vectors of major importance (Hay et al. 2010; Sinka et al. 2012). *Anopheles* mosquitoes begin their life in water as eggs. Each species differs in breeding habitat preferences. For example, some prefer temporary, shallow pools, puddles, which are usually abundant and persistent during the rainy season, or utilize flooded areas or rice fields for breeding (Caputo et al. 2008; Diabaté et al. 2008; 2005; Sogoba et al. 2007). They continue developing into larvae and pupae in such aquatic environments and finally emerge as adult. Like all mosquitoes, both male and female malaria mosquitoes depend on plant nectar as food source. However, once matured, adult female mosquitoes require a bloodmeal to produce and develop their eggs, and will generally seek their host between dusk and dawn (Becker et al. 2010).

Transmission or infection with malaria parasite can subsequently occurring during blood feeding on a host. Female malaria mosquitoes of egg-bearing age can continue producing eggs over their lifespan (Agyapong et al. 2014), increasing their chance of acquiring an infection or increasing parasite circulation.

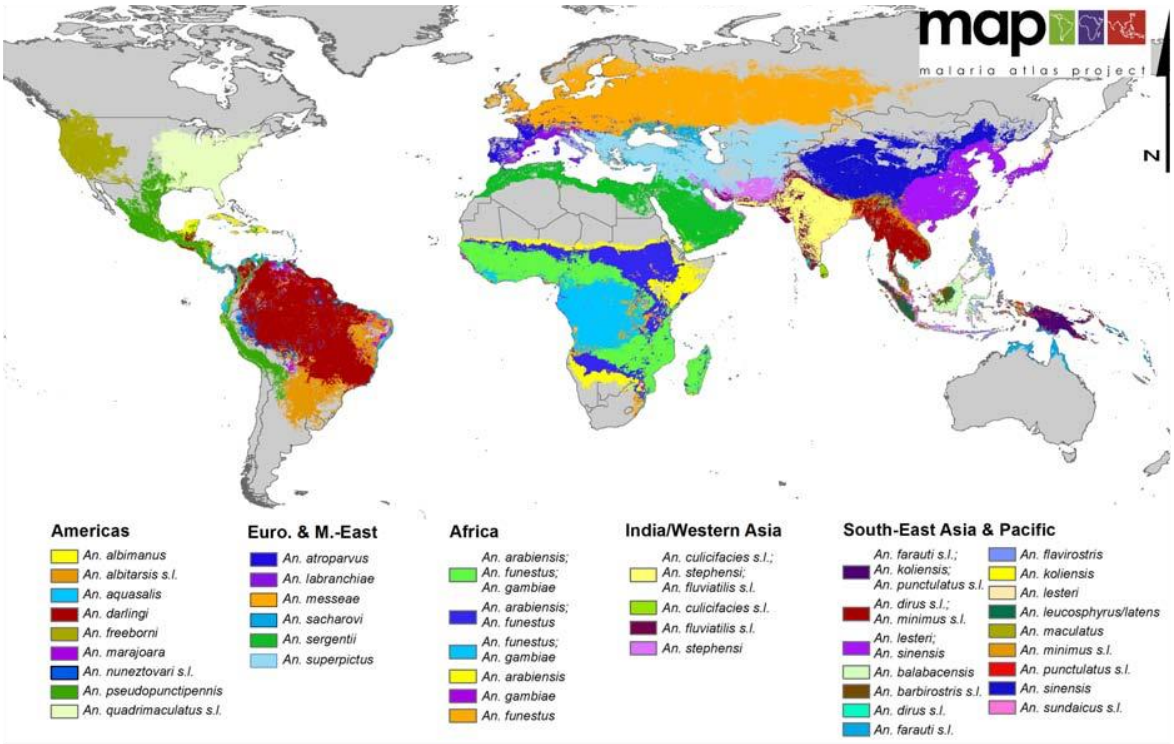

Figure 2. Global map of the distribution of major important vectors of malaria. Image credit: Sinka, Marianne E., Michael J. Bangs, Sylvie Manguin, Yasmin Rubio-Palis, Theeraphap Chareonviriyaphap, Maureen Coetzee, Charles M. Mbogo, et al. 2012. "A Global Map of Dominant Malaria Vectors." Parasites & Vectors 5 (1): 69. https://doi.org/10.1186/1756-3305-5-69.

Anopheles mosquitoes also vary in their capacity as vectors of malaria. Although different malaria vectors are found across the globe, the most highly efficient vectors of malaria are found in sub-Saharan Africa. These are the species of *Anopheles* gambiae sensu lato (s.l) and *Anopheles* funestus (Coluzzi 1999; Gillies and De Meillon 1968; Coetzee and Fontenille 2004).

High anthropophily (i.e. preference for human feeding) in these species are responsible for amplifying the intensity of malaria circulation (Sinka et al. 2010; Tirados et al. 2006; Antonio-Nkondjio et al. 2006; Awolola et al. 2005). Similarly, these vectors also show tendency to rest indoors (endophily), co-habitat close to human settlements and oviposit in near-by breeding sites (Sinka et al. 2010; Holstein 1954; Mutuku et al. 2006; N. Minakawa et al. 1999; Gimnig et al. 2001), furthering their ability to support malaria transmission.

Climate and malaria

The name malaria (meaning bad air in Italian– "mala aria") was originally coined in the 18th century following early theories that the disease was caused by fowl air from swamps and marshes that caused peak outbreaks of fever in the hot months of August and September (Constable A & Co. 1824). Although this assumption will later be refuted by Ross Ronald, who correctly demonstrated mosquitoes to be the vectors of malaria parasites (Ross 1899), early observations of malaria dynamics were not far off. Based on field and laboratory experiments, it is now widely recognized that malaria transmission is sensitive to environmental conditions, with temperature and moisture conditions, playing a wide role in the ecology of the malaria vector and parasite, consequently influencing the seasonality and intensity of local malaria dynamics (Fig. 3 & 4), alongside population-level immunity and parasite density.

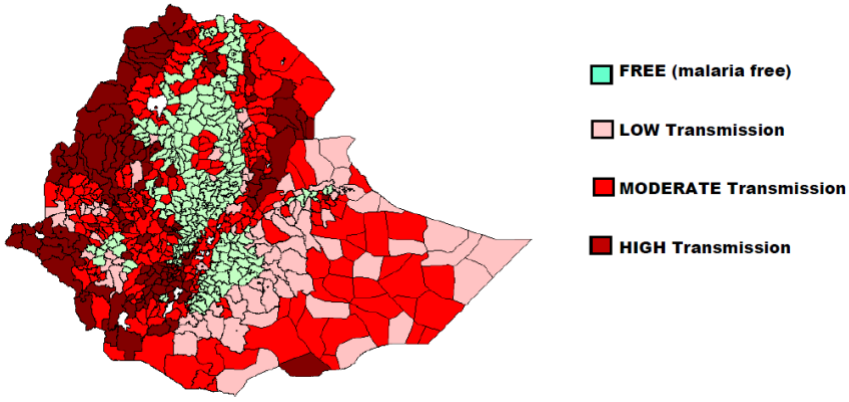

Figure 3. Map of malaria risk based on annual parasite incidence (API) by districts in Ethiopia, 2014. Image credit: United States Agency for International Development (USAID), U.S. President's Malaria Initiative. 2017. "Ethiopia Malaria Operational Plan FY 2017." Malaria free (0 API) areas are located 2000m above sea level (asl); while areas of low (0 > API < 5), moderate (5≥ API <100) and high transmission (API ≥ 100) are located below 2000m asl.

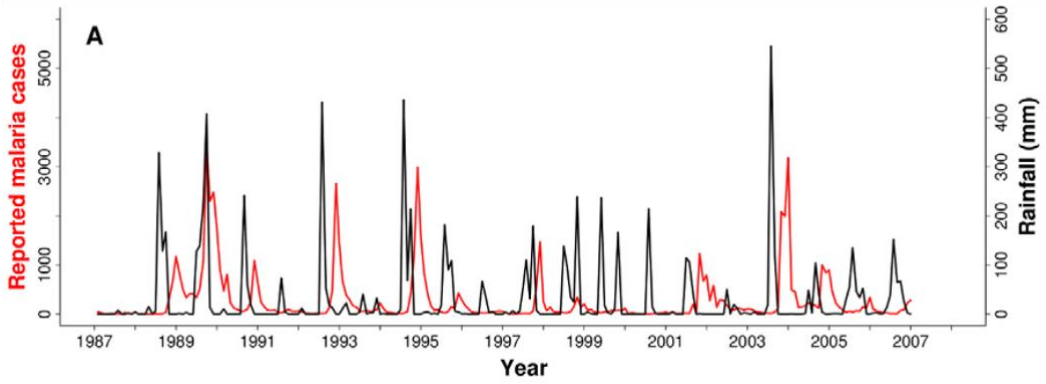

Figure 4: Monthly rainfall (black) and monthly reported cases of *Plasmodium falciparum* (red), Kutch, India, 1987-2007. Image credit: Laneri, Karina, Anindya Bhadra, Edward L. Ionides, Menno Bouma, Ramesh C. Dhiman, Rajpal S. Yadav, and Mercedes Pascual. 2010. "Forcing versus Feedback: Epidemic Malaria and Monsoon Rains in Northwest India." PLoS Computational Biology 6 (9): e1000898. https://doi.org/10.1371/journal.pcbi.1000898.

The impact of surface moisture on malaria dynamics can be profound, determining the population density of vectors and affecting the risk of malaria exposure. Many of the *Anopheles* mosquitoes that transmit malaria, prefer short-lived pools and ponds, typically created by

rainwater for breeding. As a result, abundance of these vectors changes with seasonal rainfall activity, which is a strong determinant of the number, size and persistence of these ephemeral habitats (Bomblies, Duchemin, and Eltahir 2008). The limited tolerance of subadult mosquitoes to desiccation further enlarges the dependence of mosquito numbers on surface moisture variability, as desiccation disrupts growth and causes death under prolonged exposure (J. I. Shililu et al. 2004; Koenraadt et al. 2003). In addition to moderating density, surface moisture conditions can directly impact mosquito activity. Female adult mosquitoes are sensitive to, and reliant upon, moisture levels for initiation of reproductive activities such as egg-laying and blood-feeding (Mayne 1926; Okal et al. 2013; Sumba et al. 2004; Takken, Knols, and Otten 1997). During drier humidity conditions often coincident with dry seasons and drought, these behaviors by female mosquitoes are down-regulated, resulting in a decline of malaria Vectorial Capacity (VC) (Olayemi et al. 2011; J. Shililu et al. 2004; Bigoga et al. 2007).

Temperature has been known to play a role in directly regulating the transmissibility of malaria and influencing mosquito population dynamics as well. Mosquitoes, like all insects, are poikilothermic organisms. Their inability to regulate internal body temperature results in thermodynamic and metabolic rate processes that are moderated by external temperature conditions. This connection is profound: growth rates, the survival of immature mosquitoes, and the emergence of adult mosquitoes are all influenced by environmental temperatures (M. N. Bayoh and Lindsay 2004; 2003). Oviposition and blood-feeding behavior which partly defines host contact rates are also affected by ambient temperature conditions (Shapiro, Whitehead, and Thomas 2017). Equally importantly, temperature also regulates the development of malaria parasites into sporozoites within infected mosquitoes (Shapiro, Whitehead, and Thomas 2017; Mordecai et al. 2013), altering the probability that a mosquito bloodmeal on a host will result in

malaria transmission. These effects of temperature on malaria variability are readily apparent in populations with wide-ranging annual temperatures, such as high-altitude regions where rising average temperatures have been associated with increases in malaria incidence in recent decades (Siraj et al. 2014; Shanks et al. 2005; Lindsay and Martens 1998; Omumbo et al. 2011; Lyon et al. 2017). In the tropics and subtropics where temperature conditions are warmer and vary less throughout the year, the impact of temperature can also be pronounced, as conditions are optimal all-year round, supporting a more intense Vectorial Capacity (VC) for malaria transmission (Gething, Patil, et al. 2011; Gething, Van Boeckel, et al. 2011).

Malaria immunity

Acquisition of immunity to malaria is slow and requires multiple exposures. The gradual process of immunity acquisition highly skews malaria susceptibility by age and rate of exposure. As a consequence of the short-lived and insufficient immune defense (Kinyanjui et al. 2007), young children are highly susceptible to life-threatening malaria infection. However with increasing exposure, individuals can acquire immunity that is i) anti-disease specific, which confers protection against clinical disease, reducing the risk of severe disease or ii) anti-parasite specific, which confers protection against high parasite density, or iii) premunition related, which allows tolerance of low parasite levels that is generally asymptomatic, but confers protection to re-infection (Doolan, Dobaño, and Baird 2009). Nonetheless, protection conferred by acquired immunity is non-sterilizing–adults in highly-endemic areas can still succumb to infection, while being protected from severe morbidity and mortality (Langhorne et al. 2008). Similarly, immunity to malaria is not long-lived. Previously exposed adults are likely to develop severe malaria after returning to highly-endemic areas following a couple of years in a non-endemic

region (Langhorne et al. 2008; Gupta et al. 1999). Indeed, the immunity contingent on frequent exposure has raised concerns over possible increases in susceptibility within populations undergoing malaria control. With successful control efforts reducing malaria transmission, population-level immunity is bound to decline, exposing individuals to potentially severe malaria outcomes (Ghani et al. 2009; Keegan and Dushoff 2013).

The efficacy of naturally acquired immunity can also change during pregnancy. Hormonal immunosuppression to accommodate the growing infant is primarily responsible for the increased susceptibility during pregnancy. Corticosteroids, which inhibit mechanisms of cell-mediated immunity are generally lower during pregnancy (Vleugels et al. 1987; Menendez 1995), thereby limiting the level of immune response mounted in the event of re-exposure. Even in high transmission settings, where frequency of parasite exposure is high, anti-parasite and anti-disease immunity in pregnant women can be considerably attenuated (Menendez 2006).

Malaria surveillance and diagnosis

At the early stages of malaria infection, symptoms manifesting because of parasite infections are non-specific, appearing similar to flu symptoms. Even in geographic areas with high transmission of malaria, fever is not a conclusive indication of malaria (Schellenberg et al. 1994). Therefore, diagnostic confirmation of malaria infection involves microscopic demonstration of parasites (World Health Organization 2018a). Other accurate diagnostic methods include, rapid diagnostic tests (RDT) using immunochromatographic tests to detect parasite-specific antigens and polymerase chain reaction (PCR) amplification of parasite DNA.

Through accurate diagnosis, waste of antimalaria drugs is reduced, malaria cases are better managed, and the quality of malaria surveillance is improved.

Surveillance systems for malaria typically comprise of passive case detection (PCD) of malaria within patients visiting public and private health facilities. Reports of confirmed cases are then integrated into broader health management information systems (HMIS), providing a continuum of malaria aggregates for a region. In some regions, with more proactive control programs, malaria surveillance may include community health workers (CHW). These health professionals extend malaria surveillance and the accessibility of public health services to inaccessible areas or to underserved communities, by timely report, prompt diagnosis and treatment of malaria patients. Although not currently widely integrated into many malaria surveillance systems, active case detection (ACD) may also comprise malaria surveillance– enhancing the comprehensiveness of data on malaria transmission, especially by identifying clusters or outbreaks of transmission early on or by capturing asymptomatic transmission (World Health Organization 2018a).

Malaria prevention and control

Controlling malaria requires a drastic reduction in the abundance of malaria vectors, and density of malaria parasite and limiting contact with malaria vectors. Prior to Ronald Ross' discovery that mosquitoes were the vectors of the malaria parasite (Ross 1899), unrefined natural products, such as wormwood plant and cinchona tree, from which artemisinin and quinine were later identified to be the active antimalarial compounds, were used to treat individual malaria infections (Institute of Medicine 2004a).

Control tools that target various lifestages of the malaria vector and malaria parasite have since been developed for population control of malaria transmission, including chemical insecticides and larvicides, anti-parasite and prophylactic drugs, ecological and environmental modification. The insecticide dichlorodiphenyltrichloroethane (DDT), which is highly effective against adult mosquitoes because of its long-lasting effects, was instrumental to the success of the global malaria eradication campaign in the 1960s, leading to many malaria-free communities worldwide (Shiff 2002; Institute of Medicine 2004a). However, growing resistance to DDT and high cost of implementation made eradication efforts unsustainable; and as global eradication efforts disbanded, attention to widely-available chloroquine therapeutics to reduce parasite density increased in many countries across the globe. But similarly, resistance of the malaria parasite to chloroquine increasingly weakened control efforts.

Today, widely adopted approaches to control malaria include widespread coverage of long-lasting insecticidal nets (LLINs), indoor residual spraying (IRS) of insecticides, prompt diagnosis and treatment with artemisinin combination therapies (ACTs). These highly cost-effective methods have proven successful at protecting populations from malaria, reducing malaria incidence and death by 50% and causing drastic reductions in transmission in regions with historically high malaria prevalence (World Health Organization 2016b; O'Meara et al. 2010; Lengeler 2004; Pluess et al. 2010). Seasonal malaria chemoprophylaxis (SMC), which involves administering antimalarials specifically to children to maintain concentrations of malaria therapeutics during the malaria season, is also increasingly recommended for its effectiveness in suppressing transmission (Meremikwu et al. 2012; Wilson and IPTc Taskforce 2011). However, frequent development of resistance to existing antimalaria drugs and insecticides continues to threaten public health gains in many communities across the globe.

Furthermore, issues related to quality of public healthcare systems, effects of climate variability on local mosquito ecology, as well as effects of environmental conditions, combine to complicate future outcomes of control efforts (Dhiman 2019; Thomson et al. 2017; Zhou et al. 2004).

Though vaccines are highly effective ways of controlling and eliminating many infectious diseases, an effective vaccine for malaria has remained elusive. Typically, with many infections a single inoculation of the causative agent is sufficient to induce immune response that confers lifelong protection. However, the frequent exposure required for malaria immunity as well as the complexities associated with length of immunity has made it difficult to develop efficacious vaccines. Phase III trial of the only currently approved malaria vaccine RTS, S/AS01 indicates little effectiveness– registering 39-50% efficacy against malaria (Mahmoudi and Keshavarz 2017), which is not more effective than proven current control methods. Because of the relatively low efficacy and inability to meet WHO efficacy guidelines of 75% (World Health Organization 2014), implementations of the vaccine are recommended alongside increased use of other proven malaria control methods (World Health Organization 2016b).

Mathematical Modeling of Malaria Transmission

The first global campaign to eliminate malaria was grounded on the mathematical epidemiology of malaria transmission. The basic compartmental model by Ross Ronald sought to explain the relationship between malaria incidence in human populations and mosquito abundance, and paved the way for using mathematical models to understand malaria epidemiology (Ross 1915). Building on the Ross model, Macdonald incorporated parasite latency in malaria mosquitoes and mosquito ecology and concluded that adult female mortality

was the most sensitive link in the mosquito lifecycle (George Macdonald 1957). This discovery prompted the largescale use of the insecticide DDT by the World Health Organization (WHO) in effort to eliminate malaria across Africa (G. Macdonald 1956).

Since the basic Ross-Macdonald models, mathematical transmission models of malaria have advanced to include a more complex array of human and vector processes and to allow investigation of additional features of malaria transmission dynamics and new control opportunities (Mandal, Sarkar, and Sinha 2011). Using compartmental and individual based models, the roles of climate and the environment, age-related immunity, socio-economic status, human migration, latency in vector and human hosts have now been incorporated into mathematical models and used to improve understanding of malaria transmission. Mathematical transmission models are well-suited for describing the processes of vector and parasite development that complicate vector and parasite lifecycles, as well as the multifaceted interactions between vector and host populations that change malaria susceptibility over time and space. By utilizing a well-designed model system, the defining properties of local transmission can be better characterized and provide public health control with more pre-emptive and process-informed options to properly address malaria transmission at the local level.

Recently, mathematical malaria transmission models that simplify the malaria force of infection using implicit representations have gained recognition for their ability to capture changes in malaria transmission dynamics without explicitly representing vector populations (Laneri et al. 2010; Bhadra et al. 2011; Laneri et al. 2015). These model frameworks adopt an indirect method to indicate the influence of climate, or other factors, on mosquito and parasite dynamics. However, the absence of direct relationship amongst climate, vector and parasite undermines the ecological grounding of such parsimonious and powerful model structures and

limits their potential utility in monitoring and controlling malaria. The use of climate in malaria transmission models stems from the understanding of malaria as an environmentally-sensitive transmission system with specific ecological and entomological dependencies on ambient environment. There is, therefore, a need for integration of well-elucidated, direct relationships amongst climate, mosquito and parasite behavior to allow for more realistic representation of the environmental constraint on malaria transmission by such powerful and parsimonious model structures. Furthermore, using understood relationships not only limits spurious associations within the complex and nonlinear processes of transmission but also enhances the model utility and ecological interpretability of implicitly-forced dynamical models.

Thesis Aims

The modeling research study undertaken in this dissertation demonstrates both the simplicity and interpretability of implicitly-forced mathematical transmission models of malaria that are driven by climate. In the hierarchy of mathematical malaria transmission models, implicitly-forced dynamical models driven by direct climate modulation fall in the middle of the pack– less complex than agent/individual based models and compartmental models that explicitly represent vector and human populations, but more sophisticated than process-based models that adopt a simplified representation of vector dynamics driven by indirect climate relationships. Such well-specified, climate-driven parsimonious models of transmission should occupy an important place in malaria epidemiology. By highlighting the direct ecological relationships among climate, malaria parasite and vector, the proposed climate-driven implicitly-forced model substantively advances understanding of these relationships and provides a parsimonious framework for simulating and forecasting malaria outcomes. Compared to other

implicitly-forced models, the grounding of this novel framework in malaria entomology improves realistic representation of the role of environmental conditions while simplifying the interactions of vector-host populations. Further, the modeling approach provides a means for reducing the uncertainties and complexity that arise in climate-based models that explicitly represent vector and host population dynamics. Additionally, the implicit form is flexible and powerful, and can provide first-glance, diagnostic indication of potential ecological and population drivers prior to considering more complicated assumptions on transmission dynamics.

The chapters that follow below, formulate and evaluate a mathematical model framework that acknowledges important epidemiological and ecological relationships of human and mosquito populations relevant to capturing malaria dynamics. Transmission dynamics in host population are explicitly represented. And to conserve model parsimony, explicit representation of complex vector dynamics is omitted, but the malaria force of infection is represented through direct climate-regulation of multiple aspects of the malaria Entomological Inoculation Rate (EIR), including host-feeding activity, parasite sporogony, mosquito development and mortality.

In Chapter 1, the parsimonious climate–based mathematical malaria model is developed. Malaria transmission in the human population is represented through compartmental style modeling, grouping individuals into Susceptible (S) Exposed (E) Infected (I) Treated (T) and Recovered (R) states. The population is perfectly mixed, and average rates of human demography (birth and death) and malaria epidemiology, including parasite incubation, duration of infection and clinical symptoms, period of malaria immunity for subpatent and patent infections dictate the flow of individuals through different states of the transmission system over time. Vector dynamics are represented through an environmentally-modulated Entomological Inoculation Rate (EIR). Rainfall and temperature conditions are coupled to multiple aspects of

the EIR in order to derive a climate-driven implicit force of infection. Using local climate data from four regions in Rwanda, the simple model framework generates free simulations of seasonal malaria incidence which are compared to seasonal malaria activity in those regions.

Chapter 2 explores the capacity of the simple model structure for reproducing ongoing malaria transmission at interannual and annual scales throughout Rwanda– a malaria endemic country in east Africa. The malaria model is coupled with the Ensemble Adjustment Kalman Filter (EAKF), a data assimilation algorithm, which is used in conjunction with malaria incidence data to parameterize the malaria model. For 42 regions across Rwanda, the model-inference system, driven by local meteorological conditions, generates simulations of weekly malaria incidence over a four-year period. To validate the malaria model, these estimates of malaria incidence are compared to observed malaria incidence at local and regional geographic scales to evaluate the accuracy of the implicit malaria model. Model parameters representing underlying local transmission dynamics and inferred during data assimilation are compared to existing estimates of entomological and epidemiological parameters of malaria in order to assess the validity of the developed model. Because climate impacts malaria variability through multiple pathways, the relative influence of various climate-regulated processes on local malaria variability is examined within the optimized transmission model.

Chapter 3 describes the utility of the simple model framework for forecasting local malaria incidence in Rwanda. Although process-based models of transmission have long been employed to improve understanding of malaria dynamics, the use of dynamical forecasting systems for accurate prediction of future outcomes of malaria is still in its infancy. Malaria prediction has historically relied on statistical relationships such as those utilizing generalized linear models (Gomez-Elipe et al. 2007; Teklehaimanot et al. 2004) and auto regressive

integrated moving average (ARIMA) approaches (Abeku et al. 2002; Midekisa et al. 2012) to projection future incidence. At present, only a few process-based transmission frameworks (Gaudart et al. 2009; Laneri et al. 2010; Tompkins et al. 2019) have been developed and validated for predicting malaria incidence– likely due to the difficult challenge posed by the underlying nonlinear dynamics of the transmission system, which make future predictions more prone to error growth. More so, these dynamical forecasting constructs rely on capturing recent observed malaria activity and are not equipped to approximate the evolving observed and unobserved states of the transmission system.

In Chapter 3, a dynamical forecasting system is developed that consists of the mathematical model of malaria transmission, past malaria records and the EAKF data-assimilation algorithm that enables approximation of the evolving states of the transmission system. Recently, accurate forecasts of disease incidence using similar dynamic forecasting frameworks have been developed for several infectious diseases including, dengue fever (Yamana, Kandula, and Shaman 2016), West Nile Virus (DeFelice et al. 2017; 2018), influenza (Shaman and Karspeck 2012; Shaman et al. 2013; 2017; Yang, Olson, and Shaman 2016; Yang, Karspeck, and Shaman 2014), and diarrheal disease (Heaney, Alexander, and Shaman 2020); however, a forecasting system using such a highly promising dynamic forecasting inference approach, much like those used for numerical weather prediction (NWP) (Anderson 2001; Karspeck and Anderson 2007), that recursively adjusts the dynamical model to better represent the evolving state of the underlying system, has yet to be developed and validated for malaria. Use of such model-inference frameworks for up-to-date tracking of model states is an arguably important step for malaria forecasting and could provide systems for evaluating future malaria risk and potentially improving malaria control decision-making.

Because climate is a strong driver of malaria vector and parasite activity, the forecasting system developed in Chapter three is additionally combined with local rainfall and temperature climatology. Over a four-year period, the forecasting system generates probabilistic predictions of future malaria incidence throughout Rwanda. Predictions of local malaria incidence are evaluated for their forecast accuracy, skill and reliability at regional and national levels demonstrating the statistical performance and utility of the forecasting system. Additionally, a multi-model forecasting system, comprised of the dynamic forecasting system and historical probability model predictions, is created to examine improvements to malaria forecast accuracy and uncertainty.

Chapter 1: Malaria model development and free-simulation

In this chapter, a climate-driven malaria transmission model framework is developed. The construct is a mathematical model of malaria transmission in human populations with an implicit force of infection capturing vector-host interactions through the entomological inoculation rate (EIR). Climate modulation in the model is realized through temperature and rainfall relationships with vector and parasite dynamics influencing the EIR, including mosquito development, survival, host-seeking behavior and parasite development within mosquitoes. Using seasonal climatologies of rainfall and temperature across local sites in Rwanda, the model construct is used to freely simulate transmission in order to assess whether it can accurately capture seasonal malaria dynamics. Simulation of inter-annual transmission, model inference and validation of the developed model framework are detailed in the chapter that follows.

1.1 Background

Climate-based mechanistic models of malaria can be categorized, grossly, into explicit and implicit forms. In explicit formulations, states of transmission in host and vector populations, as well as progression through stages of the mosquito lifecycle, are tracked through time. As a result, the force of infection directly evolves from interactions between host and vector populations as the transmission system changes over time. In implicit approaches, however, transmission in the host community is the primary focus. Instead of following transmission and life stages in vector populations, a parsimonious representation of mosquito dynamics is used to simulate the force of transmission acting on the host population. This allows for simpler model assumptions and may reduce the uncertainty that arises from the additional layer of complexity

that climate introduces into an already complex disease transmission system. The force of transmission, consequently, is a result of the interaction between explicitly simulated host infection dynamics and the implicitly represented mosquito dynamics.

Both explicit (Abiodun, Witbooi, et al. 2018; Alonso, Bouma, and Pascual 2011; Hoshen and Morse 2004; Jones and Morse 2010; Lou and Zhao 2010; Tompkins and Ermert 2013) and implicit (Bhadra et al. 2011; Gaudart et al. 2009; Laneri et al. 2015; 2010b) climate-based mechanistic forms are capable of simulating malaria transmission dynamics; however, current implicit models have relied on indirect climate modulation of the force of transmission (Bhadra et al. 2011; Gaudart et al. 2009; Laneri et al. 2015; 2010b). In these instances, the use of strongly correlated predictors of vector dynamics, such as observations of mosquito density or temporal seasonality and smoothing interpolations of climate, compromises meaningful investigation of the specific influence of climate on malaria. But, in explicitly forced climate-driven malaria models, climate directly regulates mosquito ecology and parasite transmissibility.

Implicit models provide a simple yet powerful form for capturing the seasonal and spatial spread of mosquito-borne diseases; however, the lack of biologically-motivated climate modulation of transmission obscures meaningful interpretation of the role of climate on disease dynamics. Similarly, the absence of a direct connection between climate and transmission limits evaluation of the specific role of climate in a biologically informative way. For example, ambient conditions regulate mosquito development rates, survivorship, host seeking behavior and parasite transmissibility (M. N. Bayoh and Lindsay 2003; 2004; Shapiro, Whitehead, and Thomas 2017; J. I. Shililu et al. 2004). It may be of interest to local epidemiology and control efforts to identify the dominant pathways of ecology through which climate supports historical and prevailing malaria activity described by these models. Therefore, there is need to enhance the implicit

model forms by providing biological grounding for the effects of climate, which may increase their attractiveness as parsimonious model constructs and enhance their utility for evaluating climate-related connections to malaria. The sections that follow detail the development of an implicitly forced climate-based transmission model. More so, it is shown that process-based, accurate simulation of malaria can be achieved using this implicit model construct, in which the force of infection is informed by direct climate relationships with several aspects of the malaria Entomological Inoculation Rate (EIR).

The EIR, defined as the number of infective bites received per day per human (David L. Smith and Ellis McKenzie 2004), represents the influence of mosquito population dynamics and infection on the host population. It incorporates mosquito population dynamics, feeding activity, development and infection in the human population, to formulate a compact measure of the transmission pressure experienced by a host population. Often estimated using information quantifying the prevalence of the *Plasmodium falciparum* parasite in the mosquito population and the human biting rate (HBR), the EIR can also be estimated directly from the basic entomological parameters of the *Anopheles* vector, namely, mosquito density (m), mosquito feeding activity (a), longevity (g), and parasite inoculation (n) within the vector and prevalence of malaria infection in the human population. These entomological variables determine the force of infection by collectively moderating the number and frequency of inoculated exposures between infectious vectors and human hosts. Temperature and rainfall impact many of the vector components affecting EIR, and as described below, consequently lead to a climate-modified risk of parasite transmission.

Many natural breeding sites are used by female *Anopheles* mosquitos for egg oviposition and larvae habitat such as temporary pools and puddles, hoof prints, edges of lakes and ponds

depend on rainfall activity. *Anopheles gambiae*, the principal vector of malaria in sub-Saharan Africa, shows high sensitivity to the amount of water in its breeding site during the egg, larvae and pupae stages of development (J. I. Shililu et al. 2004; Koenraadt et al. 2003; Krijn P. Paaijmans et al. 2007; Beier et al. 1990). Increases of moisture levels enhance the hatching success rates of eggs and progression of mosquito larvae to the pupae stage of development, whereas low moisture desiccates and causes death of the developing embryo and larvae (J. I. Shililu et al. 2004; Koenraadt et al. 2003). The eggs of *An. gambiae* are more tolerant of dry conditions than the larvae or pupae and are able to survive up to 12-15 days (J. I. Shililu et al. 2004; Beier et al. 1990) but eventually die, if dry periods are prolonged. Nonetheless, the short-term tolerance of eggs to drying conditions ensures maintenance of *Anopheles* populations during periods of low rainfall and allows rebound in mosquito population levels following the return of the wet season (Bigoga et al. 2007; Kabbale et al. 2013). The susceptibility of *Anopheles* egg, larvae and pupae to variability of surface water conditions makes rainfall a strong determinant of mosquito abundance and ultimately the capacity for transmission.

Arguably, temperature is more impactful to transmission potential. Temperature not only modulates the duration of development of immature *An. gambiae* mosquitoes, but also affects the development rate of the *Plasmodium* parasite to its infective, sporozoite stage. In 5-8 days, *An. gambiae* mosquitoes can complete the sub-adult life stages, if temperature conditions are optimal (20-22°C) (M. N. Bayoh and Lindsay 2003). Adult and pre-adult mosquitoes survive well at these optimum ranges of temperature, but experience disrupted development and death at extreme temperatures (<16°C or >35°C) (M. N. Bayoh and Lindsay 2003; Mohamed Nabie Bayoh 2001; Shapiro, Whitehead, and Thomas 2017).

The development time of the *Plasmodium* parasite in the mosquito vector, termed the Extrinsic Incubation Period (EIP), is the time needed for the parasite to reproduce within mosquitoes and form sporozoites capable of infecting a host during mosquito blood feeding. Warm temperatures (24-28°C) enhance the speed of parasite development (5-7days) (Eling et al. 2001a; Shapiro, Whitehead, and Thomas 2017) and consequently raise the probability of an infective bite from an infected mosquito. In contrast, extreme low or high temperatures (<16 or >35°C) result in delayed development of the parasite, death of the mosquito vector and a lack of malaria transmission.

Temperature also plays a part in the host-seeking behavior associated with parasite transmission and oviposition. *Anopheles* mosquitoes require a blood meal in order to successfully develop and mature their eggs (Becker et al. 2010). Female *Anopheles* take at least one blood meal during the gonotrophic cycle (Scott and Takken 2012)– the interval between blood feeding, egg development and egg-laying. Blood feeding activity and the duration of gonotrophy in female *An. gambiae* is well moderated by temperature (Shapiro, Whitehead, and Thomas 2017; Gillies 1953). After taking a blood meal, female *Anopheles* mosquitoes enter a resting phase during which proteins from the blood meal are digested and used for egg production (A.N. Clements 1992; M.J. Lehane 2005). Once matured eggs are oviposited, ending the gonotrophic cycle, surviving female *Anopheles* may then seek another meal. Temperature has been shown to alter the duration of the gonotrophic cycle, with increasingly warm conditions decreasing the interval between feeding and oviposition (Shapiro, Whitehead, and Thomas 2017; Gillies 1953). The resulting higher frequency of host-seeking supports more oviposition and further inflates the malaria force of transmission.

These various modulatory roles of ambient climate conditions on the malaria mosquito and parasite enable derivation of a climate-driven transmission pressure through the EIR. Using EIR to simplify mosquito dynamics is not uncommon in dynamical malaria modeling, as it readily relates to the intensity of transmission, which can be useful for malaria control and risk monitoring efforts. Thomas Smith et al. 2006 used field estimates of EIR in within-host mathematical models to predict the potential impact of vaccination on infection rates in human populations. Ermert et al. 2011b; Tompkins and Ermert 2013 used climate-driven explicit mosquito and human population models to simulate EIR values as crude estimates of malaria activity and for validation against field estimates. Here, the EIR is used to represent transmission forcing; multiple components of EIR are directly modulated by climate through established empirical relationships between climate and the malaria vector and parasite. Similar climate expansion of malaria indicator variables, such as Vectorial Capacity (VC) and Reproductive number (R_0), in connection with climate regulation has been demonstrated (Ceccato et al. 2012; Mordecai et al. 2013). Expansions for the EIR in conjunction with simple dynamical models of transmission implicitly forced by direct influence of climate on parasite and vector entomology have not been described.

In the sections that follow detail the mathematical expansion of the EIR to include modulation by climate conditions. This modulation is represented through influence upon a variety of important features, including mosquito population density, parasite transmissibility, and mosquito feeding activity. Descriptions of this climate-coupled malaria model and summary of the relative effect of EIR variables on malaria risk are provided. Results show that the entomological climate-model is capable of accurately capturing the seasonal dynamics of malaria incidence, when coupled to temperature and rainfall climatology from four regions in Rwanda.

1.2 Materials and Methods

1.2.1 Study region

The study region is Rwanda– a small, landlocked country in eastern sub-Saharan Africa. Rwanda has diverse terrain, with elevations up to 4200m above sea level in the north and west and as low as 900m above seas level in the east and south (Henninger 2013). The large difference in geography is associated with distinct climate regimes across the country (Fig. 1). The highlands experience year-round temperate temperatures that hover around 17.5°-19°C, compared to the warmer tropical temperatures (20°-24°C) found across the lowlands. Two rainy seasons exist in the country, primarily because of the seasonal progression of the Inter-Tropical Convergence Zone (ITCZ)– a longer season lasting from February–June and peaking in April and a shorter one between September–December, peaking in November. Additionally, across the country rainfall varies distinctly, increasing from the east and southeast (~900mm annual average) to the west and northwest (~1500mm annual average) (Henninger 2013; National Institute of Statistics of Rwanda 2015a).

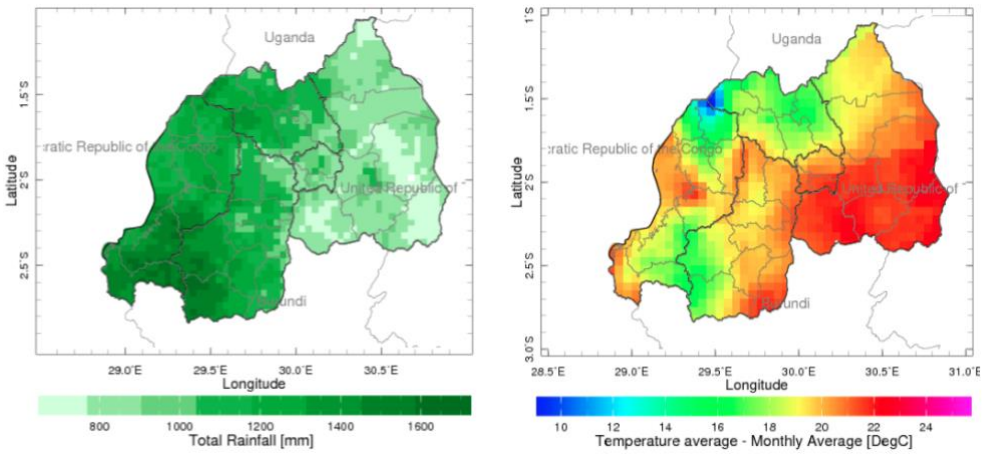

Figure 1. Map of rainfall (left panel) and temperature (right panel) climatology (1981-2016) in Rwanda. Image credit: Dinku, Tufa, Madeleine C. Thomson, Rémi Cousin, John del Corral, Pietro Ceccato, James Hansen, and Stephen J. Connor. 2017. "Enhancing National Climate Services (ENACTS)

for Development in Africa." Climate and Development 0 (0): 1–9. https://doi.org/10.1080/17565529.2017.1405784.

Malaria transmission in Rwanda occurs year-round, and has two seasons, one peaking around April–May and the other during November–December. Both seasons follow the bimodal rainy season. Although the entire population is at risk of transmission, malaria varies geographically across the country. In the highlands in the west and north, the burden of malaria is lower compared to the lowlands in the south and east (Ministry of Health, Rwanda 2017). In Rwanda, as is in most of sub-Saharan Africa, *Plasmodium falciparum* is the prevalent cause of malaria disease (World Health Organization 2018c; 2017c; 2016a); and *Anopheles gambiae* sensu lato (*s.l.*), a highly efficient vector of the parasite (Gillies and De Meillon 1968; Coluzzi 1999) is the most common malaria vector across the country (Hakizimana et al. 2018; Murindahabi et al. 2021; Nyirakanani et al. 2017). *Anopheles funestus* and other *Anopheles* species are also found throughout the region but in fewer numbers.

2.2.2 Study data

Malaria incidence data were obtained from the Rwanda Ministry of Health (MoH). The MoH, beginning in 2011, established nationwide diagnosis and cases-management protocols that include parasitological confirmation of all suspected malaria cases (National Institute of Statistics of Rwanda 2015a) and mandatory reporting of malaria cases on a weekly basis to health district centers. Weekly counts of malaria incidence from 2016 to 2019 for four health districts located in the East province (Kibungo district), South province (Gitwe district), West province (Kirinda district) and North province (Rutongo district) were obtained, and a seasonal average cycle of weekly malaria incidence for each site was computed.

Long term temperature (1981-2016) and rainfall (1981-2019) data were acquired from the University of California, Santa Barbara Climate Hazards Group InfraRed Precipitation and Temperature with Station dataset (CHIRPS and CHIRTS) products (Funk et al. 2019; 2015). Due to the lack of long-term malaria data, rainfall and temperature climatologies based on 2006-2016 and 2005-2019 periods were computed for each study site. The computed climatologies were used to force model simulations of malaria incidence, which were compared to the observed cycle of malaria incidence for each study site.

1.2.2 Model description

1.2.3.1 Compartmental model

To represent malaria transmission, a compartmental model with a Susceptible Exposed Infected Recovered and Susceptible (SEIRS) form (Eq. 1-5) is developed. Within this system (Fig. 2), the human population is divided among individuals who are susceptible to infection(S), exposed to the parasite but not yet infectious (E), have clinical infection and are treated (T), have clinical infection and are untreated (I), and recovered from clinical disease (R). Hosts transition between susceptible, exposed, infected and recovered states at rates determined by model parameters, which represent key epidemiological and human demographic characteristics. Based on birth rate estimates (μ_{BS}) from recent census data, individuals enter the Susceptible (S) group; previously infected individuals can also return to the susceptible state due to loss of immunity (end of patency) or treatment–related prophylaxis. The immunity structure employed here is a simplification of more complex dynamics, which are age and parasite specific and vary with repeated exposure. To maintain model parsimony, immunity within the system follows a simple structure in which previous infection confers non-sterilizing immunity and recovered individuals

become susceptible again. Similar simplified representations of malaria immunity have provided reasonable fittings of observed malaria incidence (Laneri et al. 2010b; Griffin, Ferguson, and Ghani 2014).

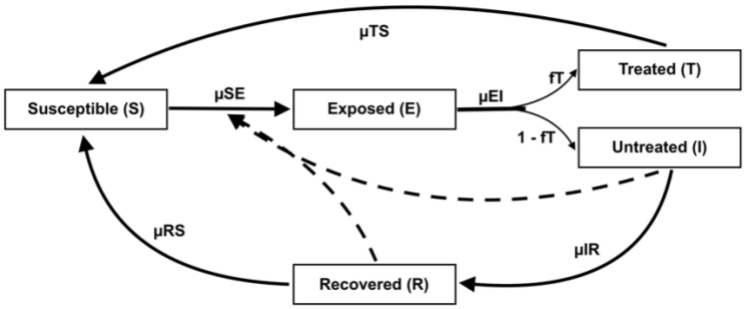

Figure 2. Flow diagram of the malaria transmission model. Individuals within the transmission system are divided into those who are susceptible to infection (S), exposed to the parasite (E), have clinical infection and are treated (T), have clinical infection and are untreated (I), and have recovered from clinical disease (R). Individuals are susceptible at birth (μ_{BS}) or following loss of immunity (end of patency) or end of treatment–related prophylaxis. Susceptible individuals become exposed at a rate determined by the force of infection (μ_{SE}). Exposed hosts (E) then undergo intrinsic incubation of *Plasmodium falciparum* at a rate determined by μ_{EI}. Following parasite incubation, infected cases begin to show clinical symptoms, a fraction (fT) of which are assumed to be fully treated (state T) with the remainder untreated (state I). Treated individuals return to the susceptible state at a rate determined by the duration of the prophylactic effect (μ_{TS}) due to antimalarial therapy. Untreated infections recover naturally (μ_{IR}) from clinical disease and show no further symptoms of clinical infection. Hosts that naturally recover, enter a state of low level parasitemia (state R) that is tolerated by the immune system. Under this patent/subpatent state, individuals are protected from reinfection and have a relatively lower infectivity to mosquitoes (qR) compared to full-blown clinical infections. Once patent/subpatent infections are cleared (μ_{RS}), recovered hosts again become susceptible.

Following exposure to an infectious mosquito bite, susceptible individuals move into the exposed group at a certain rate of infection, determined by the force of transmission. While in the exposed state, individuals undergo intrinsic incubation of *Plasmodium falciparum* during which parasites transition to gametocytes – the parasitic stage infectious to mosquitoes. Following this incubation period, which typically lasts 8-21 days in humans, individuals begin to show clinical symptoms, and are caught by the surveillance system. Malaria incidence in the transmission system is tracked by μ_{EI}*E, the number of newly infected individuals per unit time. These

clinical infections may be fully treated (state T) by anti-malaria therapy drug or remain untreated and infectious (state I). Based on recent Demographic and Health Survey (DHS) data on treatment seeking behavior of individuals with fever in Rwanda (Battle et al. 2016), half of newly occurring infections (f_T) are assumed to seek and receive full treatment.

Following treatment, infected cases (in state T) return to being susceptible after the duration of the post-treatment prophylactic effect (μ_{TS}) provided by antimalarial therapy. Only untreated infections (I) contribute to the force of infection and can transmit the parasite to mosquitoes with a certain probability (P_{HM}), as not all blood meals result in mosquito infection. Several factors such as human gametocyte density and antimalarial treatment may affect the likelihood of infecting a blood-feeding mosquito (Collins and Jeffery 2003; Alves et al. 2005a; Targett et al. 2001). Untreated infections recover naturally (μ_{IR}) from clinical disease and show no further symptoms of clinical infection. However, given that malaria infection can outlive clinical symptoms (Langhorne et al. 2008; Doolan, Dobaño, and Baird 2009), recovered individuals enter a state of low level parasitemia (state R) that is tolerated by the immune system. During this period of patent/subpatent infection, individuals are protected from reinfection and have a relatively lower infectivity to mosquitoes (q_R) compared to full-blown clinical infections (Slater et al. 2019; Tadesse et al. 2018; Kim A. Lindblade et al. 2013). As the host immune system steadily clears patent and sub-patent infections, individuals return to susceptibility after a time based on the duration of the patency and sub-patency period μ_{RS}. The set of ordinary differential equations representing this malaria transmission system are as follows:

$$\frac{dS}{dt} = \mu_{BS}P - \mu_{SE}S + \mu_{RS}R + \mu_{TS}T - \delta S \quad (1)$$

$$\frac{dE}{dt} = \mu_{SE}S - \mu_{EI}E - \delta E \quad (2)$$

$$\frac{dI}{dt} = (1 - fT)(\mu_{EI}E) - \mu_{IR}I - \delta I \quad (3)$$

$$\frac{dT}{dt} = fT(\mu_{EI}E) - \mu_{TS}T - \delta T \quad (4)$$

$$\frac{dR}{dt} = \mu_{IR}I - \mu_{RS}R - \delta R \quad (5)$$

$$P = S + E + I + T + R \quad (6)$$

Environmental and population factors, such as proximity to mosquito breeding sites, area vegetation, human genetics and behavior, and mosquito biting behavior have been recognized for creating malaria transmission hotspots (Bousema et al. 2010; Kreuels et al. 2008; Ernst et al. 2006; R. L. Clark 2009). These transmission hotspots reflect the so-called 20/80 rule (T. D. Clark et al. 2008; Woolhouse et al. 1997; David L. Smith et al. 2007; D. L. Smith et al. 2005), common in infectious diseases, in which a small proportion (e.g. 20%) of the population bears most of the burden of transmission (80%) and contributes considerably more to the force of transmission than surrounding communities in the same region (Bousema et al. 2010; T. D. Clark et al. 2008; Woolhouse et al. 1997). Because of this heterogeneity, the effective number of individuals actively involved in malaria transmission may be lower than the total human population in a region. Therefore, estimate an effective population size *P* models the population size of the transmission system. *P* is the product of scaling parameter *s* and *N*, the human census population.

Table 1. Description and prior ranges of the parameters of the malaria transmission model.

Parameter	Description	Prior ranges	Unit	Reference
μ_{BS}	Birth rate	$(57*365)^{-1}$	day^{-1}	Census
$\delta S, \delta E, \delta U, \delta T, \delta R$	Death rate	$(53*365)^{-1}$	day^{-1}	Census

$\mu_{EI}^{\ddagger}$	Duration of parasite incubation	7 – 14	day	Lit(Boyd and Kitchen 1937)
μ_{TS}	Duration of treatment + prophylaxis	30	day	Lit(Watkins et al. 1997; Trigg et al. 1997; Kamya et al. 2007; Yeka et al. 2008; Cisse et al. 2009; Kakuru et al. 2013)
μ_{IR}	Duration of untreated infection	5	day	Lit(Drakeley et al. 2006; Zwang et al. 2009; Miller 1958; Church et al. 1997)
fT	Proportion of infected receiving full treatment	0.5	-	Lit(Battle et al. 2016)
$\mu_{RS}^{\ddagger}$	Duration of patent/sub-patent period	120 –365	day	Lit(W. Sama, Dietz, and Smith 2006; Bretscher et al. 2011; Felger et al. 2012; Wilson Sama, Killeen, and Smith 2004; Keegan and Dushoff 2013)
P_{MH}	Probability of transmission from mosquito to human	0.5	-	Lit(Churcher et al. 2017a; Filipe et al. 2007)
P_{HM}	Probability of transmission from human to mosquito	0.125	-	Lit(Boudin et al. 1993; Jeffery and Eyles 1955; Alves et al. 2005b)
qR	Infectivity of non-clinical cases relative to clinical cases	0 – 0.5 * (P_{HM})	-	Lit(Slater et al. 2019; Tadesse et al. 2018; Kim A. Lindblade et al. 2013)
ε	Number of eggs laid per gonotrophic cycle	50	-	Lit(Hogg, Thomson, and Hurd 1996; Hogg and Hurd 1997; Lyimo and Takken 1993)
μ_M	Daily adult mortality rate	-ln 0.98	-	-
a.R‡	Egg-adult sensitivity to surface moisture	0 – 1	-	See supplement in Chapter 1
b.R‡	Mean anomaly of accumulated rainfall	-5 – 5	-	See supplement in Chapter 1
D‡	Length of accumulated rainfall contributing to mosquito breeding	7 – 200	day	Lit(Laneri et al. 2010b; Yazoumé Yé et al. 2009; McCann et al. 2014; Lindsay, Parson, and Thomas 1998)
s‡	Population scaling factor	0 – 1	-	-
S_0,E_0, I_0, T_0, R_0	Initial state conditions	0 – P, P = total model population	-	-

‡Model parameter values to be inferred from observed data

1.2.3.2 Force of infection

The force of infection in the transmission system is dependent on the collective pressure exacted by the infectious populations of humans and vectors and is directly related to the EIR–

the number of infectious bites received per person per unit time. Often estimated in the field as the product of the Human Biting Rate (HBR) and sporozoite rate (the proportion of infectious mosquitoes), the EIR at time *t* also can be expressed mathematically (Eq. 7) using assumptions of human infectiousness and mosquito infectiousness, density, feeding activity and survivorship (David L. Smith and Ellis McKenzie 2004):

$$EIR\ (t) = \frac{ma^2 P_{HM}\ X\ e^{-gn}}{g + aP_{HM}X} \qquad (7)$$

where *m* is the number of mosquitoes per human, *a* is the mosquito biting rate, P_{HM} the probability of transmission from human to mosquito, *g* the adult mosquito death rate, *n* sporogony duration and *X* the proportion of infectious humans at *t*. $X = \frac{I + qR*R}{S+E+I+T+R}$ defines the fraction of human states (i.e *I* untreated clinical infections and *R* non-clinical infections adjusted by their lower infectivity, *qR*) contributing to the force of infection.

Analyses of EIR data and occurrence of new malaria infections indicate the existence of a nonlinear relationship with the force of infection (David L. Smith and Ellis McKenzie 2004; T. Smith et al. 2004; David L. Smith et al. 2010) in which risk of infection saturates at high EIR. These findings show a clear deviation from the assumptions of the Ross-Macdonald model (George Macdonald 1957; David L. Smith et al. 2012) that infectious bites are linearly proportional to the rate of new infections. Therefore, to follow T. Smith et al. 2004 and T. A. Smith 2008, the modified force of infection (μ_{SE}) below acknowledges nonlinearity between infectious mosquito bites and the risk of new infections, and the saturation of new infections as EIR increases:

$$\mu_{SE}(t) = 1 - e^{-pMH*EIR(t)} \qquad (8)$$

The density of parasite in a vector, host immune status, and failure of the parasite to advance to blood stages all can affect whether an infectious bite produces infection in a human host

(Churcher et al. 2017b). Therefore, only a proportion of infectious bites P_{MH} (i.e. the probability of mosquito to human transmission) lead to human infection.

1.2.3.3 Climate regulation of parasite and vector ecology

Mosquito density (m)

Following the simple model of Parham and Michael 2010 describing a mosquito population at equilibrium, adult mosquito density is defined as:

$$m = \frac{L}{\mu_M} \qquad (9)$$

$$L\ (T, R) = \frac{B(T)\ P_{EA}(T, R)}{\tau_{EA}(T)} \qquad (10)$$

The abundance of adult mosquitoes is tied to the population birth rate of adult mosquitoes (L) and the mortality rate of adult mosquitoes (μ_M). While existing mature mosquitoes must survive long enough to feed, reproduce and oviposit eggs at available breeding sites, pre-adult mosquitoes need to successfully move through egg, larvae and pupae stages in a timely manner to emerge and contribute to the naive adult population. Temperature conditions and water habitat availability can severely change the population balance by altering survival probabilities at all life stages and as well as female oviposition. Increased adult mortality and failure of pre-adult development because of suboptimal conditions jointly lower the reproductive power of the mosquito population and consequently adult density. These environmentally driven effects are reflected in the population model by setting the probability that eggs survive to adults (P_{EA}), the egg-to-adult development time (τ_{EA}), and the lifetime number of eggs laid by female adults (B), as functions of temperature and rainfall. The following section describes each of these components and how temperature (T) and rainfall (R) simultaneously modulate their outcomes.

Lifetime number of eggs (B)

The typical number of eggs laid by female *Anopheles* mosquitoes during oviposition may range from 50 to 290 (Hogg, Thomson, and Hurd 1996; Hogg and Hurd 1997; Lyimo and Takken 1993). Although the number of eggs laid have not been linked to ambient conditions, the frequency of oviposition, which is determined by the length of the gonotrophic cycle– the time between a blood meal and egg production– varies as a function of temperature (Shapiro, Whitehead, and Thomas 2017). Thus, by influencing the frequency of oviposition, temperature affects the number of eggs laid during the adult lifespan of a female *Anopheles*. Assuming a female mosquito oviposits every few days, depending on the length of the gonotrophic cycle, and experiences a constant rate of mortality (μ_M), an exponential relationship with egg laying is expected. Given these assumptions, and following White et al. 2011, the number of eggs produced over the female mosquito lifespan is:

$$B(T) = \frac{\varepsilon}{e^{GP\mu_M - 1}} \qquad (11)$$

$$GP(T) = \frac{1}{0.017T - 0.165} \qquad (12)$$

where ε is the number of eggs laid per gonotrophic cycle, GP is the length of the gonotrophic cycle, and μ_M is daily adult mortality rate.

Bloodfed mosquitoes must survive the gonotrophic cycle in order to oviposit their eggs. Though temperature in general affects adult mosquito mortality (Mohamed Nabie Bayoh 2001), during gonotrophy when time is spent resting, digesting a blood meal and developing eggs, mortality may be more affected by predation or by the use of endophily (i.e. resting indoors)

versus exophily (i.e. resting outdoors) (Pates and Curtis 2005; Faye et al. 1997; Mahande et al. 2007), confounding the relationship with temperature. Therefore, adult mosquito mortality in the mosquito population is fixed to a constant, temperature-independent rate (μ_M).

Egg to adult survivorship

Mosquitoes begin their life in water as eggs and continue developing into larvae and pupae in this aquatic environment before emerging as adults. Though sub-adult mosquitoes are adapted to aquatic environments, they are highly sensitive to changes of temperature and the water level of their breeding habitat. Near the optimal 24-28°C water temperature, larval development can be completed in about 9-14 days (M. N. Bayoh and Lindsay 2003); at colder temperatures, larval duration can take 7-14 days longer. Larval mortality also increases by 30-70% (M. N. Bayoh and Lindsay 2004), as temperature shifts away from optimality. Additionally, significant drops in water habitat level or prolonged periods of desiccation, rapidly decreases the probability of egg, larvae and pupae survival (J. I. Shililu et al. 2004; Koenraadt et al. 2003). The critical roles of temperature and water availability are readily highlighted by the spatial and seasonal dynamics of *Anopheles* mosquitoes, with peaks in vector abundance occurring following the peak of the rainy season (Kabbale et al. 2013; Bigoga et al. 2007) and declines in vector populations and malaria risk with increasing altitude (M. Aregawi et al. 2014; Lyon et al. 2017). Transmission risk is also shown to drop in arid regions or during periods of drought compared to wetter regions and the rainy season (Bigoga et al. 2007; Patz 1998; Gagnon, Smoyer-Tomic, and Bush 2002).

Survivorship due to rainfall

A sigmoidal function, based on several studies on the survival of immature *Anopheles gambiae* as surface water level changes in the breeding site (J. I. Shililu et al. 2004; Koenraadt et al. 2003; Beier et al. 1990) models the probability of subadult survival as a function of hydrologic conditions. Chances of survival and successful completion of development increases with increasing surface water levels, here estimated by cumulative rainfall, but are near zero when hydrologic conditions are anomalously low and gradually plateaus when surface water levels are high. Survival due to water variability shows similar trends across the egg, larvae and pupae development stages, although with varying degrees of sensitivities. To limit model complexity, survivorship due to hydrologic changes during egg-adult development is modeled aggregately as:

$$P_{EA}(R) = \frac{1}{1 + e^{-a.R(c.R_D - b.R)}} \qquad (13)$$

where $a.R$ relates the egg-adult sensitivity to surface water levels and $c.R_D$ is the standardized anomaly of cumulative rainfall (over D previous days) relative to historical cumulative rainfall conditions (2005–2019). The parameter $b.R$ indicates the mean anomaly level at which 0.5 survival is expected. Prior ranges on length of cumulative rainfall are informed by some understanding on rainfall activity and mosquito density (Laneri et al. 2010b; Yazoumé Yé et al. 2009; McCann et al. 2014; Lindsay, Parson, and Thomas 1998). The model form for moisture-regulated survival, and the prior ranges on mean anomaly and the slope are informed by empirical fittings on *Anopheles* egg survival and moisture changes from literature (see supplement).

Survivorship and development time due to temperature

Several studies on the immature stages of *Anopheles gambiae* have shown that overall

survival and development rates, from egg to adult emergence, are linked with water habitat temperature through the quadratic relationships below (M. N. Bayoh and Lindsay 2003; Mordecai et al. 2013; M. N. Bayoh and Lindsay 2004). Survival and development rates are highest around 24-28°C and exposure to temperatures far from this optimal level results in death or delayed and disrupted development of mosquitoes into the next life stage. Therefore, within the modeled EIR, the rate of immature survival (P_{EA}) and duration (τEA) of egg-adult stage vary as follows:

$$P_{EA}(Tw) = -0.00924Tw^2 + 0.453Tw + -4.77 \quad (14)$$

$$\tau\mathrm{EA}(T_w) = \left(0.000111Tw(Tw - 14.7)\sqrt{34 - \mathrm{Tw}}\right)^{-1} \quad (15)$$

where T_w is habitat water temperature. Water temperature of mosquito habitats highly correlates with surrounding ambient air temperature. However, air temperature can underestimate mosquito survival and development, as it can be up to 6°C cooler than breeding site water temperature. Thus, to estimate the water temperature (T_w) of breeding sites, a simple linear model $T_w = k*T_{air} + \Delta T$ is employed as per Krijn P Paaijmans et al. 2010; A. F. G. Jacobs, Heusinkveld, and Nieveen 1998. Here, *k* is the slope and ΔT is a constant >0 capturing all antecedent impacts that raise the energy balance of the breeding site. Estimates of *k*, which represents the strength of the relationship between T_{air} and T_w have been shown to vary from 0.5 to 0.9 (Krijn P Paaijmans et al. 2010; A. F. G. Jacobs, Heusinkveld, and Nieveen 1998) with broad uncertainty, depending on location and size of the breeding sites. Rates of evaporation, wind conditions and season also affect the strength of the relationship between air temperature and water temperature of aquatic habitats (Krijn P Paaijmans et al. 2010; A. F. G. Jacobs, Heusinkveld, and Nieveen 1998; Adrie F. G. Jacobs et al. 2008; K. P. Paaijmans et al. 2008). As estimates of *k* has shown large variability and high specificity to local features, *k* is set to unity and ΔT to a constant value of

2°C due to absence of information on the location, size and ambient features of aquatic habitats in the study region. Sensitivity analyses to examine the effect of various values for k and ΔT on malaria transmission and model inference are addressed in the subsequent chapter that focuses on inference and validation of the dynamic model.

Mosquito biting rate (a)

Female mosquitoes require blood meals for egg development and will feed periodically on blood hosts to obtain the proteins and calories needed to support development (Fernandes and Briegel 2005). After eggs mature and are oviposited, surviving females can again seek a host for blood feeding and repeat this cycle of gonotrophy. The amount of time spent in blood meal digestion and egg development is strongly impacted by temperature (Shapiro, Whitehead, and Thomas 2017; Lardeux et al. 2008) and does not appear to depend on infection status of mosquitoes in the egg generation state (Norris et al. 2010). The temperature-dependent estimate of the mosquito biting rate is found by inversion of the duration of gonotrophy:

$$a(T) = 0.017T - 0.165 \qquad (16)$$

Sporogony (n)

Plasmodium parasites within infected mosquitoes must develop further into sporozoites to produce infections in humans (Vanderberg 1975; Matuschewski 2006; Sato, Montagna, and Matuschewski 2014). The duration of sporogony (i.e. the extrinsic incubation period) is modulated by ambient temperature (Shapiro, Whitehead, and Thomas 2017; Waite et al. 2019; Noden, Kent, and Beier 1995) in a nonlinear fashion similar to mosquito development (Eq. 17). Under warm temperatures, mosquitoes spend less time incubating the parasite and are likely to

have more infective bites, whereas under colder conditions mosquitoes may not live long enough to feed again and transmit the pathogen. The relationship depicting the influence of temperature on the development of the *Plasmodium* parasite within the vector can be summarized mathematically as (Krijn P. Paaijmans, Read, and Thomas 2009; Briere et al. 1999):

$$\mathrm{n}(T) = \left(0.000112T(T - 15.384)\sqrt{35 - \mathrm{T}}\right)^{-1} \qquad (17)$$

1.2.4 Simulation of malaria incidence

The present study assesses the ability of the environmentally-driven entomological framework to capture seasonal malaria transmission at local levels. Using climate data from four regions of Rwanda with differing climatology, this simplified entomological approach, when in free simulation, can generate simulations of malaria incidence comparable to the seasonal malaria for these regions.

To generate malaria simulations for the four health districts, 10,000 sets of initial model state conditions and parameters were randomly selected from prior parameter ranges (Table 1). Model integrations commenced at the beginning of the calendar year, and the transmission model (Eqs. 1-5) was integrated forward for 20 years using temperature and rainfall climatological forcing. These simulations reached a relatively steady seasonal cycle of malaria incidence in the later years of the integration. To focus on the differences due to the random selection of parameters, the first 10 years of each integration was discarded, and simulated malaria incidence was defined as the weekly average over the last 10 years. Mean absolute percentage error (MAPE) was computed between seasonal incidence data of individual sites and each of the 10,000 simulations. Also for each simulation, MAPE was averaged across the four sites to acquire an average error (AE) per parameter combination.

$$MAPE = \frac{1}{n}\sum_{t=1}^{n}\left|\frac{y_t - \widehat{y_t}}{y_t}\right| \qquad (18)$$

$$AE = \frac{1}{k}\sum_{i=1}^{k} MAPE_i \qquad (19)$$

where $\widehat{y_t}$ is simulated malaria incidence and y_t is seasonal malaria incidence at week *t (t = 1,2,3…,52)*, for each simulation for site *i (i =1,2,3,4)*. From the 10,000 simulations, the top 10 simulations with the lowest AE were retained for further analysis.

As part of the study, the relative effect of the various climate-based EIR pathways on seasonal malaria dynamics was assessed. To do this, the values of B, P_{EAR}, P_{EAT}, a, and n, informed by rainfall and temperature climatology were replaced with a constant value determined by annual mean rainfall and temperature. The malaria model was re-run with these alternate values in conjunction with the transmission parameters from the top 10 simulations and again allowed to reach a steady-state. The percent change in error (ΔE) was calculated between the MAPE of the original top model simulation and the $MAPE_{const}$ from the alternate simulations.

$$\Delta E = \frac{MAPE - MAPE_{const}}{MAPE} * 100 \qquad (20)$$

The effect of temperature and rainfall climatology to seasonal dynamics was also assessed. Instead of seasonal climate data, annual average temperature and rainfall were used to modulate malaria entomology. In this configuration, the transmission model was re-run for each study site using parameters from the top 10 simulations until steady-state was reached. The

percent change in error (ΔE) allowed assessment of the relative importance of rainfall and temperature on capturing seasonal dynamics of malaria.

1.3 Results

1.3.1 Free simulation of malaria

Of the 10,000 random simulations, the top 10 model simulations with the lowest error for the four sites were retained as best-fit models. There is good agreement between the seasonal pattern of best-fit models and seasonal malaria data, with correlations ranging from high in Kibungo (0.66-0.94), to moderate in Kirinda (0.66-0.74) and modest in Gitwe (0.47-0.68) and Rutongo (0.45-0.65) (Fig. 3). Across the sites, the trend in simulated transmission closely match observed seasonal activity, especially around the timing of peaks and troughs in transmission. Similarly, the best models were in close agreement regarding the level of malaria burden predicted among the sites (Fig. 4).

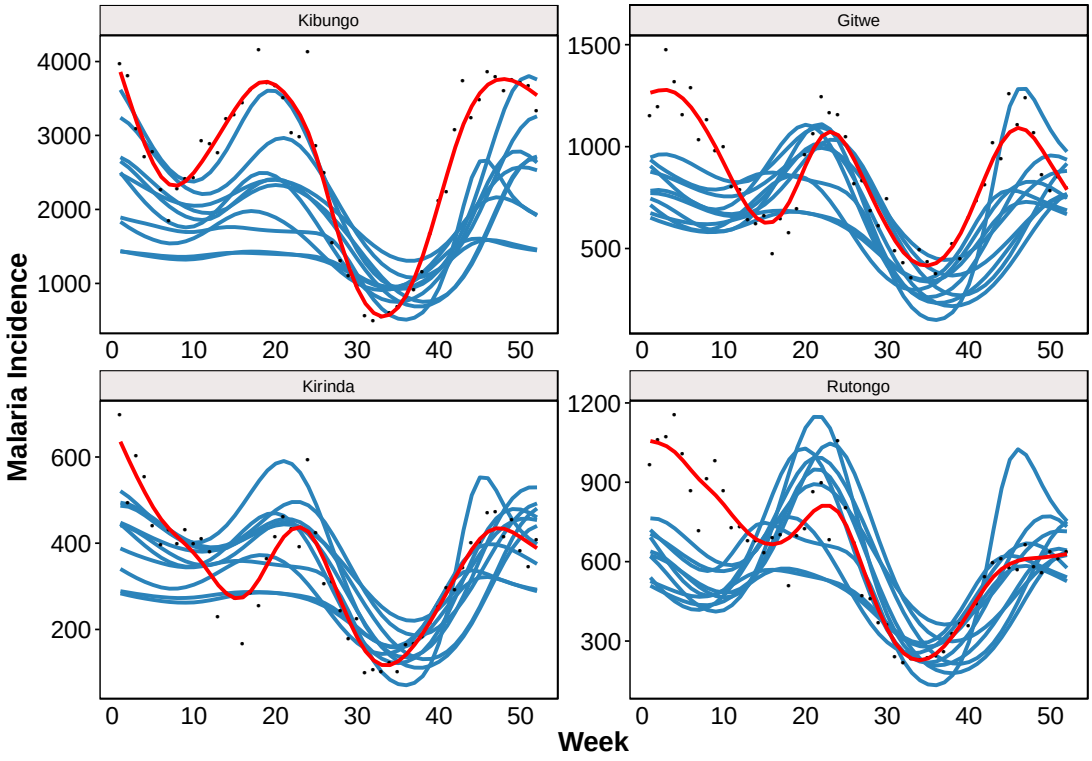

Figure 3. Simulations of seasonal malaria incidence from the environmentally-driven malaria transmission model in free simulation. Blue lines are the model simulations of seasonal incidence; black dots and red solid lines show the observed and smoothing of the seasonal values of reported malaria incidence. Range of correlation coefficient (Pearson) between modeled incidence and seasonal average malaria incidence: 0.66-0.94 (Kibungo), 0.47-0.68 (Gitwe), 0.66-0.74 (Kirinda) and 0.45-0.65 (Rutongo).

Under free simulation, the parameters of the top climate models revealed a common region of parameter space supporting malaria transmission regardless of study region. Although some variability in best-fitting parameter values was observed, similarity among the top models was high. In particular, a clear localization towards a common domain for parameters describing moisture-dependent mosquito survivorship (D, a.R, b.R), was observed among top models. Similarly, models best describing seasonality showed general consensus on the effective size of the transmission population (i.e. model population). Although, a central tendency in the posterior domain could be defined for duration of subpatent/patent infection (μ_{RS}), parasite incubation

(μ_{EI}), and relative infectivity of non-clinical infections (qR), localization was less clear (Fig. 5).

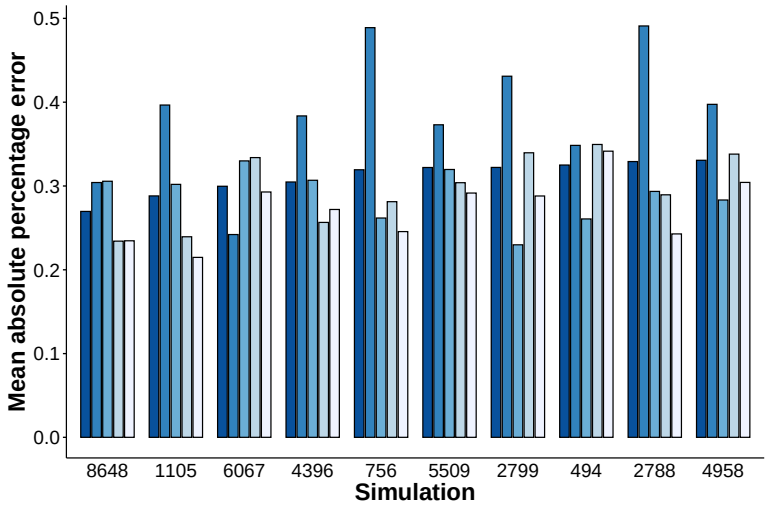

Figure 4. Mean absolute percentage error (MAPE) of the top 10 seasonal models. MAPE calculated for across all sites, and individually for Kibungo, Gitwe, Kirinda, and Rutongo are indicated by dark blue to light blue bars, in decreasing order of shading.

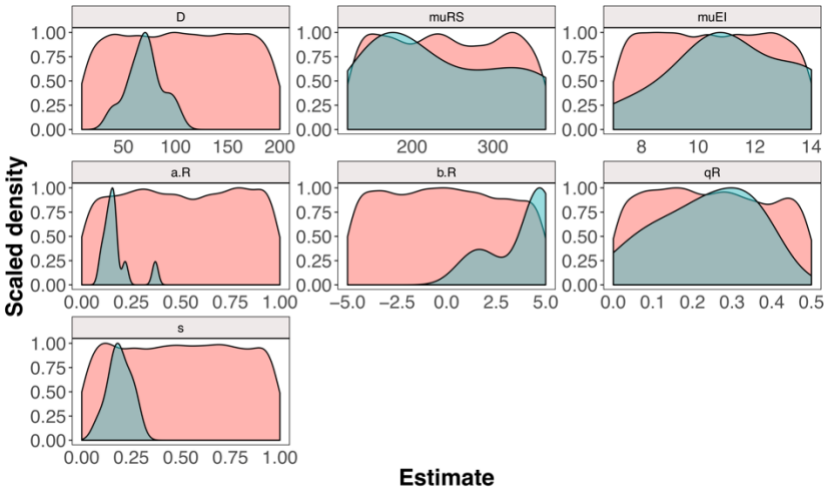

Figure 5. Distribution of posterior parameters of seasonal malaria simulations. Spread of the set of best-fitting parameters (in green) are compared to distribution of the prior parameters (red).

1.3.2 Relative benefit of temperature/rainfall regulation on seasonal dynamics

The benefit of the various individual temperature and rainfall forcing functions was also evaluated. Results indicate that the transmission model benefited the most from including

moisture regulated mosquito survivorship during sub-adult development (Fig. 6). Without moisture modulated egg-adult survivorship within the transmission model, model error generally increased across sites and among top models, with MAPE increasing on average across sites by 40.32% – 94.30% compared to the full model. Omission of temperature regulated variables of the EIR created far less deficit to the fitness of the top models with a mean increase of 0.051–4.61% in MAPE across sites.

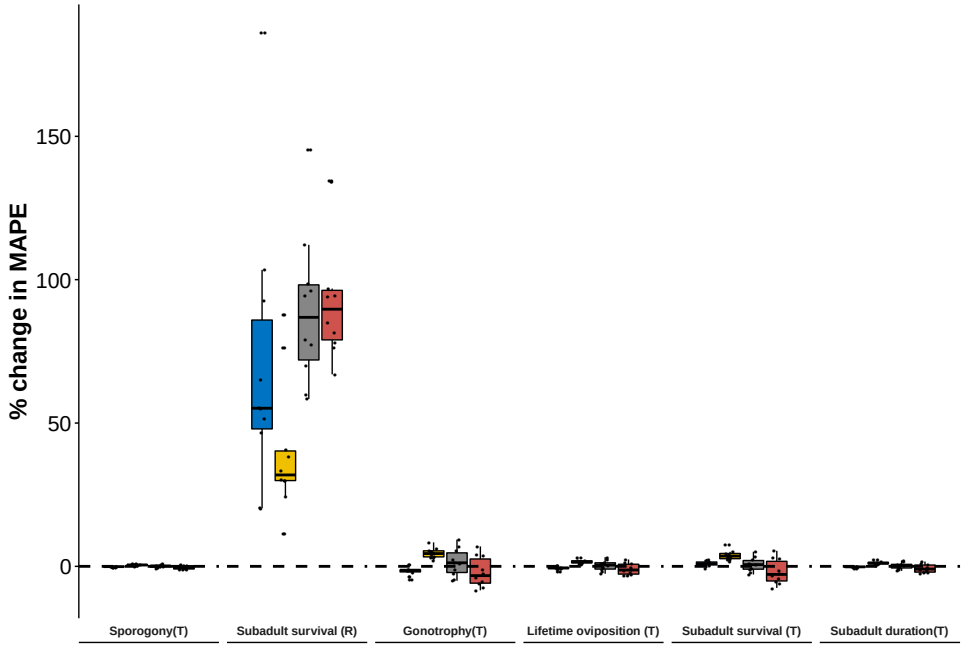

Figure 6. Percent change in error of seasonal malaria, when individual entomological functions are decoupled from climate. A function is decoupled from temperature or rainfall by setting the function to a constant value. Boxplots are showing the median (thick line), interquartile range (box bounds), Q1 -1.5*IQR (lower whiskers) , Q1 +1.5*IQR (upper whiskers) of the deviation of top 10 models from simulated malaria incidence in Kibungo (blue), Gitwe (yellow), Kirinda (grey), and Rutongo (red) districts. Jittered black dots indicate the deviation value for each model. Dashed horizontal line indicates no change in model MAPE due to decoupling.

Model analyses also investigated the overall importance of temperature or rainfall forcing on malaria simulation. The transmission model benefited the most from rainfall forcing. Absence of seasonal rainfall alone produced an average increase in MAPE of 40.32% – 94.30% (Fig. 7).

Lack of seasonal temperature forcing also decreased model performance but to a lesser degree than seasonal rainfall: error in simulated malaria incidence for the top seasonal models rose on average by 3.78 – 11.04%. In Gitwe, seasonal temperature coupling appears to be more significant to capturing malaria dynamics than in other sites. On the other hand, the influence of rainfall coupling is less pronounced in Gitwe compared to the other regions. When seasonal rainfall and temperature effects were simultaneously omitted, moderate to large declines in model fitness were observed generally, except in Gitwe where the effect of seasonal temperature and rainfall omission was less pronounced but still increased model error. Overall, modeling of malaria transmission improved with inclusion of seasonal rainfall and temperature forcing of the EIR; however, seasonal rainfall provided the greater constraint and was consistent across study sites.

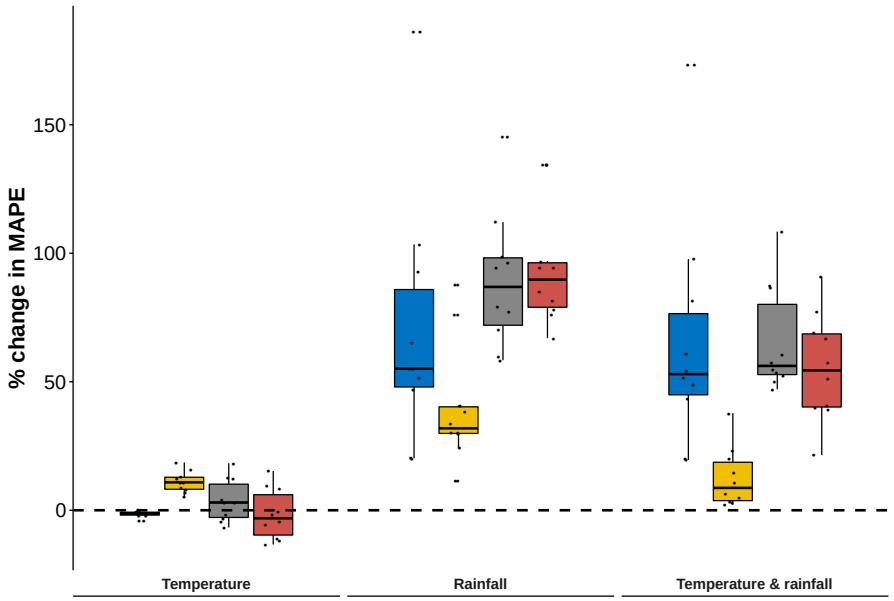

Figure 7. Percent change in error of simulated incidence, when the transmission system is decoupled entirely from climate modulation. Forcing from temperature, rainfall or from both rainfall and temperature are replaced instead with an annual average. Boxplots are showing the median (thick line), interquartile range (box bounds), Q1 -1.5*IQR (lower whiskers) , Q1 +1.5*IQR (upper whiskers) of the deviation of top 10 models from simulated malaria

incidence in Kibungo (blue), Gitwe (yellow), Kirinda (grey), and Rutongo (red) districts. Jittered black dots indicate the deviation value for each model. Horizontal dashed line indicates zero change in model MAPE.

1.3.3 Influence of climate conditions on host and vector dynamics

The effect of the environmentally-driven force of infection on the transmission system is evident in the seasonal variations of the susceptible, exposed, and infected human populations (Fig. S1). Risk of parasite exposure is highest when ambient conditions are most suitable for mosquito activity and parasite development; consequently, shortly after the onset of the rainy season, the number of exposed individuals increases, and the number of susceptible individuals declines. The number of recovering individuals grows as well, as more exposed individuals become infectious and eventually recover. However, at the start of the dry season, transmission decreases, as the availability of mosquito habitats diminishes, even though temperature conditions remain conducive for mosquito activity and parasite transmission. Fewer individuals are exposed in the dry season, and the susceptible population steadily increases as the risk of parasite exposure falls. In general, the malaria transmission model, as driven by local temperature and rainfall, captures the seasonal dynamics of malaria incidence at the study sites.

Estimated rainfall climatology follows a seasonal trend similar to seasonal malaria incidence (Fig. S2). Although, daily rates of rainfall are similar among the four sites, a wide variation in seasonal rainfall exists, making rainfall a potential limiting environmental variable in the study region. In general, mosquito activity and risk of parasite exposure (measured by the EIR) rise markedly following the rainy months but decline sharply following the dry season, as egg-adult mosquito survival rises and falls with changes in surface water availability (Fig. S3).

Within Rwanda, temperature increases from West to East. Kibungo health district located in the East province experiences the warmest seasonal temperatures, ranging from 22-24°C and Rutongo, in the northern province, the coolest, 20-22°C, according to satellite-based CHIRTS data (Fig. S2). In general, mean weekly temperature, among the four health districts, is well above the critical threshold of 18°C and shows little seasonal variation within districts. As a result, seasonal changes in parasite development and mosquito biting and survival rates are vary only slightly over time, although differences among districts still exist. Overall, parasite development, mosquito biting, and egg-adult survival rates follow similar trends among the sites, peaking during the warmest months and declining during the cooler months, except in Kibungo the warmest study site, where egg-adult survival rates are inverted during the hottest months (Fig. S3).

1.4 Conclusion

This study developed a malaria transmission model in which the entomological inoculation rate (EIR) is modulated by both temperature and rainfall conditions. The force of transmission for malaria is directly related to the EIR (David L. Smith and Ellis McKenzie 2004), which measures the risk of parasite exposure through multiple aspects of the malaria vector lifecycle—development, survival and parasite transmissibility—all of which are regulated by ambient conditions experienced by the mosquito vector. Results of this approach indicate that an implicit model with an environmentally-driven force of infection can capture the seasonal dynamics of malaria transmission, using local rainfall and temperature data. Model analysis also revealed a set of generally similar parameter values supporting malaria transmission in the study

regions.

In the climate-forced model, malaria transmission relies on both temperature and rainfall mediation of multiple aspects of the EIR to properly capture seasonal dynamics of local malaria transmission. Temperature drives sub-adult mosquito development and survival, adult mosquito feeding activity, and parasite infectiousness. Rainfall impacts mosquito population density, by modulating sub-adult survivorship as a function of surface water availability. Although the roles of temperature and rainfall are apparent in the individual components of the EIR, the downstream impact on local malaria seasonality is mostly dominated by rainfall. Model description of malaria transmission risk is more substantially improved by rainfall forcing than temperature. Weekly average temperatures for the study regions are well above the critical threshold required for *Anopheles* mosquito development and *Plasmodium* transmission (Shapiro, Whitehead, and Thomas 2017; Mordecai et al. 2013) and do not vary widely during the season. As a result, seasonal changes in parasite transmissibility, mosquito development, and or feeding activity due to temperature are slight and lead to negligible impacts on the seasonality of malaria transmission.

On the other hand, results indicate a well-defined connection between seasonal rainfall variability and malaria transmission in the study regions. Malaria transmission relies on rainfall for creating and sustaining mosquito breeding habitats to support the development and survival of aquatic sub-adult mosquitoes. Seasonal rainfall in the study regions is widely varying and creates a clear disparity in mosquito activity during the rainy and dry months. Sub-adult *Anopheles* mosquitoes are highly sensitive to hydrologic changes during development (J. I. Shililu et al. 2004; Koenraadt et al. 2003) and with marked declines in surface water availability experience lower chances of survival and progression through lifecycle stages. As a result,

parasite transmission falls when conditions cannot support sub-adult development.

In this work, a simple implicit climate model of malaria is shown capable of describing seasonal malaria incidence and allowing in-depth evaluation of the role of climate on vector lifecycle and survival, parasite transmissibility and ongoing transmission. Results from free simulations indicate that the environmentally-driven model can generate malaria simulations comparable to observed seasonal malaria at the local level. Moreover, a uniform explanation for the processes underlying disease risk in the four different regions examined could be achieved with similar parameters. The use of the biologically mediated model approach employed here, which incorporated vector entomology and parasite transmissibility, not only reduces model complexity but also creates opportunity for formal assessment of the roles of vector and parasite activity in implicit models. The findings show that malaria simulation can be improved using environmentally-driven entomology in a simple and biologically-relevant form. Nonetheless, future work applying more rigorous inference methods in conjunction with observed malaria data is needed to further validate the climate-forced model for describing interannual malaria variability and evaluate its utility in improving predictions of future malaria incidence.

1.6 Supplemental text

1.6.1 Parameterization of moisture-regulated subadult survivorship

Here, parameterization of mosquito-dependent subadult survivorship modeled in Eq. 18 is described. While prior ranges indicating the period of cumulative rainfall (D) on subadult mosquito survivorship are based on some understanding of rainfall activity and mosquito density (Laneri et al. 2010b; Yazoumé Yé et al. 2009; McCann et al. 2014; Lindsay, Parson, and Thomas 1998), the prior ranges for the mean anomaly (b.R) and the slope (a.R) are informed by least-

square fitting to *Anopheles* mosquito survival given changing surface moisture conditions (J. I. Shililu et al. 2004).

Under laboratory conditions J. I. Shililu et al. 2004 exposed equal numbers of eggs of field-caught *Anopheles gambiae* mosquitoes to soil with different soil moisture levels. After pre-defined days (1, 5, 10, 15), the soil moisture content and proportion of eggs hatching to larvae under the different settings were assessed. The resulting relationship between soil moisture level and egg survival to larvae stage are fitted to Eq. 18 below.

$$H = \frac{1}{1 + e^{-a.R_0(m - b.R_0)}} \qquad (18)$$

where H is the age-adjusted larval hatching success of eggs under moisture level, m_{std}, which is computed as the standardized anomaly of experimental soil moisture conditions, m; and a.R is the sensitivity of eggs to moisture and b.R is the mean moisture level at which 50% survivorship is observed. The value of m used in Eq. 18 above is derived from the logistic function below (Eq 19) relating soil moisture content left given the length of the experiment (J. I. Shililu et al. 2004).

$$m = m_0 e^{-\lambda d} \qquad (19)$$

where m_0 is set to the known moisture content (20%) at the start of the experiment (d=0) and λ is the moisture loss rate during the experiment and is estimated by least-squares as 0.1028 (99% CI= 0.0903 – 0.1153), with R (Pearson Correlation) = 0.9888.

Finally, adjusting for the effects of aging on egg survival (J. I. Shililu et al. 2004) given the length of days under desiccation, survivorship due to soil moisture levels is defined as $H = H_0^{1/d}$, where H_0 is the observed proportion of anopheles eggs hatching following d days of desiccation. Using least-square fitting on the Eq. 18 relating H and m, $a.R_0$ = 0.3296 (99% CI=

0.0137 – 0.6455), and b.R_0 = -2.980 (99% CI= -5.7167 – -0.2425), with R (Pearson Correlation) = 0.7514. Based on preliminary analysis from malaria simulations on select sites showing poor fitting, the bounds of uncertainty on *a.*R_0 and b.R_0 are slightly relaxed to 0 – 1, and -5 – 5, respectively to account for the limited range in the anomalous moisture conditions to which experimental mosquitoes were exposed.

1.7 Supplemental figures

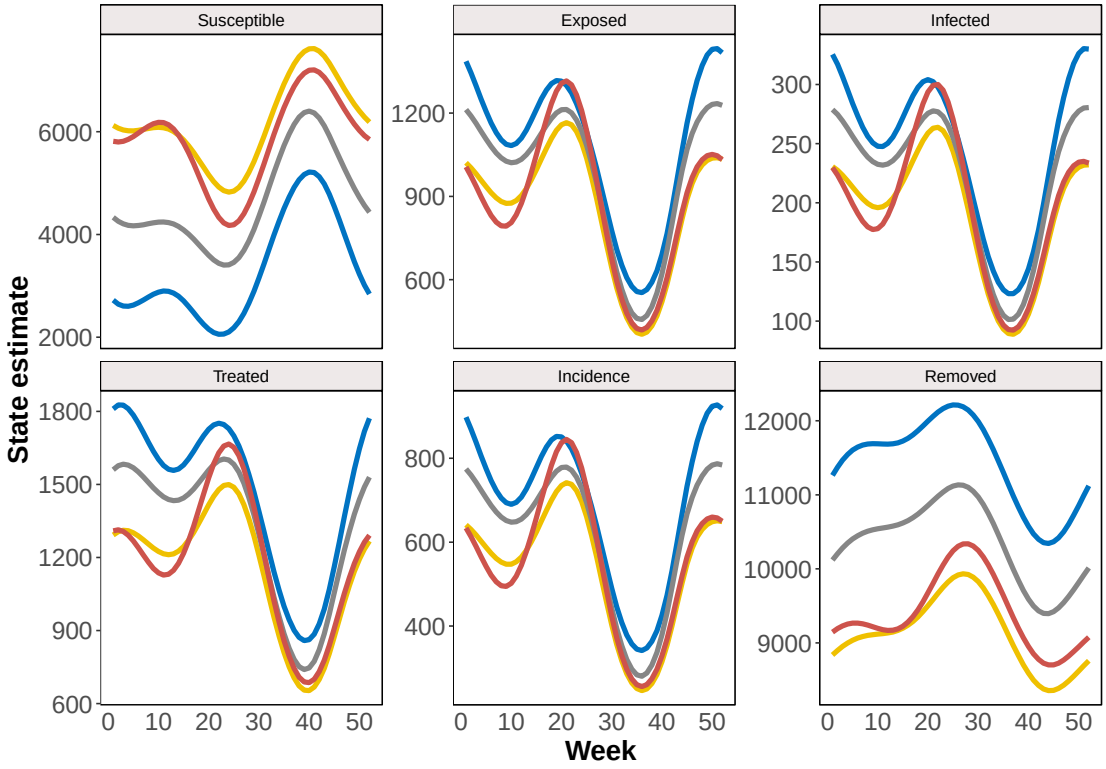

Figure S1. Averaged seasonal dynamics of state variables of the model system. State estimates are shown for Kibungo (blue), Gitwe (yellow), Kirinda (grey) and Rutongo (red).

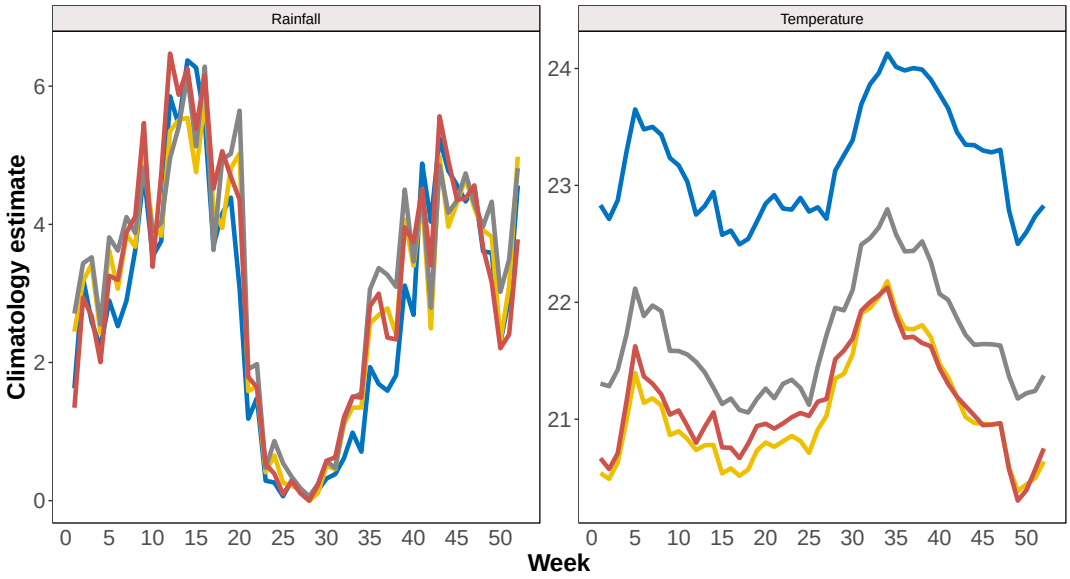

Figure S2: Seasonality of weekly climatology of rainfall and temperature (CHIRPS and CHIRTS). Kibungo (blue), Gitwe (yellow), Kirinda (grey) and Rutongo (red).

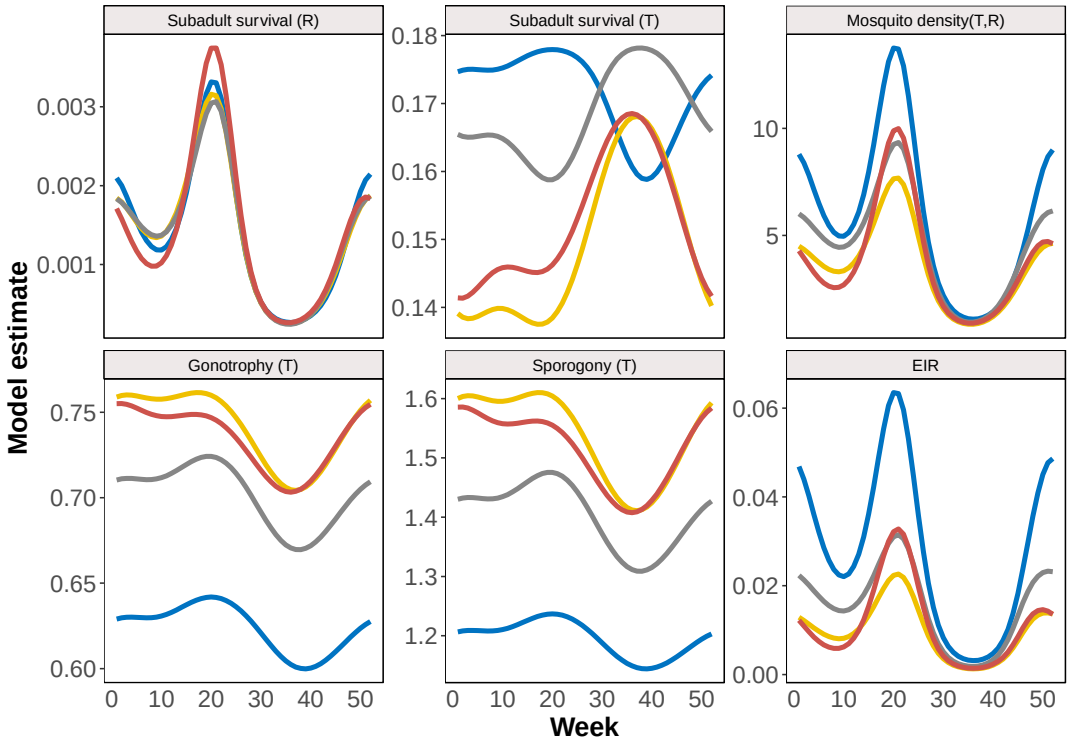

Figure S3. Average seasonality of entomological parameters from the top 10 malaria models. Rainfall (R) and temperature (T) modulated parameter values of the EIR are shown for Kibungo (blue), Gitwe (yellow), Kirinda (grey) and Rutongo (red). All parameters are in weekly units and rates.

Chapter 2: Model inference and dynamic simulation

In this chapter, the climate-driven malaria transmission model developed in Chapter 1 is paired with a data-assimilation technique that utilizes observed malaria incidence data for state variable optimization and inference of transmission parameters. This combined model-inference system enables dynamic simulation of interannual malaria transmission at the local level throughout Rwanda. This model-inference system is validated against observed malaria incidence, and parameters of the optimized model are externally validated against existing estimates of malaria entomology and epidemiology from other studies.

2.1 Background

Every year, malaria infects more than 200 million people and causes about 400,000 deaths (World Health Organization 2019). More than 90% of this burden of disease is borne by individuals in sub-Saharan Africa, most of whom are children and pregnant women (World Health Organization 2019). Global efforts to combat the disease have led to sharp declines in rates of malaria deaths; however, malaria incidence has decreased at a slower rate (World Health Organization 2019). Understanding the local drivers of transmission and conditions promoting exposure to the malaria vector are important for effectively controlling the spread of malaria.

The malaria parasite is transmitted to individuals by infected female *Anopheles* mosquitoes. The population dynamics of these vectors, like all insects, are moderated by ambient conditions such as rainfall and temperature (M. N. Bayoh and Lindsay 2004; 2003). Additionally, temperature influences transmissibility of the malaria parasite (Shapiro, Whitehead, and Thomas 2017; Eling et al. 2001b). Recognition of these effects of climate has led

to the formulation of explicit and implicit mechanistic climate-based models to elucidate the role of local conditions on mosquito populations and malaria transmission.

However, existing lower dimension process-based models of malaria have relied on indirect predictors of vector dynamics, such as temporal seasonality or interpolations of rainfall/temperature, to simulate malaria dynamics. While this is an effective approach to limiting model complexity and assumptions on vector interaction, to enable capture of malaria dynamics, the specific influence of environmental conditions on relevant vector and parasite ecology is obscured. Meaningful interpretation of climate variability within these models is also compromised.

The climate-driven malaria model framework, developed in the previous chapter, leverages the direct relationships between climate and the malaria vector and parasite to implicitly express the force of transmission through the Entomological Inoculation Rate (EIR). This EIR-model framework is combined with Bayesian inference method– Ensemble Adjustment Kalman Filter (EAKF), in the sections below, to evaluate the model's ability to reproduce local transmission over a four-year period, across 42 regions in Rwanda. Parameters of local transmission are compared against existing estimates of parameters of malaria to externally validate the implicit process-based malaria model. In addition, the EIR-based framework directly investigates the relative significance of the diverse pathways, including mosquito feeding behavior, parasite inoculation, mosquito development and survivorship, through which climate influences local malaria.

2.2 Materials and Methods

2.2.1 Simulation of malaria incidence

The EIR-model developed in Chapter 1 is combined with data assimilation for inference and simulation of local malaria transmission dynamics in Rwanda. Briefly, the transmission model explicitly tracks transmission in human hosts, and divides the population into individuals that are susceptible (S), exposed (E), infected (I) treated (T) and recovered (R) states, in a SEIRS compartmental style model. Flow of individuals across the system and through different states of transmission are determined by an average rate defined from parameters of human demography and malaria epidemiology (see supplement, Table S1). Interaction between vectors and hosts in the system are implicitly represented through the EIR, which is modulated by various climate-mediated vector and parasite ecology to derive a climate-informed force of infection.

2.2.2 Data and study region

Malaria data used in this study were acquired from the Rwanda, Ministry of Health (MoH) and are publicly available via the Rwanda Biomedical Center (RBC) web portal (Ministry of Health 2016). In an effort to improve control of malaria transmission and lower the burden of malaria, Rwanda established improved reporting and laboratory testing practices for suspected malaria and other infectious diseases beginning in 2011, as well as greater Insecticide-treated bed net (ITN) coverage, Indoor Residual Spraying (IRS), and community-level case management (National Institute of Statistics of Rwanda 2012; 2015b; Ministry of Health, Rwanda 2017). From the health repository, weekly parasitologically-confirmed malaria incidence reported during 2016 to 2019 for 42 public health catchment areas was obtained. These

datasets were used to train the climate-malaria model in conjunction with data assimilation approaches for each catchment site.

Weekly rainfall (2016-2019) and temperature (2006-2016) data were obtained from the publicly available University of California, Santa Barbara Climate Hazards Group InfraRed Precipitation and Temperature with Station dataset (CHIRPS and CHIRTS) products (Funk et al. 2015; 2019). These data were then re-gridded to match each catchment site. Due to a lack of up-to-date data, weekly temperature averages derived from the 2006-2016 CHIRTS data were used to drive the climate-malaria model in conjunction with contemporaneous weekly CHIRPS rainfall estimates.

2.2.3 Model inference system

To simulate malaria transmission and infer model parameters, the climate-malaria model is paired with malaria incidence data using a data assimilation method for state-space models: the Ensemble Adjustment Kalman Filter (EAKF). Using Bayes' Rule, the EAKF optimizes current model parameters and state variables, so that the first and second moments of the currently observed model state (i.e. incidence, $\mu EI*E$) align with those of the observed incidence data (Anderson 2001; Karspeck and Anderson 2007). Various process-based infectious disease models have been optimized using EAKF and have demonstrated reasonable fit to data and parameter convergence under synthetic testing (DeFelice et al. 2017; Shaman et al. 2013a; Shaman and Karspeck 2012; W. Yang, Karspeck, and Shaman 2014). Further assessment of the EAKF performance in accurately estimating parameters of the malaria transmission model under synthetic testing is described (see supplement).

An ensemble of 300 simulations with parameter values (D, μRS, μEI, a.R, b.R, qR and s) and initial state estimates (S_0, E_0, I_0, T_0, R_0) randomly drawn from uniform distributions, U (a, b), in which a and b indicate lower and upper boundary values (Table S1), is used to initialize the model-EAKF system. In iterated filtering, the EAKF repeatedly assimilates the same time series (Pei et al. 2018) in a stepwise approach in order to improve convergence to more probable parameter and state variable solutions. Specifically, starting from time *t =1*, the EAKF uses observation at t=1 to update prior ensemble members into posteriors. To assimilate the next observation, the EAKF system is re-initialized from t=1 using these same posteriors parameters as priors, filtering observations again from t=1 to t=2 and generating new posteriors. The EAKF-model system continues this recursive filtering and assimilation of observed data in a growing, stepwise fashion, until the final observation, t=208, is assimilated, producing the filter estimates for the first iteration. A total of 10 iterations were performed using the observed time series, with subsequent iterations initialized with ensembles drawn from N (u, sigma) of the previous iteration. The annealing factor α_i used in computing sigma for each iteration *i*, is defined as follows:

$$\alpha_i = \left(1 + \frac{0.5}{(1+i)^{0.75}}\right) \qquad (18)$$

During data assimilation, divergence of the EAKF system from observed data can occur. To limit this, the variance is inflated (3%) and the prior ensembles are randomly re-probed (5%) before each filter update (Karspeck and Anderson 2007). Even with measures in place to prevent filter divergence issues, it was observed that assimilation of periods of anomalously low malaria activity typically in the later years of the study resulted in failure of EAKF filter. Among the explanations considered for these failures was the absence of data on intensified malaria control deployed across Rwanda, particularly in the last years of the study (Ministry of Health, Rwanda

2017; U.S. President's Malaria Initiative 2018a; 2019a). To ensure that the model-EAKF system is properly constrained by the data at hand, the loglikelihood (ll_t) of the full timeseries following each update is evaluated to track filter failure (Eq 19). Filter failure was heuristically defined as a 5% departure from the current maximum loglikelihood. If this condition is violated, assimilation of an observation that results in massive failure is skipped and the prior is integrated forward to the next observation. The loglikelihood is

$$ll_t = -\frac{n}{2}\ln 2\pi - \frac{n}{2}\ln \sigma^2 - \frac{1}{2\sigma^2}\sum_{j=1}^{n}(x_j - \mu)^2 \qquad (19)$$

where x is the reported malaria incidence at week *j*; μ is the ensemble mean and σ the ensemble standard deviation of malaria incidence simulations for week *j*, generated from posteriors following updates at time *t.*

Inferred parameter values and uncertainty are reported as the mean and 95% credible Interval (CI) of the posterior ensemble from the final iteration. Using these mean and 95% CI values, together with rainfall and temperature data for each year, the transmission model was integrated forward to estimate the true state of observed malaria incidence and the uncertainty of that estimate. Coefficient of Determination (R^2) and Mean Absolute Relative Error (MARE) assessed agreement between model simulated incidence by the model-EAKF system and observed data. Similarly, model-EAKF inferred parameters was compared to prior estimates from other studies.

Additionally, analyses using synthetically generated incidence data evaluated the capability of the model-inference system to capture underlying parameters of a synthetic transmission. Estimated parameters inferred by the model-EAKF system are then compared to the parameter values used to generate the synthetic data (see supplement). All simulations and analyses were conducted in R statistical software (R Core Team 2019).

2.3 Results

2.3.1 Model simulation of interannual and seasonal malaria

The malaria model system captures the seasonal dynamics and some of the interannual variability observed in malaria at aggregated province (Fig. 1) and public health catchment levels (supplemental Fig. S1). With model simulations aggregated at the province level as shown in Figure 1, the climate model explained 27.75 – 65.64% of malaria variability; at the finer catchment level, it captured 3.6% – 80.82% of the variability observed in malaria transmission in all sites from 2016-2019. Performance of the climate model was generally higher earlier in the study period, with a median of 43.66% and 41.19% of malaria variance explained across all sites in 2016 and 2017 respectively (Fig. 2). Model error was also lower during these seasons. Subsequent years saw diminished model fit, having a median variance of 20.47% and 16.58% explained by climate in 2018 and 2019. During these seasons, the climate model predicted more intense transmission in 2018, followed by more stable conditions during the 2019 season. In contrast, large declines of malaria incidence occurred, including a complete disruption of malaria seasonality. This disconnection between the climate-model and malaria incidence is further highlighted by the progressively dwindling association between malaria incidence and rainfall conditions within the model for most of Rwanda (Fig. 3).

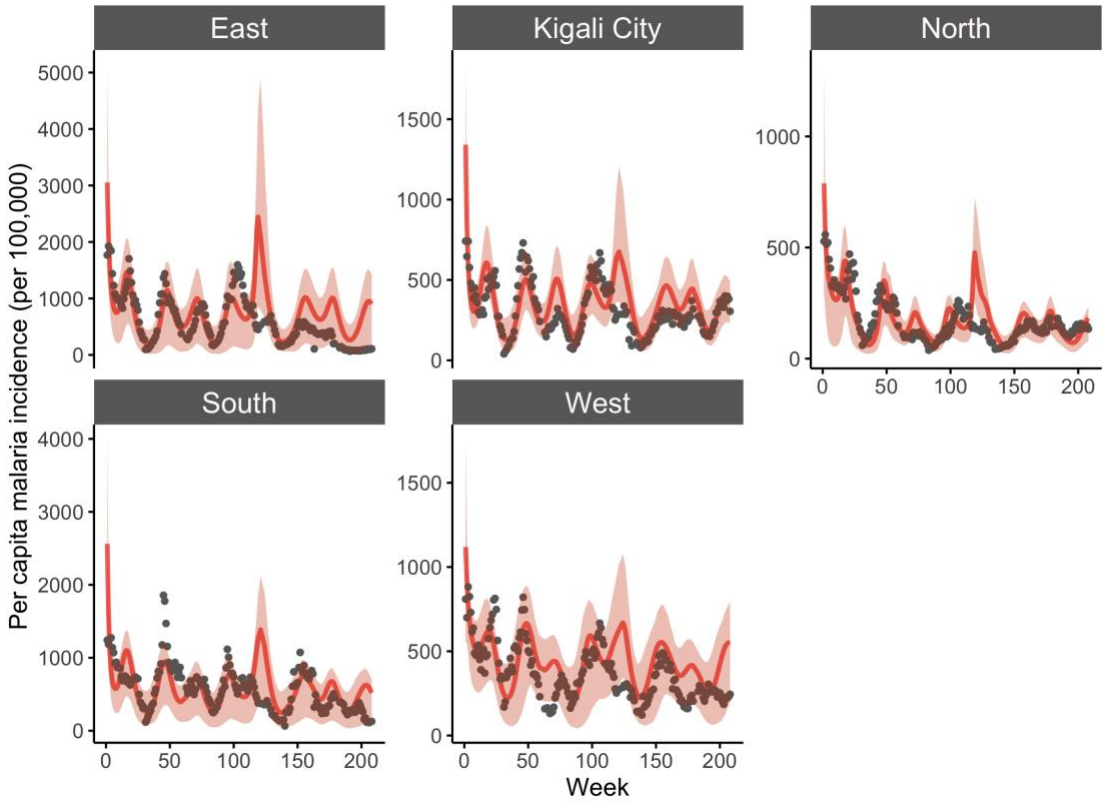

Figure 1. Model-EAKF simulated incidence of malaria at the province level from 2016-2019. The aggregated results (per capita incidence) from simulations of malaria transmission using the EAKF-model system are shown in red dots and lines, with red shading indicating the 95% CI of model estimated incidence. Reported incidence are shown as gray dots.

Because of the large disruption in the year-to-year cycle of malaria transmission, the model-EAKF system re-initialized each year to investigated whether the model could better constrain intra-annual malaria activity (Fig. 4). By simulating each year separately, malaria variability was better captured at the province level, with 41.18%–86.89% of variance explained. While at the more resolved catchment level, median variance explained rose as well– 60.84%, 58.62%, 70.77% and 52.55% in 2016-2019 respectively (Fig. 2, yellow).

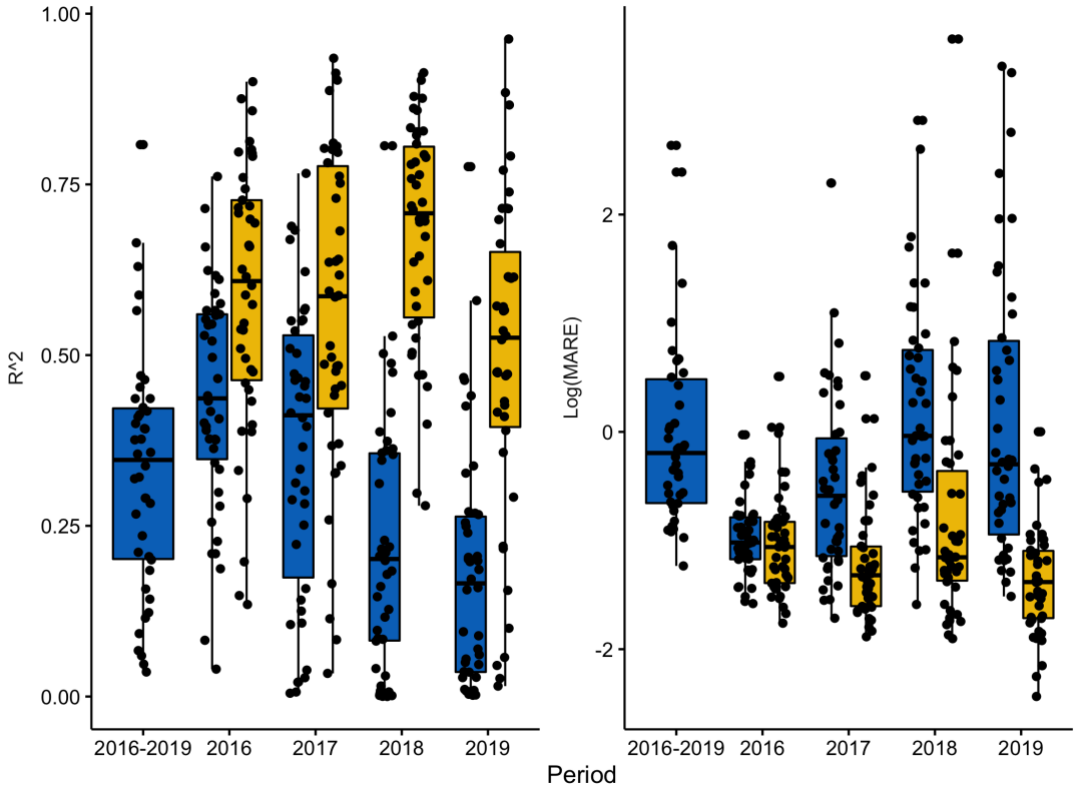

Figure 2. Fit of model predicted malaria incidence, across all 42 catchment sites, computed over various study periods, during inter-annual (light blue) and intra-annual (yellow) simulations. Boxplots are showing the median (thick line), interquartile range (box bounds), range (whiskers) of coefficient of determination (left, R2) and log-scaled Mean Absolute Relative Error (right, MARE) of different sites (jittered black dots).

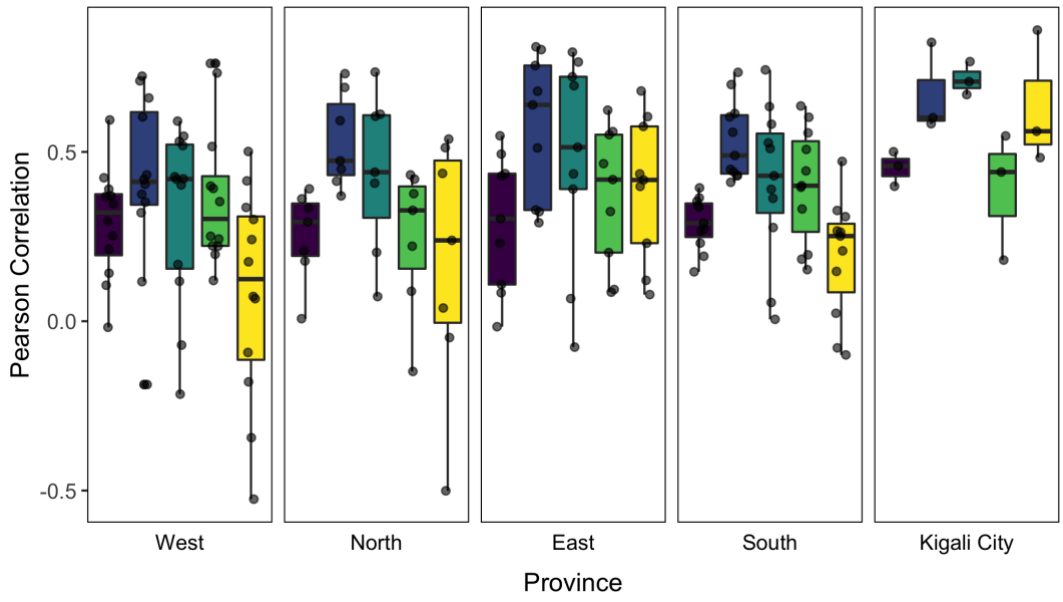

Figure 3. Correlation between malaria incidence and cumulative moisture conditions of the final model. Boxplots are showing the median (thick line), interquartile range (box bounds), range (whiskers) of the Pearson Correlation coefficient estimated for study sites (jittered black dots) over the entire study period (in purple) and for each individual year between 2016 to 2019 (in blue, green, light green, and yellow).

2.3.2 Ento-epidemiological parameters of malaria

Malaria parameters estimates were highly similar across study sites (see Table S1 for list of model parameters). For *Plasmodium falciparum* parasite incubation, which typically lasts 7–18 days before symptom onset (Boyd and Kitchen 1937), a duration of 9.17–13.08 days was inferred across Rwanda (Table 1). And across the sites, duration of parasite incubation was found to vary similarly from region to region (Fig. S3). The duration of patency for individuals recovering from untreated *Plasmodium* infections typically has an expected duration of about 200 days (W. Sama, Dietz, and Smith 2006; Bretscher et al. 2011; Felger et al. 2012; Wilson Sama, Killeen, and Smith 2004; Keegan and Dushoff 2013) to clear the parasite. Here, model estimates of malaria patency showed a wide spread among individual sites (Fig. S3). For study sites in the East, Kigali City, North, South, and West provinces, median durations of 265.59

days, 240.08 days, 231.21 days, 246.13 days and 274.85 days were estimated, respectively (Table 1 and Table S2).

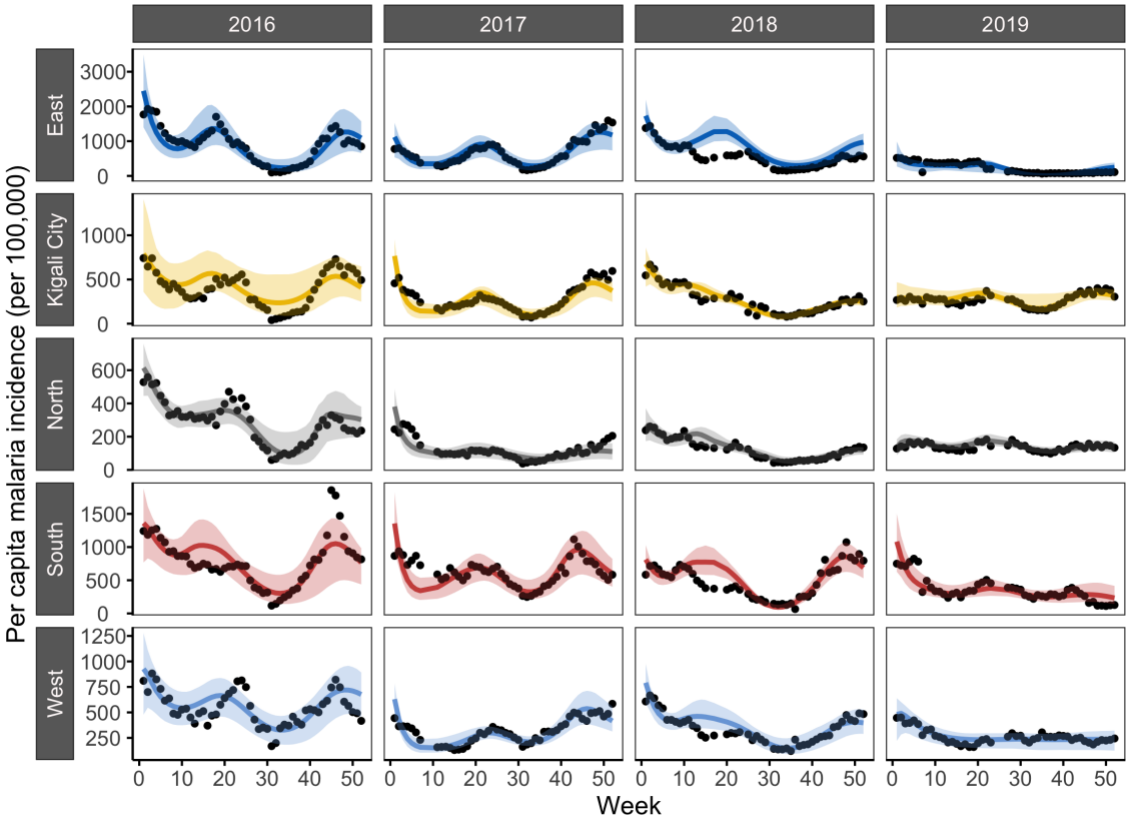

Figure 4. Incidence of malaria simulated for individual years by the model-EAKF. The aggregated results (per capita incidence) from simulations of malaria transmission using the EAKF-model system are shown in colored lines. Colored shading indicates the spread of the 95% CI of model estimated incidence. Aggregated simulated incidence for sites in East, Kigali City, North, South and West provinces are indicated in blue, yellow, grey, red and light blue. Reported incidence are shown as black dots.

Estimates of relative infectivity of patent/subpatent infections (q_R) compared to full-blown infections ranged from 0.0025– 0.4385 across Rwanda (Table S2). In the majority of the sites (12.5^{th} and 87.5^{th} percentile representing 75% of the sites), relative infectivity ranged from 0.05–0.125, close to previously estimated levels of subpatent infectivity compared to symptomatic infections (Slater et al. 2019; Tadesse et al. 2018; Kim A. Lindblade et al. 2013).

Among the regions, spread and tendency of relative infectivity rates of sites was found to vary similarly (Fig. S3).

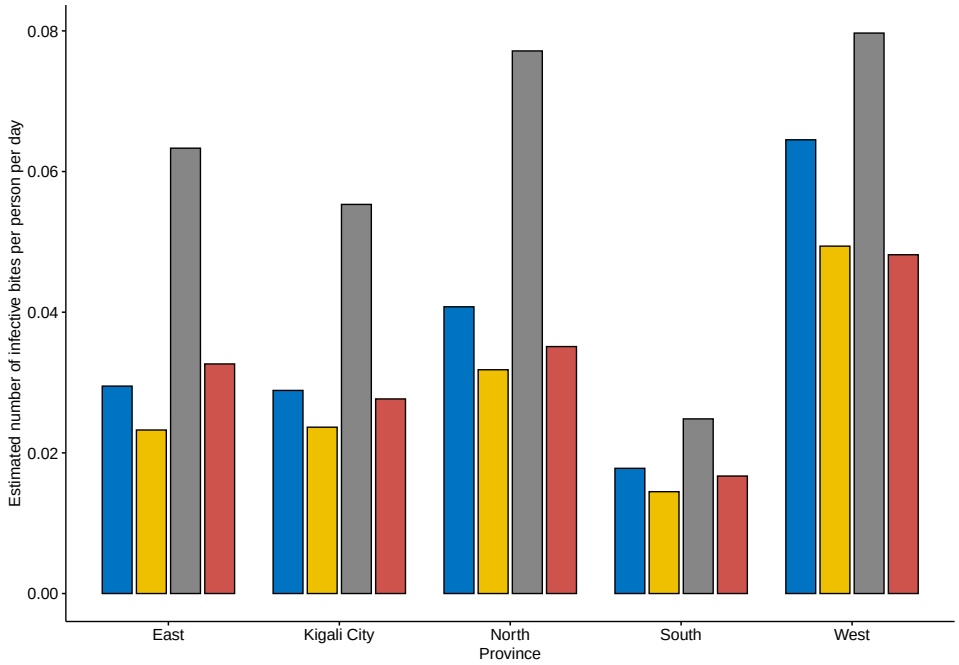

Figure 5: Model estimated annual average for the daily Entomological Inoculation Rate (EIR). Values for 2016-2019 indicated in blue, yellow, gray and red colored bars, respectively.

Additionally, estimates of the length of accumulated rainfall conditions contributing to mosquito habitat levels (D) were generally in agreement throughout Rwanda (Fig. S3). The median cumulative rainfall conditions in the preceding days found to be important for mosquito and malaria activity was 68, 81, 101, 70, and 87 days respectively for sites in the East, Kigali City, North, South, and West provinces (Table S2). In a majority of the sites, the parameter estimate for the length of cumulative moisture conditions affecting mosquito breeding, tended to vary similarly throughout Rwanda, however, some differences in site estimates were also observed (Table S2).

Sensitivity of subadult mosquitoes to moisture conditions (a_R) estimated for sites was found to be within similar ranges throughout Rwanda (Fig. S3). Estimated sensitivity ranged from 0.0555– 0.2286, and a slightly narrower range (0.0849–0.1883) was observed in a majority of the sites (75%). Mean moisture anomaly (b_R) also showed a high tendency of being in ranges similar across Rwanda (Fig S3). Inferred estimates across most sites showed a narrower concentration around 4.

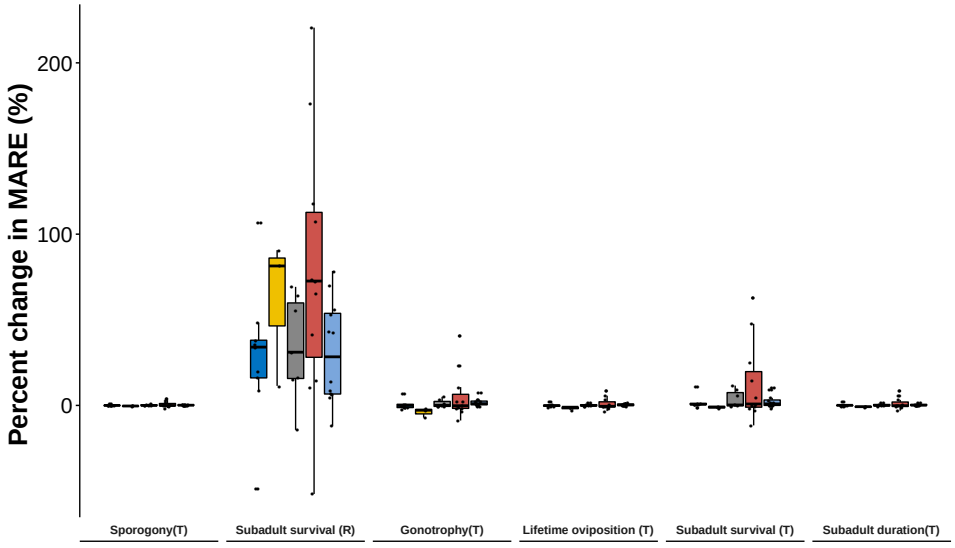

Figure 6. Percent change in MARE of simulated malaria when individual entomological functions are decoupled from climate. A function is decoupled from temperature (T) or rainfall (R) by setting the function to a constant value, determined by the annual temperature or rainfall for each year. Change in MARE observed for site located in East, Kigali City, North, South and West provinces are shown in blue, yellow, grey, red and light blue.

Model estimates of the population scaling factor (s) also revealed that generally a small proportion of the total population comprised the model population (Fig. S3; Table S2). Effective population sizes consisting 0.15–0.35 of the census population (N) were found for most sites (i.e., 75% of sites). However, some sites, specifically, in the South and East regions, had effective population sizes representing 0.5 or more of the census population. In contrast, sites

located in the North and West provinces typically showed the least estimated proportion of the census population involved in the transmission model (Table S2). With relatively lower census numbers (National Institute of Statistics of Rwanda 2015b), this indicates a smaller number of people generally involved in transmission the North and West than in the South and East provinces.

Table 1: Range of the mean posterior estimates for two epidemiological parameters of malaria. μ_{EI} is the average duration of parasite incubation in humans and μ_{RS}, the average duration of subpatent infection.

Province	Posterior estimate (in days)	
–	μ_{EI} median (range)	μ_{RS} median (range)
East (N=9)	10.58 (10.39 -13.08)	265.59 (140.74-345.08)
Kigali City (N=3)	11.22 (11.14 - 11.67)	240.08 (238.85-281.20)
North (N=7)	11.05 (9.65-12.08)	231.21 (124.22-344.36)
South (N=11)	10.68 (9.17-12.72)	246.13 (151.62-348.75)
West (N=12)	10.64 (9.56-12.26)	274.85 (145.01-355.16)

N = number of sites located within a province.

Estimates of entomological exposure (EIR) were relatively stable from year-year, though the 2018 transmission season was expected to have a wide-spread rise in entomological activity (Figure 5). This was in accordance with the intense transmission predicted for 2018 due to heightened environmental capacity and suitability for mosquito survivorship and development (see supplement, Fig. S2). On average, individuals were estimated to experience 0.018 – 0.06 infective bites per person per day (bpd) in a year across Rwanda (Figure 5) within the range of field estimates (0.0067 – 0.11 bpd) reported in five districts across the East and South provinces during 2016-2019 (U.S. President's Malaria Initiative 2017b; 2018b; 2019b). Additionally, estimated entomological exposure varied regionally across Rwanda. Populations in the North and West experienced the highest EIR (Figure 5), even though malaria burden is historically heaviest

in the East and South Provinces (National Institute of Statistics of Rwanda 2015b; Ministry of Health, Rwanda 2017). Similarly, sites in these communities were predicted to have higher mosquito-survivorship due to more suitable surface moisture conditions than the rest of the country (see supplement, Fig. S2).

Malaria transmission within the climate model is regulated through a number of pathways. Analyses indicate that malaria dynamics were most affected by rainfall regulation of sub-adult survivorship. Without rainfall-modulated subadult development, model fitness decreased across sites, with MARE climbing by more than 40% in the final model (Fig. 6). Temperature-regulated conditions such as parasite EIP, biting rate (a) and development rate (P_{EAT}) contributed to model fitness but played a far less substantive role constraining the model fitting. The absence of these temperature-forced pathways only slightly decreased model fitness by about 3% maximum.

2.4 Conclusion

Temperature and rainfall are major drivers of malaria vector population dynamics and parasite transmission. The effects of these meteorological conditions on the ecological life traits of the malaria vector and parasite make them important for accurately describing transmission risk. Several malaria modeling studies have demonstrated that malaria and other mosquito-borne diseases indeed can be accurately described using an implicit force of transmission that depends on indirect climate predictors of mosquito dynamics (Laneri et al. 2010b; Bhadra et al. 2011; Li et al. 2019). In these instances, implicit models have used highly collinear variables, like observations of mosquito density, temporal seasonality and smoothing interpolations of climate to represent mosquito force of transmission. However, the present study finds that lower

transmission models of malaria are capable of reproducing seasonal and inter-annual malaria activity, by leveraging the direct ecological role of climate without need for explicit representation of vector population and transmission dynamics. The developed model structure not only captures malaria across the varied climate regimes of Rwanda but also enables formal investigation of the role of climate in mediating risks of malaria transmission.

Over the long term, the climate model reproduced malaria incidence fairly well. However, some notable disagreement, specifically in the last two years of study, between observations and model simulations was evident. Throughout Rwanda, a varied connection between climate and malaria activity is observed, with weak connections to climate detected and linked to declining transmission in many locations, over certain periods. This observed disconnection suggests action of external factors disrupting vectorial capacity and precluding transmission. For example, a nationwide increase in transmission was predicted following initial years of high agreement between climate-signaled transmission and malaria incidence. However, across Rwanda declines and disrupted seasonal activity were reported. Indeed, starting in 2018, several high malaria burden regions in Rwanda began intensified malaria control in an effort to recover gains toward malaria elimination lost due to relaxed malaria control (Ministry of Health, Rwanda 2017; U.S. President's Malaria Initiative 2018a; 2019a). Malaria intervention and vector control are highly effective measures for targeting and attenuating entomological exposure risk. Thus, re-adoption and adherence to routine blanket indoor residual spraying (IRS) and insecticide treated nets (ITN) campaigns could have drastic suppressed seasonal malaria incidence and low entomological inoculation rates reported in the last two study years across Rwanda (U.S. President's Malaria Initiative 2018a; 2019a).

The absence of these exogenous effects in the climate-forced model could explain the lack of agreement between simulations and observations. Widespread ITNs coverage and frequent usage act against malaria incidence by decreasing the proportion of infected and susceptible individuals available for potentially infective contacts with vectors. This shrinkage in the number of available hosts bottlenecks parasite circulation and further weakens the malaria force of infection. Similarly, the increased adult female mosquito mortality rates dilute the vectorial capacity and mosquito oviposition as rates of bloodmeal in the female adult population plummet due to ITNs (Kawada et al. 2014; Charlwood and Graves 1987). Changes to mosquito gonotrophy may also decrease breeding rates because of ITN repellence of mosquitoes. Resistant *Anopheles* females or those behaviorally adverse to insecticide treated bed nets are likely to experience an increased period of time between bloodmeal acquisition and egg development, as they spend more time and calories seeking hosts that are less accessible, and less time acquiring bloodmeals and laying eggs (Hauser, Thiévent, and Koella 2019). Additionally, as more mosquitoes resort to feeding on non-human hosts in the vicinity, which has been noted to occur among *Anopheles gambiae* (Sinka et al. 2010; Tirados et al. 2006; Antonio-Nkondjio et al. 2006; Awolola et al. 2005), and also proposed as a potential control tool (Donnelly et al. 2015; Asale et al. 2017), the force of infection is diluted further.

IRS further contributes to reducing transmission pressures by targeting the resting behavior of blood-fed *Anopheles* mosquitoes. Mosquitoes that manage to evade ITNs and acquire bloodmeals from human or non-human hosts are eliminated by IRS, further shrinking parasite exposure and mosquito breeding rates. Unfed populations of *Anopheles* mosquitoes are also likely to decline, as a result of resting on IRS applied surfaces, leading to further widespread decreases in adult populations.

Indeed, without data on these strong external forces on vector density and entomological activity that change vector-host contact rates, the model inference system is not capable of capturing associated changes to model states and parameters. As a result, model projections may fail to reflect the dramatic declines or disruptions in malaria activity that is contrary to the climate-forced constraints on the system.

In addition to capturing local dynamics, the climate-driven model also was able to identify parameters best describing local malaria that are similar to previous malaria estimates, lending more external validity to the model. Malaria in Rwanda, like in all of sub-Saharan Africa, is largely dominated by infections from species of the *Plasmodium falciparum* parasite (World Health Organization 2019). *Plasmodium falciparum* infections are characterized by short incubation periods before symptom onset as well as relatively short periods of patency for untreated infections compared to other malaria species. Model estimates of *P. falciparum* incubation only varied slightly across Rwanda; however, malaria patency estimates were less uniform. This variation in susceptibility could be a result of differences in malaria burden, which may complicate acquired immunity across populations (Felger et al. 2012; Filipe et al. 2007; Gupta et al. 1999).

The intensity of malaria transmission is also not uniform across Rwanda, but varies from region to region (National Institute of Statistics of Rwanda 2015b; Ministry of Health, Rwanda 2017). The level of parasite circulation within a community alters the rate of repeated exposure to malaria parasites and expectedly may lead to differential rates of susceptibility and acquired immunity observed within a population (Keegan and Dushoff 2013; Filipe et al. 2007). Additional population factors at play include community age structure, level of general health,

and migration (Felger et al. 2012; Filipe et al. 2007; Gupta et al. 1999), which may lead to heterogeneity of susceptibility and acquisition of malaria immunity across study populations.

The malaria model framework also allowed approximation of the EIR– an indicator of the intensity of transmission. Model predicted levels of EIR (0.018 – 0.06 bpd) were low compared to levels in other neighboring malaria endemic countries (Hay et al. 2000). Other researchers using empirical relationships (0.0013 bpd) and dynamic simulation (0.006 bpd) (Penny et al. 2015) have also estimated a less intense transmission in Rwanda. Based on field studies (U.S. President's Malaria Initiative 2017b; 2018b; 2019b; Hakizimana et al. 2018), Rwanda indeed has low but widely variable levels of malaria intensity. A comprehensive entomological study (Hakizimana et al. 2018), consisting of malaria sentinel sites spanning the country, indicated EIR ranging from 0.0027–0.9014 infective bites per day throughout Rwanda. While model estimates are in line with the field estimated levels, they suggest a lower range of malaria intensity. However at the lowest spatial level (i.e. catchments), where populations are less aggregated, model estimates of EIR rose closer to observed entomological data (Hakizimana et al. 2018).

Across the diverse mountainous geography of Rwanda, a non-uniform rate of entomological exposure was found among the five provinces, but not as fully expected. With most lowlands situated in the South and East provinces, climate suitability for malaria is thought be highest because of improved vector survivorship and parasite transmissibility brought on by warmer conditions. And in the highlands located mostly in the West and North, climate suitability for malaria is expected to be lower. In contrast, model estimates suggest higher EIR levels in the less warm but wetter West and North regions. And lower levels were observed in the East and South, where rates of malaria incidence are typically higher (National Institute of

Statistics of Rwanda 2012; 2015b; Ministry of Health, Rwanda 2017). It is unclear whether rates of reporting specifically for malaria vary differentially between the areas, even though rates of treatment seeking for fever are similar between the regions in question (Ministry of Health, Rwanda 2017). However, increased population-level immunity due to a higher malaria burden in the South and East could produce milder malaria episodes (Gupta et al. 1999; Langhorne et al. 2008), differentially impacting treatment seeking behavior. As a consequence, a lower entomological exposure could be inaccurately inferred for the region. In addition, the high EIR rates in the West and North may be explained by a more focal transmission suggested by the smaller effective transmission population size estimated for regions in the North and West. Indeed, conditions are relatively cooler in these parts and could limit the geographical range of malaria activity relative to similarly low lying altitude areas (Lyon et al. 2017; Shapiro, Whitehead, and Thomas 2017; Baidjoe et al. 2016). The lower denominator population from the pockets of sub-communities with more climatically suitable environments combined with comparatively low population-level immunity (Ernst et al. 2006; Brooker et al. 2004; Baidjoe et al. 2016; Langhorne et al. 2008) could result in higher EIR rates, while much of the high-altitude populations could remain generally less involved due to increasingly lower parasite suitability.

An important benefit of the model developed here with direct climate-mediation of transmission pressures is the ability to examine the relative contribution of climate-driven vector ecology on malaria risk. The model form allows interrogation of malaria vector dependency on environmental conditions. In this study, rainfall-regulated sub-adult survivorship proved to be the entomological factor most impactful to local transmission, well above the temperature-regulated vector and parasite dynamics represented in the transmission system. Note that temperature acting on adult mortality was not assessed due to the lack of temperature-regulated

adult mortality in the model. Thus, the system may underestimate the role of temperature, as adult mortality is recognized to be a major driver of malaria vectorial capacity (Macdonald 1956; Brady et al. 2016; 2015). However, among the temperature-dependent ecology evaluated, seasonal effects of parasite transmissibility, sub-adult duration and survivorship or feeding activity were slight and lead to negligible impacts on the seasonal dynamics of malaria transmission. The effect of rainfall on malaria vectorial capacity in the region is highlighted further by the distinct dynamics of malaria seasonality, which correlate with the two rainy seasons. This finding is in agreement with several other studies (Patz 1998; Abiodun et al. 2018; Adeola et al. 2019; Ebhuoma and Gebreslasie 2016; Thomson et al. 2005) that have linked rainfall and soil moisture conditions in East and sub-Saharan Africa to *Anopheles* mosquito activity and malaria transmission more than to temperature. The environmental carrying capacity for malaria mosquitoes (i.e., the population size that resources in the environment can support) are thought to be defined by moisture conditions (White et al. 2011; Yé et al. 2009). *Anopheles* mosquitos begin their life in water and continue developing in aquatic environments until adult emergence. The formation and stability of these rain-fed, short-lived water pools are likely to be more impacted by rainfall variability than temperature, which is near optimal levels for mosquito development throughout the year for much of Rwanda.

This study demonstrates that seasonal and interannual malaria incidence can be relatively accurately reproduced by combining the climate-based malaria transmission model with a data-assimilation system. This model-inference system also enabled estimation of entomological and epidemiological parameters of malaria transmission, with inferred values highly were similar across the region and comparable to estimates from prior studies. The environmentally EIR-driven modeling framework also identified important climate relationships within parasite and

vector dynamics that dominate seasonal malaria variability across local populations in Rwanda. Future studies will evaluate the benefit of using similar climate-forced dynamic model for forecasting local malaria incidence and will also assess the predictive utility of the entomological model framework in supporting ongoing local malaria control efforts in sub-Saharan Africa.

2.6 Supplemental text

2.6.1 Synthetic testing

Here, the identifiability of the model-EAKF inference system using 'synthetic' observations generated with the model in free simulation is assessed.

2.6.1.1 *Synthetic transmission*

Fifteen sets of prescribed model parameters and initial state conditions were used as truths in this experiment. These sets of parameters (Table S1) were originally selected from among a randomly generated set (N=1000) for freely simulated incidence that were highly similar to seasonal malaria in Kibungo and for having attack rates within typical ranges observed in the Rwanda malaria data (2016-2019, across all sites). Using rainfall and temperature data from 2016 for the Kibungo catchment site, along with the 15 sets of parameters, the climate-model was integrated starting from week 1, at a weekly time step, for 52 weeks under free simulation. Weekly incidence of malaria (μ_{EI}*E) during synthetic transmission was recorded.

2.6.1.2 *Data assimilation and inference*

For data assimilation using the EAKF, observational error variance (OEV) of the data must be defined. For these synthetic experiments (and for reported malaria incidence data),

observability of weekly data is defined assuming the malaria data are overdispersed and follow a negative-binomial specification:

$$OEV_t = \gamma_t + \frac{\gamma_t^2}{\gamma_t^k} \quad (1)$$

where γ is the true incidence at time t, and k is the common rate of dispersion as γ changes over time. For the synthetic analysis, k was set to a constant value of 0.5. To generate observed incidence for each true incidence, five realizations are taken from NB ($\gamma_t, \frac{1}{\gamma_t^k}$) and paired separately with the model-EAKF system for data-assimilation.

With an ensemble of 300 simulations from randomly drawn parameters and initial state conditions, the model-EAKF assimilates the synthetic data in an iterated approach (see main text). A total of 10 iterations over each full timeseries of synthetic malaria incidence data was conducted. The ensemble mean of the final posterior, *x*, was the estimate for each model parameter inferred. For each of the five stochastic realizations of the 'true' synthetic malaria incidence, the model-EAKF was re-initialized five times, each time with a new ensemble of 300 parameters and state variables, resulting in total of twenty-five estimates per parameter. The relative error (RE) of final parameter estimates *x* of each true parameter, inferred from realization *j*, during re-initialization *i*, is calculated as follows:

$$RE_{ij} = \frac{truth - x_{ij}}{truth} \quad (2)$$

Results from synthetic testing, shown in Fig. S4, indicate that EAKF inference system is highly capable of capturing the underlying parameters of transmission of the developed model. Regardless of the sets of true parameters, error in posteriors is substantively reduced across all model parameters, although wider variation in posterior accuracy was observed in some parameters.

2.6.2 Observation Error Variance (OEV) of malaria data

Given that true incidence of malaria across study sites is unknown, γ_t the true mean (in Eq. 1) is taken as the response at time t from a cubic spline smoothing of the full malaria timeseries for a site; and k is the common aggregation parameter for observing malaria incidence. Maximum likelihood estimates of k (Table S3) were determined for each site by numerical maximization of the negative binomial log-likelihood function (Piegorsch 1990), using batch-gradient optimization within the optim function in R (R Core Team 2019).

The OEV seeks to address variance of the true mean of observed cases, such as caused by random measurement error of the unknown mean. Systemic issues such as poor surveillance catchment and high rates of under-reporting that could lead to significant changes and variance in the measured mean are not explicitly accounted for by the OEV. Surveillance of malaria and other serious infectious diseases has significantly improved in Rwanda and have been exemplary across sub-Saharan Africa. This is owing to major government undertakings (National Institute of Statistics of Rwanda 2012; 2015b) to transform the health system, eliminate malaria, and improve healthcare accessibility, especially through the universal health insurance that enables individuals to visit and receive treatment for malaria without cost barriers (Karema et al. 2020). In addition to the regional health center, local public health facilities and health posts that make up the passive surveillance network, active surveillance are set-up through Community Health Workers (CHW) at the Village administrative level throughout Rwanda (National Institute of Statistics of Rwanda 2015b). These health personnel are specially trained to actively detect cases at the household level, to treat and report confirmed malaria cases to the regional surveillance network. The wide catchment system in place in Rwanda gave high confidence at the onset of

the study to omit explicit estimation of reporting rates or surveillance coverage. However, the effect of the spread of the surveillance network on the modeled dynamics can readily be incorporated by $\rho * \mu_{EI} * E$, where $\mu_{EI} * E$ is the true incidence of the transmission system and ρ is the rate of under-reporting, and by default set to 1 within the transmission model.

2.6.3 Water temperature (Tw) sensitivity of the malaria model

To estimate the water temperature (Tw) of breeding sites, a simple linear model as per Krijn P Paaijmans et al. 2010; A. F. G. Jacobs, Heusinkveld, and Nieveen 1998 is adopted. In the model, $T_w = k * T_{air} + \Delta T$, where *k* is the slope and ΔT is a constant >0 representing antecedent effects with a net increase in radiative energy of the breeding site. Temperature of breeding sites can be up to 6°C warmer than surrounding ambient air temperature. Additionally, the magnitude of association between T_{air} and T_w have been shown to vary from 0.5 to 0.9 (Krijn P Paaijmans et al. 2010; A. F. G. Jacobs, Heusinkveld, and Nieveen 1998), depending on size of water pool and ambient features of location. In the transmission model, *k=1* and ΔT to a constant value of 2°C. Therefore, the following analyses examine the robustness of the malaria model to changing conditions of the water temperature model. A total of 500 random combinations of k and ΔT were drawn from Latin Hypercube Sampling (LHS), with the boundary values [0,1] and [1, 5], respectively. Using the mean posterior parameter estimates from the model-EAKF system, the final malaria model for each catchment site was integrated to the end of the study period using the randomized Tw conditions. The relative change in mosquito density and root mean squared error (RMSE) in model simulated incidence assess the level of disparity between outcomes from the randomized Tw conditions and those of the optimized malaria model.

Analyses indicate that malaria incidence simulations generated by the optimized climate-based model were generally robust. Model fit to malaria incidence across the 42 local catchment sites on average did not deteriorate markedly and changes to mosquito density were moderate as values of k and ΔT varied (Fig. S5). Improvements to model fit outside the default conditions were slight on average– about 5%, occurring typically at increasingly larger values of ΔT and increasingly lower values of k.

2.7 Supplemental figures

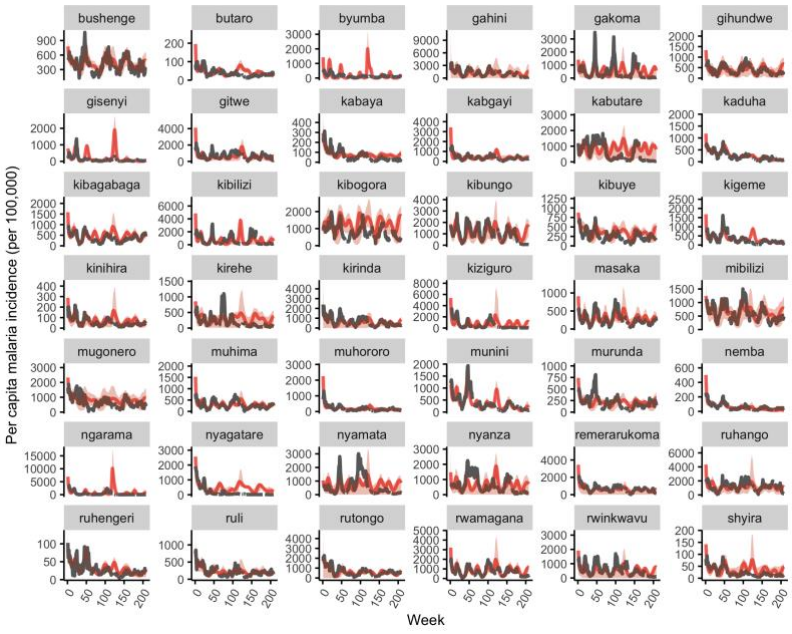

Figure S1. Model-EAKF simulated incidence of malaria from 2016-2019 for the 42 catchment sites. In red dots and lines, with red shading are per capita incidence simulations of malaria transmission and the 95% CI estimated by the EAKF-model system. Reported incidence are shown as gray dots.

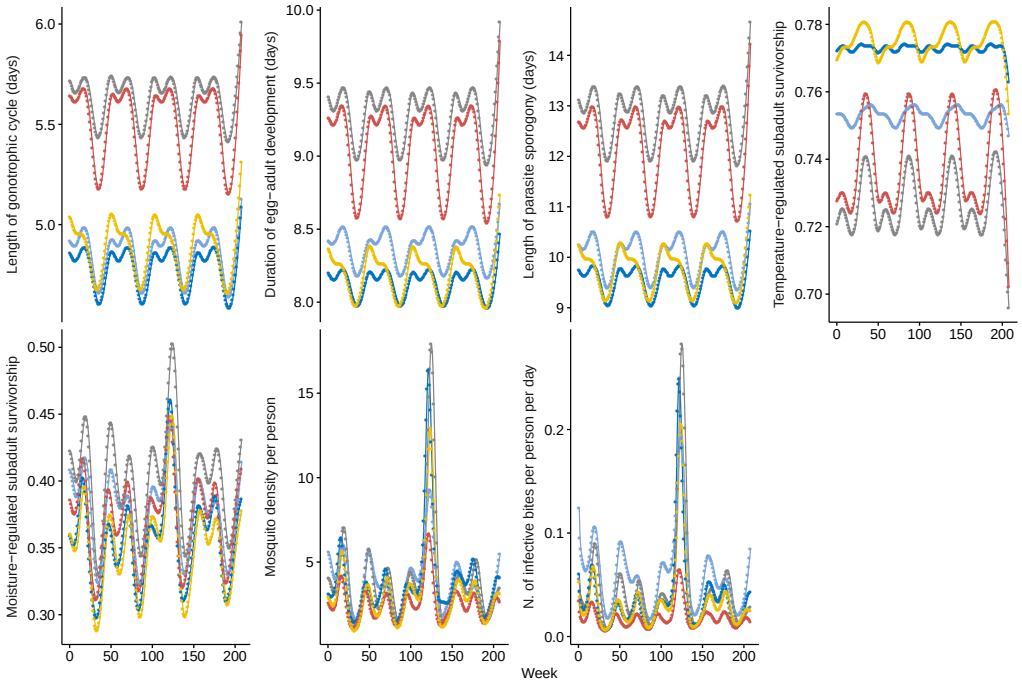

Figure S2. Mosquito development and estimated survivorship as modulated by temperature and rainfall in model simulations. Colored lines and points indicate the average estimate of duration of gonotrophy, duration of subadult development, extrinsic parasite incubation, temperature-regulated egg-adult survival, moisture-dependent egg–adult survivorship, mosquito density, entomological inoculation rate, for sites within the East (blue), Kigali City (yellow), North (grey), South (red) and West provinces (light blue).

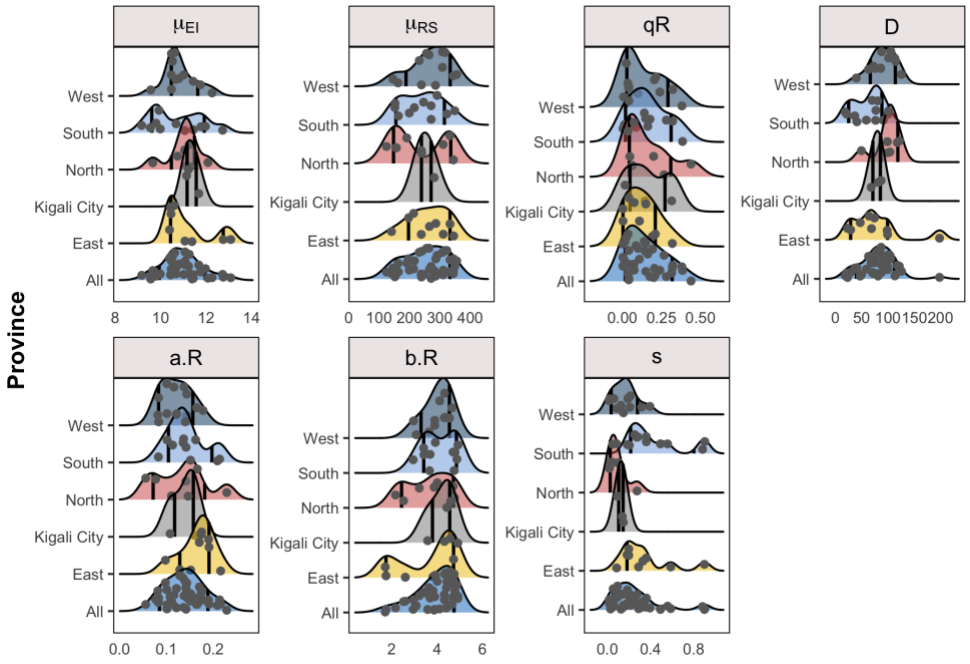

Figure S3. Posterior parameters of the malaria transmission model estimated from the EAKF-model inference system. Shaded density plots show spread of the estimated parameter values for sites in all of Rwanda (blue) and for those in East (yellow), Kigali City (gray), North (rose), South (light blue) and West (grayish blue) provinces, respectively. Jittered dots indicate the actual values, and the solid vertical lines mark the 12.5th and 87.5th percentiles, representing a majority (75%) of the sites.

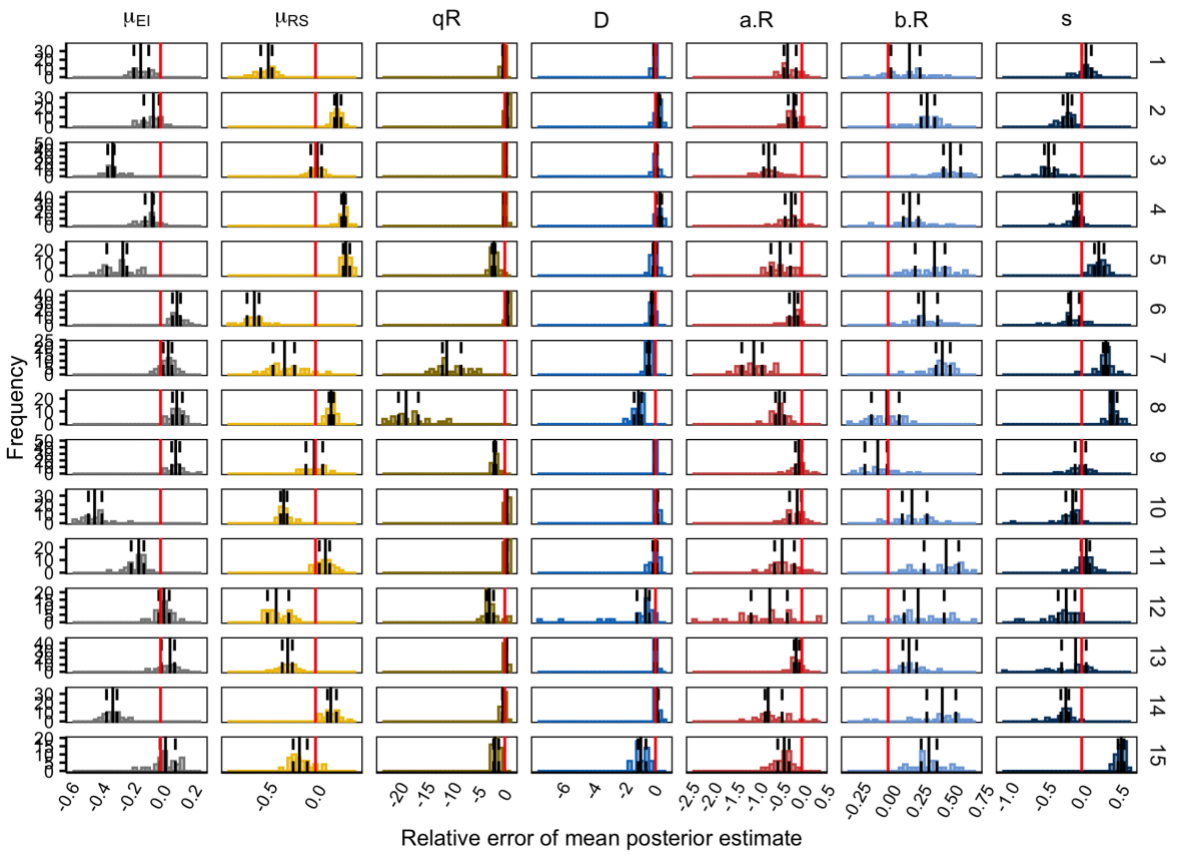

Figure S4. Relative error of mean posterior estimate of true parameters made by the EAKF system during synthetic testing. Each histogram (N=25) represents the spread of RE for each parameter (column panels) from 5 realizations and 5 re-initializations for each synthetic truth (row panels). The median RE is shown in solid blue lines, and dashed blue lines indicate the 1st (25th percentile) and 3rd quartiles (75th percentile) of the RE. Solid red line indicates zero error relative to the truth.

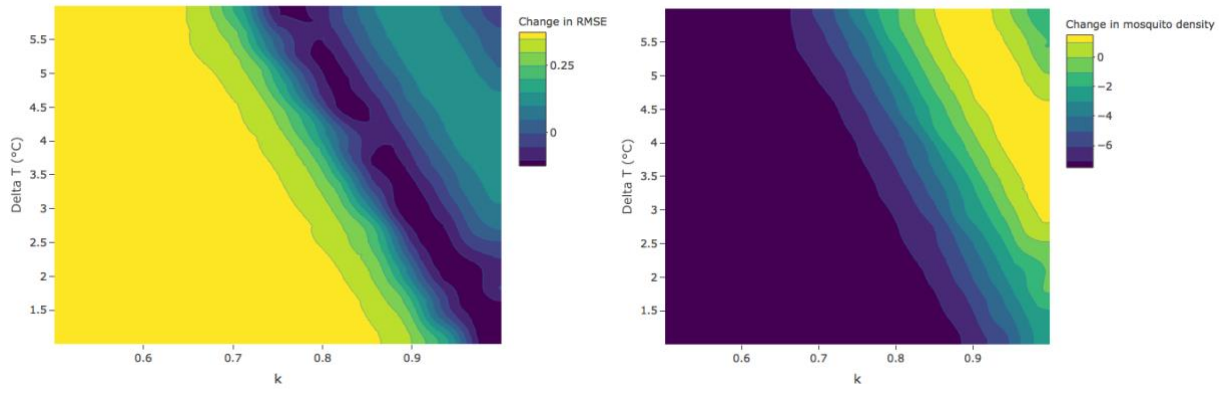

Figure S5. Contours of percent change in RMSE of malaria incidence simulations and change in mosquito density of the final climate model under various conditions of the water temperature (Tw) model. Zero indicates no change in RMSE as k, the slope and ΔT deviates from default parameters of Tw model; $Tw = k*T_{air} + \Delta T$, where k=1 and ΔT=2.

2.8 Supplemental tables

Table S1. Description and prior range of the parameters of the transmission model.

Parameter	Description	Prior ranges	Unit	Reference
μ_{BS}	Birth rate	$(57*365)^{-1}$	day^{-1}	Census
$\delta S, \delta E, \delta U, \delta T, \delta R$	Death rate	$(53*365)^{-1}$	day^{-1}	Census
μ_{EI}^{*}	Duration of parasite incubation	7 – 14	day	Lit(Boyd and Kitchen 1937)
μ_{TS}	Duration of treatment + prophylaxis	30	day	Lit(Watkins et al. 1997; Trigg et al. 1997; Kamya et al. 2007; Yeka et al. 2008; Cisse et al. 2009; Kakuru et al. 2013)
μ_{IR}	Duration of untreated infection	5	day	Lit(Drakeley et al. 2006; Zwang et al. 2009; Miller 1958; Church et al. 1997)
fT	Proportion of infected receiving full treatment	0.5	-	Lit(Battle et al. 2016)
μ_{RS}^{*}	Duration of patent/sub-patent period	120 –365	day	Lit(W. Sama, Dietz, and Smith 2006; Bretscher et al. 2011; Felger et al. 2012; Wilson Sama, Killeen, and Smith 2004; Keegan and Dushoff 2013)
P_{MH}	Probability of transmission from mosquito to human	0.5	-	Lit(Churcher et al. 2017a; Filipe et al. 2007)
P_{HM}	Probability of transmission from human to mosquito	0.125	-	Lit(Boudin et al. 1993; Jeffery and Eyles 1955; Alves et al. 2005b)
qR	Infectivity of non-clinical cases relative to clinical cases	0 – 0.5 * (P_{HM})	-	Lit(Slater et al. 2019; Tadesse et al. 2018; Kim A. Lindblade et al. 2013)
ε	Number of eggs laid per gonotrophic cycle	50	-	Lit(Hogg, Thomson, and Hurd 1996; Hogg and Hurd 1997; Lyimo and Takken 1993)
μ_M	Daily adult mortality rate	-ln 0.98	-	-
a.R*	Egg-adult sensitivity to surface moisture	0 – 1	-	See supplement in Chapter 1
b.R*	Mean anomaly of accumulated rainfall	-5 – 5	-	See supplement in Chapter 1
D*	Length of accumulated rainfall contributing to mosquito breeding	7 – 200	day	Lit(Laneri et al. 2010b; Yazoumé Yé et al. 2009; McCann et al. 2014; Lindsay, Parson, and Thomas 1998)
s*	Population scaling factor	0 – 1	-	-
S_0,E_0, I_0, T_0, R_0	Initial state conditions	0 – P, P = total model population	-	-

*Model parameter values to be inferred from observed data

Table S2. Mean and 95% credible interval of posterior ensemble of model parameter estimates.

Sites	μ_{EI}	μ_{RS}	q_R	D	a.R	b.R	s
East province sites							
Gahini	10.58 (7.11–13.98)	333.28 (189.28–365)	0.21 (0.12–0.46)	98.19 (79.71-114.46)	0.19 (0.15–0.24)	3.64 (2.56–4.77)	0.9 (0.59–1)
Kibungo	10.45 (7–13.73)	310.9 (214.45–365)	0.32 (0.04–0.44)	47.06 (29.5-66.51)	0.17 (0.15–0.21)	4.89 (4.54–5)	0.33 (0.17–0.55)
Kirehe	10.45 (7.31–13.66)	238.61 (135.82–350.37)	0.11 (0.02–0.24)	99.02 (20.63-186.57)	0.15 (0.04–0.26)	4.13 (2.47–4.96)	0.08 (0.04–0.14)
Kiziguro	10.43 (7.47–14)	345.08 (251.06–365)	0.04 (0–0.14)	63.95 (50.03-77.88)	0.22 (0.17–0.29)	2.54 (1.91–3.11)	0.36 (0.24–0.48)
Ngarama	13.08 (10.06–14)	140.74 (120–171.11)	0 (0–0.01)	23 (12.13-39.19)	0.19 (0.13–0.27)	1.73 (1.32–2.04)	0.59 (0.39–0.81)
Nyagatare	12.75 (11.35–13.85)	213.43 (171.37–252.29)	0 (0–0)	197.8 (195-199.95)	0.1 (0.05–0.17)	1.2 (–2.41–2.69)	0.18 (0.15–0.21)
Nyamata	10.39 (7.27–13.67)	196.76 (121.12–311.57)	0.08 (0–0.23)	28.77 (10.77-52.77)	0.13 (0.06–0.2)	4.69 (3.9–5)	0.2 (0.09–0.32)
Rwamagana	11.07 (7.02–13.98)	265.59 (137.51–365)	0.15 (0.03–0.45)	73.99 (54.59-96.18)	0.17 (0.1–0.23)	4.39 (2.43–5)	0.29 (0.17–0.46)
Rwinkwavu	11.37 (7.08–14)	286.52 (174.4–355.05)	0.19 (0–0.42)	68.43 (48.14-95.38)	0.17 (0.13–0.24)	4.26 (2.81–4.86)	0.2 (0.13–0.28)
Kigali City province sites							
Kibagabaga	11.22 (7.28–14)	238.85 (120–348.79)	0.31 (0.09–0.5)	81.03 (59.88-102.92)	0.16 (0.12–0.22)	4.49 (3.24–5)	0.15 (0.09–0.21)
Masaka	11.14 (7.14–13.65)	240.08 (130.74–365)	0.02 (0–0.05)	67.78 (46.95-93.47)	0.11 (0.05–0.18)	3.08 (–5–4.45)	0.09 (0.05–0.14)
Muhima	11.67 (7.91–14)	281.2 (171.11–365)	0.14 (0.07–0.29)	86.77 (68.69-108.26)	0.15 (0.1–0.2)	4.29 (2.91–4.95)	0.14 (0.07–0.22)
North province sites							
Butaro	12.08 (9.06-14)	124.22 (120-165.36)	0.05 (0.03-0.08)	99.63 (87.38-110.13)	0.08 (0.07-0.09)	4.75 (4.32-5)	0.05 (0.04-0.07)
Byumba	11.25 (7.67-14)	190.95 (143.37-281.08)	0.06 (0.02-0.13)	98.67 (81.01-115.92)	0.15 (0.1-0.19)	2.74 (-5-4.1)	0.05 (0.02-0.09)
Kinihira	11.29 (7.94–13.83)	310.59 (238.08–363.5)	0.07 (0.01–0.14)	103.48 (81.26-126.18)	0.14 (0.07–0.22)	3.9 (2.76–4.62)	0.03 (0.02–0.04)

Nemba	10.74 (7.2–14)	156.84 (120–218.91)	0.04 (0.02–0.06)	49.32 (37.47-62.61)	0.06 (0.04–0.07)	4.65 (4.01–5)	0.1 (0.07–0.15)
Ruhengeri	10.81 (7.4-13.96)	231.21 (131.05-342.17)	0.37 (0.22-0.5)	106.2 (92.3-121.02)	0.13 (0.08-0.2)	3.35 (1.91-4.42)	0.03 (0.02-0.04)
Ruli	11.05 (7.76–13.92)	344.36 (312.22–364.23)	0.2 (0.04–0.41)	117.55 (93.51-140.78)	0.17 (0.07–0.25)	1.88 (–0.05–3.01)	0.08 (0.06–0.11)
Rutongo	9.65 (7–13.05)	332.75 (248.73–353.32)	0.44 (0.27–0.5)	121.38 (107.9-139.87)	0.23 (0.18–0.29)	2.46 (1.98–3.23)	0.27 (0.2–0.39)
South province sites							
Gakoma	9.98 (7.21–14)	290.87 (165.09–365)	0.18 (0–0.4)	21.12 (12.57-39.23)	0.21 (0.15–0.3)	3.23 (1.1–4.64)	0.18 (0.1–0.35)
Gitwe	11.43 (7.83–14)	270.66 (143.95–365)	0.04 (0–0.1)	76.85 (37.64-128.86)	0.11 (0.07–0.17)	4.65 (3.9–5)	0.36 (0.22–0.54)
Kabgayi	12.72 (8.75–14)	348.75 (295.11–365)	0.15 (0.09–0.26)	69.83 (60.37-79.66)	0.16 (0.15–0.18)	3.04 (–5–4.56)	0.25 (0.16–0.36)
Kabutare	11.97 (8.28-14)	163.33 (135.19-213.38)	0.38 (0.25-0.5)	76.3 (56.22-95.31)	0.14 (0.1-0.18)	3.38 (2.95-3.85)	0.2 (0.04-0.43)
Kaduha	9.55 (7.17–13.91)	151.62 (133.79–195.8)	0.32 (0.21–0.43)	90.96 (82.42-98.97)	0.12 (0.11–0.13)	4.91 (4.61–5)	0.49 (0.34–0.76)
Kibilizi	9.93 (7.01–13.19)	246.13 (132.38–365)	0.28 (0.09–0.5)	18.38 (10-31.42)	0.21 (0.14–0.27)	4.77 (4.38–5)	0.56 (0.27–0.91)
Kigeme	11.77 (7.86–13.58)	199.23 (168.93–242.22)	0.01 (0.01–0.02)	58.69 (47.16-71.39)	0.1 (0.09–0.11)	3.68 (3.48–3.98)	0.9 (0.65–0.95)
Munini	9.79 (7-12.5)	152.44 (120-207.54)	0 (0-0.01)	36.69 (26.81-47.37)	0.08 (0.08-0.09)	4.86 (4.55-4.98)	0.88 (0.65-1)
Nyanza	10.67 (7.39–13.69)	215.82 (123.05–336.33)	0.16 (0.01–0.37)	40.82 (13.63-72.75)	0.14 (0.08–0.21)	4.72 (4.23–5)	0.27 (0.14–0.4)
Remera rukoma	9.16 (7–13.39)	322.72 (219.07–365)	0.14 (0–0.34)	99.69 (87.98-113.14)	0.14 (0.11–0.17)	3.38 (3.06–3.77)	0.28 (0.2–0.4)
Ruhango	11.06 (7.72–13.87)	271.14 (156.79–365)	0.09 (0.01–0.2)	80.16 (26.77-139.67)	0.14 (0.03–0.28)	2.76 (1.26–3.7)	0.36 (0.21–0.52)
West province sites							
Bushenge	10.52 (7.17–14)	285.44 (184.48–365)	0.03 (0.02–0.06)	85.94 (50.77-124.04)	0.08 (0.05–0.13)	2.55 (–5–4.05)	0.15 (0.09–0.22)
Gihundwe	10.81 (7.25–13.88)	317.09 (232.56–363.03)	0.04 (0.01–0.07)	39.61 (22.01-58.32)	0.12 (0.04–0.19)	3.82 (2.92–4.4)	0.32 (0.24–0.41)

Gisenyi	10.47 (7.14-13.75)	255.66 (133.47-353.19)	0.02 (0.01-0.05)	114.38 (74.38-154.09)	0.16 (0.1-0.23)	4.62 (4.04-4.99)	0.12 (0.06-0.21)
Kabaya	9.56 (7–12.82)	355.16 (300.52–365)	0.38 (0.17–0.5)	125.56 (106.03-161.23)	0.14 (0.11–0.18)	3.71 (–2.63–4.73)	0.02 (0.01–0.03)
Kibogora	11.43 (8.08–14)	162.31 (120–256.69)	0.2 (0–0.45)	75.13 (26.37-133.46)	0.14 (0.08–0.21)	4.44 (3.34–5)	0.21 (0.14–0.28)
Kibuye	10.47 (7.06–13.9)	264.26 (170.81–351.87)	0.21 (0.02–0.46)	100.94 (25.63-187.92)	0.14 (0.07–0.22)	4.25 (2.72–4.99)	0.09 (0.06–0.12)
Kirinda	11.75 (7.78–14)	343.91 (244.88–365)	0.32 (0.15–0.5)	85.83 (67.66-102.87)	0.18 (0.16–0.21)	4.51 (3.98–4.78)	0.39 (0.3–0.55)
Mibilizi	10.46 (7.52–13.54)	308.06 (231.66–363.15)	0.04 (0.01–0.07)	62.75 (25.81-100.91)	0.1 (0.03–0.18)	2.74 (1.06–3.78)	0.19 (0.11–0.28)
Mugonero	10.61 (7.12–13.9)	232.01 (130.67–352.91)	0.24 (0.03–0.47)	105.17 (23.24-192.28)	0.12 (0.02–0.22)	4.06 (1.6–4.96)	0.19 (0.13–0.26)
Muhororo	12.26 (8.03–13.78)	145.01 (120.64–199.82)	0.1 (0.06–0.16)	72.02 (59.51-85.13)	0.1 (0.09–0.12)	3.59 (3.21–4.22)	0.21 (0.14–0.3)
Murunda	10.66 (7.05–13.97)	239.05 (156.38–347.02)	0.04 (0–0.09)	112.91 (13.85-198.92)	0.08 (0.02–0.15)	4.04 (1.53–4.96)	0.06 (0.04–0.08)
Shyira	11.01 (7.38–13.87)	308.39 (230.14–364.51)	0.01 (0–0.02)	87.63 (49.86-124.96)	0.08 (0.01–0.15)	3.59 (1.26–4.72)	0.02 (0.01–0.02)

Table S3: Mean and 95% confidence interval estimates of *k*, the common rate of dispersion within the OEV for model-EAKF simulation.

Site	k estimate (95% CI)
East province sites	
Gahini	0.353 (0.285-0.421)
Kibungo	0.317 (0.254-0.381)
Kirehe	0.368 (0.297-0.439)
Kiziguro	0.313 (0.244-0.383)
Ngarama	0.365 (0.27-0.46)
Nyagatare	0.473 (0.397-0.55)
Nyamata	0.275 (0.211-0.338)
Rwamagana	0.319 (0.254-0.385)
Rwinkwavu	0.323 (0.253-0.393)
Kigali City province sites	
Kibagabaga	0.395 (0.329-0.461)
Masaka	0.374 (0.303-0.446)

Muhima	0.444 (0.372-0.516)
North province sites	
Butaro	0.758 (0.654-0.862)
Byumba	0.435 (0.363-0.508)
Kinihira	0.608 (0.509-0.707)
Nemba	0.689 (0.595-0.783)
Ruhengeri	0.739 (0.633-0.845)
Ruli	0.598 (0.511-0.684)
Rutongo	0.521 (0.447-0.594)
South province sites	
Gakoma	0.271 (0.198-0.345)
Gitwe	0.384 (0.315-0.453)
Kabgayi	0.485 (0.419-0.552)
Kabutare	0.45 (0.379-0.52)
Kaduha	0.562 (0.481-0.642)
Kibilizi	0.284 (0.215-0.354)
Kigeme	0.493 (0.418-0.568)
Munini	0.469 (0.396-0.541)
Nyanza	0.382 (0.314-0.45)
Remera Rukoma	0.449 (0.382-0.515)
Ruhango	0.412 (0.345-0.478)
West province sites	
Bushenge	0.609 (0.536-0.683)
Gihundwe	0.566 (0.489-0.642)
Gisenyi	0.372 (0.295-0.448)
Kabaya	0.726 (0.618-0.834)
Kibogora	0.432 (0.365-0.499)
Kibuye	0.518 (0.442-0.594)
Kirinda	0.443 (0.363-0.524)
Mibilizi	0.441 (0.372-0.511)
Mugonero	0.633 (0.55-0.716)
Muhororo	0.651 (0.564-0.738)
Murunda	0.514 (0.439-0.588)
Shyira	0.775 (0.649-0.9)

Chapter 3: A dynamic forecasting system for malaria incidence

In this chapter, a malaria forecasting system for the climate-driven malaria transmission model is developed. The system utilizes a Bayesian algorithm for dynamical tracking of the evolving states of transmission– a technique successfully used in accurately forecasting a number of recurrent infectious diseases including influenza, diarrheal disease and dengue. The probabilistic forecasts generated by the system are retrospectively validated with malaria incidence data from 42 regions over four years in Rwanda. In an effort to reduce forecast uncertainty and improve reliability, a multi-model forecasting system comprising of the dynamic model and historical expectance predictions is also developed. Verification of both forecasting systems are conducted to assess the statistical reliability and overall utility of the malaria forecasting systems as forecasters of local malaria incidence in Rwanda.

3.1 Background

Every year, malaria causes 200 million cases and about 400,000 deaths worldwide (World Health Organization 2019). Accurate prediction of future malaria incidence, including the timing and intensity of outbreaks, could provide better insight for malaria preparedness. For more than a century, mathematical models have deepened understanding of malaria transmission; their ability to describe complex, nonlinear system dynamics can, in theory, support accurate prediction of the changes to malaria risk. State-of-the-art forecasting has yet to become an integral component in the fight against malaria, but as decades of global gains made against malaria incidence and morbidity have stalled (World Health Organization 2019; Dhiman 2019), it has become imperative to seek more proactive approaches to back control efforts.

Recently, accurate forecasts for a number of infectious diseases, including dengue fever (Yamana, Kandula, and Shaman 2016), West Nile Virus (DeFelice et al. 2017; 2018), influenza (Shaman and Karspeck 2012; Shaman et al. 2013b; 2017; W. Yang, Olson, and Shaman 2016; W. Yang, Karspeck, and Shaman 2014), and diarrheal disease (Heaney, Alexander, and Shaman 2020), have been developed using dynamic forecasting systems. Many of these systems combine a mathematical model of disease transmission with data-assimilation methods, much like those used for numerical weather prediction (NWP) (Anderson 2001; Karspeck and Anderson 2007), that recursively adjust the dynamic model to better represent the evolving state of the actual system. Using the most up-to-date estimates of the system, the model can then be used to generate probabilistic projections of future outcomes and their uncertainty. Infectious disease outbreaks, due to their underlying nonlinear dynamics, can be prone to error growth that undermines accurate prediction (Lighthill et al. 1986). The use of a model-inference approach helps to reduce forecast error while still representing nonlinear infectious disease processes. Information systems used to evaluate future malaria risk and advise antimalaria decision-making could benefit from such model-inference frameworks that contemporaneously track model state and forecast disease incidence.

A variety of forecasting methods have been developed for malaria including generalized linear models (Gomez-Elipe et al. 2007; Teklehaimanot et al. 2004), auto regressive integrated moving average (ARIMA) approaches (Abeku et al. 2002; Midekisa et al. 2012), and mathematical transmission models (Gaudart et al. 2009; Laneri et al. 2010a; Tompkins et al. 2019). Even though accurate forecasts of various vector-borne and non vector-borne infectious diseases have been demonstrated using data assimilation combined with dynamic modeling, to date, the feasibility of this potentially valuable system for malaria has not been investigated.

This study develops and validates a malaria forecasting system comprised of a parsimonious model of malaria transmission and a data assimilation technique– the Ensemble Adjustment Kalman Filter (EAKF) (Anderson 2001). Within the forecasting system, model outputs and malaria incidence data are combined using the EAKF and generate probabilistic forecasts of malaria incidence in Rwanda. The accuracy, skill and statistical reliability for midrange forecasts generated by the system at national and regional levels are evaluated. Additionally, because ensemble forecast systems are generally more accurate than single prediction systems (Yamana, Kandula, and Shaman 2017; Reich et al. 2019; Krishnamurti et al. 1999), the dynamic forecasting system combines with historical probability predictions to create a more reliable multi-model system for malaria forecasting.

3.2 Materials and Methods

To forecast local malaria conditions, the developed forecasting system comprises of a mathematical transmission model of malaria driven by rainfall and temperature conditions, a data assimilation algorithm and observations of malaria incidence. Components of the forecasting system are detailed below.

3.2.1 The malaria model

The recently developed climate-driven compartmental model of malaria (Figure 1) is employed to simulate transmission. Detailed description of the development and validation of the model with malaria data are provided in Chapters 1 and 2. Briefly, individuals within the host population are divided between Susceptible, Exposed, Untreated (infected), Treated (infected) and Recovered states. Transition between model states is dictated by an average rate based on

human demography and parameters of malaria epidemiology related to immunity, parasite incubation and clinical infection.

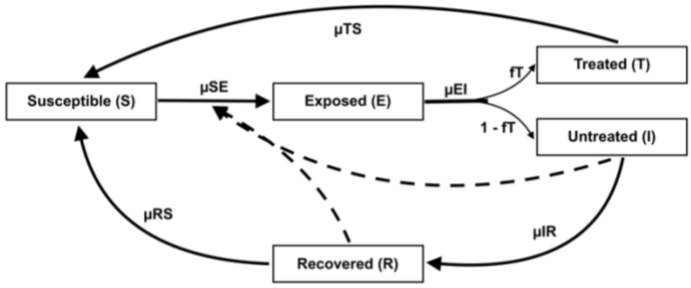

Figure 1. Flow diagram of the malaria transmission model. Individuals within the transmission system are divided into those who are susceptible to infection (S), exposed to the parasite (E), have clinical infection and are treated (T), have clinical infection and are untreated (I), and have recovered from clinical disease (R). Individuals are susceptible at birth (μ_{BS}) or following loss of immunity (end of patency) or end of treatment–related prophylaxis. Susceptible individuals become exposed at a rate determined by the force of infection (μ_{SE}). Exposed hosts (E) then undergo intrinsic incubation of *Plasmodium falciparum* at a rate determined by μ_{EI}. Following parasite incubation, infected cases begin to show clinical symptoms, a fraction (fT) of which are assumed to be fully treated (state T) with the remainder untreated (state I). Treated individuals return to the susceptible state at a rate determined by the duration of the prophylactic effect (μ_{TS}) due to antimalarial therapy. Untreated infections recover naturally (μ_{IR}) from clinical disease and show no further symptoms of clinical infection. Hosts that naturally recover, enter a state of low level parasitemia (state R) that is tolerated by the immune system. Under this patent/subpatent state, individuals are protected from reinfection and have a relatively lower infectivity to mosquitoes (qR) compared to full-blown clinical infections. Once patent/subpatent infections are cleared (μ_{RS}), recovered hosts again become susceptible.

Susceptible individuals become exposed at an average rate determined by the force of transmission(μSE). Following completion of *Plasmodium falciparum* incubation, determined by μEI, exposed individuals show clinical symptoms, a proportion of whom will be fully treated (fT) or untreated (1-fT). Treated cases eventually return to the susceptible state after a duration of prophylaxis (μTS) from antimalaria therapy. However, untreated infections recover naturally (μIR) from clinical disease and at the end of patent and sub-patent (μRS) infection subsequently become susceptible to reinfection.

Within the model, rainfall and temperature regulate various aspects of mosquito survival, development and parasite infectivity, and in so doing modulate vector-host contact rates and the force of transmission (μSE). These effects are represented through climate-mediated adjustment of the entomological inoculation rate, as previously described in Chapter 1. Incidence of malaria within the model is tracked over time by the number of newly infected individuals presenting clinical symptoms per unit time.

3.2.2 Malaria and climate data

Malaria data used in this study are obtained from the Rwanda Ministry of Health (MoH). Beginning in 2011, Rwanda established standard nationwide malaria surveillance and case management practices, which included parasitological confirmation of malaria cases. Weekly data were acquired for reported lab-confirmed malaria cases in Rwanda's 42 health catchment sites, during 2016-2019 (Ministry of Health 2016). These weekly datasets were then used to train the malaria model and evaluate the accuracy of retrospective, model-generated out-of-sample predictions for each site.

Weekly rainfall (1980-2019) and temperature (2006-2016) data were acquired from the University of California, Santa Barbara Climate Hazards Group InfraRed Precipitation and Temperature with Station products (CHIRPS and CHIRTS) (Funk et al. 2015; 2019). Due to an absence of temperature data during 2016-2019, weekly averages of temperature from 2006-2016 in conjunction with current rainfall data were used to force the climate malaria model during training periods. During forecasting, weekly historical averages of rainfall (1980-2019) and temperature (2006-2016) were used to drive the climate model.

3.2.3 Model inference

The malaria transmission model is trained by the Ensemble Adjustment Kalman Filter (EAKF), a data assimilation, or Bayesian inference, technique for state-space models (Anderson 2001; Karspeck and Anderson 2007). The EAKF recursively adjusts the first and second moments of the currently observed model state (i.e. case incidence within the model) to better match those of the observed malaria data as the transmission model system evolves over time. Additionally, the ensemble of model parameters and state variables are adjusted based on cross-ensemble co-variability to reflect the projected change in the observed model state.

For data assimilation using the EAKF, observational error variance (OEV) of the data must be prescribed. The OEV expresses to the model-inference system the uncertainty surrounding the observability of true malaria incidence. Malaria incidence data are assumed to be over-dispersed and follow a negative binomial distribution, and consequently the OEV of weekly malaria observation for the model-EAKF system is defined as:

$$OEV_t = \gamma_t + \frac{\gamma_t^2}{\gamma_t^k} \qquad (1)$$

As true incidence is unknown, γ_t is taken as the response at time t from a cubic spline smoothing of the current timeseries training set of malaria incidence; and k the common aggregation parameter for observing malaria incidence is set to a constant value of 0.5.

To parameterize the model, the EAKF system is initialized with 300 simulations of randomly drawn combinations of parameters and initial state variable estimates. These 300 initial conditions are then integrated forward to the first observation at time *t*=1, which the EAKF uses to update the prior ensemble of model parameters and state variables to posteriors. The model is then integrated forward to the next observation at time *t*=2 using the updated ensemble parameter and state variables. Observations of malaria at t=2 are assimilated and the system state variables

and parameters are again adjusted, generating new posteriors. The EAKF-model system continues this recursive filtering and model integration until the training timeseries of observations have been assimilated. In an iterated filtering approach, the EAKF repeatedly assimilates the same time series (Pei et al. 2018) to enhance convergence of model parameter and state variables. A total of 10 iterations (*i*) were performed, with subsequent iterations initialized with model parameters state variables drawn from N(μ, σ^2), where μ is the mean of the posterior parameters from the previous iteration. σ is a product of the variance of the posterior ensemble of the previous iteration and an annealing factor α_i, which is defined as:

$$\alpha_i = \left(1 + \frac{0.5}{(1+i)^{0.75}}\right) \qquad (2)$$

3.2.4 Retrospective malaria forecast

Malaria in Rwanda is typically characterized by two distinct transmission cycles separated by troughs in incidence following the short and long dry seasons. To forecast malaria, the climate-forced transmission model is trained on the immediately preceding cycle, and also on the current cycle in a rolling fashion, until observations of the current cycle up to the date of forecast initiation are fully assimilated by the EAKF. Specifically, beginning at the first observation of the previous cycle, which is say 30 weeks long, the EAKF starts at *t*=1 with an ensemble of 300 model simulations initialized with random initial state variables and parameters. The EAKF-model continues updating and integrating after each observation until the preceding full cycle has been assimilated (*t*=30), producing the final posteriors of the i^{th} iteration. At the end of the 10th iteration, posteriors of the EAKF system together with weekly historical average temperature and rainfall are used to integrate the transmission model forward from week 30 to 8 weeks ahead, without further training. To generate more forecasts of the current cycle, the training dataset is extended by one week; and the EAKF-model inference system starts afresh

from *t*=1, with random ensemble of parameters and state variables. The process of updating and integrating after each observation continues until the extended training dataset has been assimilated (*t*=31). Using the model state variables and parameters to which the system has converged, EAKF-model generated forecasts of future malaria incidence initialized from *t*=31 to 8 weeks ahead. The training, forecasting, and rolling extension of data continues until the malaria data for the current cycle have been fully assimilated. To examine forecast performance the forecast mean and 95% Credible Interval (CI) generated by the ensemble of retrospective forecasts are compared with observed malaria incidence.

3.2.5 Historical probability model

Historical probability models can provide useful foreknowledge of seasonal dynamics for systems with relatively stable transmission outcomes. Here, historical expectance of malaria across Rwanda is used to construct a probability model of weekly malaria incidence. Annual malaria records at site-level are relatively short (n=4) and thusly could strongly bias out-of-sample predictions. Therefore, to form more robust weekly probabilities, records of sites possessing similar transmission profiles are pooled. Mean elevation is known to spatially auto-correlate and determine the malaria transmission intensity and vectorial capacity (Bødker et al. 2003; Noboru Minakawa et al. 2002; Kulkarni et al. 2006) for neighboring populations. Based on this, local populations were pooled into two regional groups– low altitude with mean elevation <1500m and high altitude with mean elevation >=1500 m, reflecting a distinct break in temperature suitability for vector abundance and parasite transmission (Bloland and Williams 2002; World Health Organization 2012b; Baidjoe et al. 2016). Historical predictions for a site during a particular week of the year are derived from the group mean and range of historical

malaria incidence, excluding data from that site for the given week and year. All malaria record pooling, forecasts, and comparisons were based on per capita case incidence.

3.2.6 Multi-model ensemble forecast

The model-EAKF forecasts combines with the historical expectance predictions using simple weighted-averages to create multi-model ensemble forecasts. A total of five weighted-average models were generated with weights, $w = 0.5, 0.6, \ldots 0.9$, given to the model-EAKF forecast and 1-w weights placed on the historical probability forecasts. They are hereafter referred to as multi-model I, II, III, IV and V. Every week, forecast mean, variance, and quantiles (5^{th}, 10^{th}, … , $95^{th,}$ with increments of 5) for the multi-model predictions were determined by weighted-averages of these statistics based on the joint forecast distribution of the model-EAKF system (weight =w) and historical probability model (weight = 1-w). Analyses outcome is reported for the best performing multi-model form.

3.2.7 Forecast Analysis

The usefulness of a forecasting system for better decision-making is partly evident in the objective evaluation of prediction quality. And several measures described below verify the overall utility of the forecasting systems for predicting local malaria incidence across Rwanda.

Logarithmic Scoring

Forecasts of 1, 2, 4, 6, and 8 weeks ahead predictions for malaria incidence were generated by the model-EAKF, historical expectance and multi-models for 2016-2019 for all study sites. For each prediction method, the probability of observing malaria incidence each

week was determined by integrating over the likelihood profile. Specifically, taking the mean forecast (μ) and variance of the forecast spread (σ^2) of each prediction method *m*, the log score (LS) of the forecast following Gaussian specification is computed as follows:

$$LIK_t = \int_{y-j}^{y+j} P_{fc_m}(y_t)\, dy \qquad (3)$$

$$LS = \frac{1}{n}\sum_{t=1}^{n} \log(LIK_t) \qquad (4)$$

where P_{fcm} is the probability density function of the forecast system *m*, and *y* is the observed incidence at time *t*. Because the probability of a continuous variable can be infinitesimal, P_{fc} is integrated over a slightly larger width *j*. The value of *j* is allowed to be proportional to *y* by setting it to a small fraction (0.05) of the observed incidence.

Forecast accuracy

The average correspondence between individual pairs of weekly forecasts and observations was also assessed. For historical expectance predictions, the historical mean observed within pooled sites for a given week represents the point forecast. Point forecasts for model-EAKF were taken as the weekly predictions generated from integrating the transmission model forward using the mean posterior state variables and parameters of the optimized model. For multi-model forecasts, the weighted-average of predicted weekly incidence for a given week was taken as the point forecast. Reports of 1) the Mean Absolute Percentage Error (MAPE) over the four-year period and across all sites for each model, 2) site-level Pearson Correlation estimate (R) between point predictions made over the study period and observed malaria

incidence, and 3) the forecast target accuracy of local forecasts, defined as proportion of point predictions that came within ± 25% of observed data over the study period (P± 25%) measured the performance of point predictions of the forecasting systems.

Forecast skill

Additionally, the forecast skill compared the skills of the historical expectance and multi-model systems in accurately predicting malaria incidence, relative to the model-EAKF system. As computed below, the Skill Score (SS) expressed the added benefit of including weighted historical expectance. The forecast skill (SS) of the five multi-models and historical prediction models are based on Mean Absolute Percentage Error (MAPE) and calculated as follows:

$$SS_m = 1 - \frac{MAPE_M}{MAPE_{ref}} \qquad (5)$$

where $MAPE_m$ is the point forecast error computed over the 4-year period, across all 42 study sites for historical probability predictions or individual multi-model, and $MAPE_{ref}$ is the point forecast error of the model-EAKF system model. Skill scores range between -∞ and 1. Higher is better, with perfect skill = 1.

Forecast reliability

As part of forecast verification, the distribution of predictions made by the multi-model and EAKF-model forecasts are comparing to the distribution of observed occurrence of malaria

incidence, to examine the forecast reliability of each system (D. Wilks 1995). Specifically, the probability of observing a predicted event given the forecast probability is computed. The lower and upper bounds of the *pth* percentile (i.e. p = 5, 10, 20, 25, ..., 95th) of the full ensemble of forecast trajectories (model-EAKF) represent the probability of a given forecast. Based on this distribution, the proportion of times weekly malaria incidence falls within the forecasted intervals is quantified over time and all of Rwanda to obtain the overall statistics of observing a prediction. In a well calibrated forecast, 20% of observations should fall within the 20% prediction interval, 80% of observations should fall within the 80% prediction interval, etc. The resulting reliability plot, which graphically depicts the concordance between predictions and observed occurrence, visualizes this agreement between the observed probability and forecasted probability.

3.3 Results

Over the four-year period, probabilistic forecasts made by the model-EAKF system showed strong overall agreement with malaria incidence at the province level, as shown in Figure 2. At the more resolved local level, malaria point forecasts likewise showed high agreement with local malaria incidence across Rwanda (Figure 3). Across the local sites, dynamical point predictions made at short to mid-range lead times strongly correlated with malaria outcomes on aggregate with 1-week lead median R = 0.851, 2-week lead median R = 0.773 and 4–week lead median R = 0.681. Similarly, point accuracy and target accuracy were highest for these short- to mid-range predictions across the sites in Rwanda. At longer lead times (≥ 6 weeks), however, correlation between point predictions and malaria incidence at the local level was moderate on aggregate– with 6-week lead forecasts having median R = 0.599 and 8-

week lead $R = 0.534$. Accuracy of point predictions also declined at these longer terms compared to shorter-term forecasts.

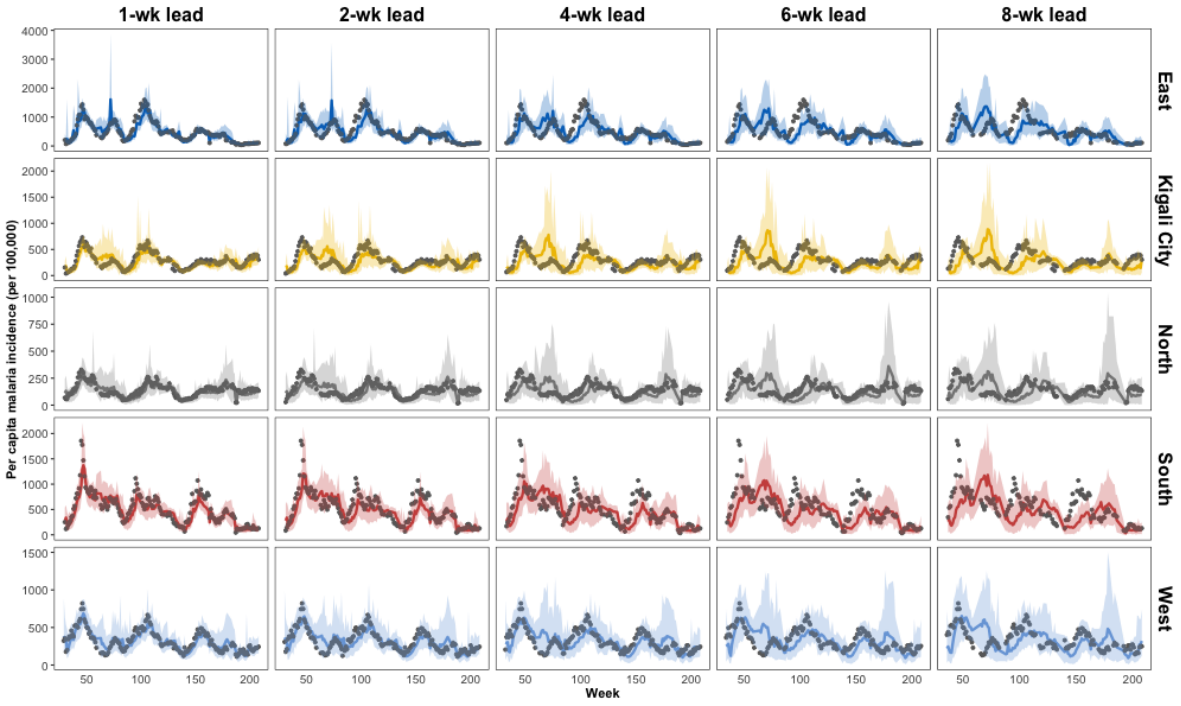

Figure 2. Province-level forecast of malaria incidence (2016-2019) at varied lead times. Climate model predictions are generated at the more resolved site level and results are aggregated and shown below by province. Colored lines and shading indicate aggregated forecast mean and 95% CI for provinces in the East (blue), Kigali City (yellow), North (grey), South (red) and West (light blue). Observed malaria incidence is indicated in black dots.

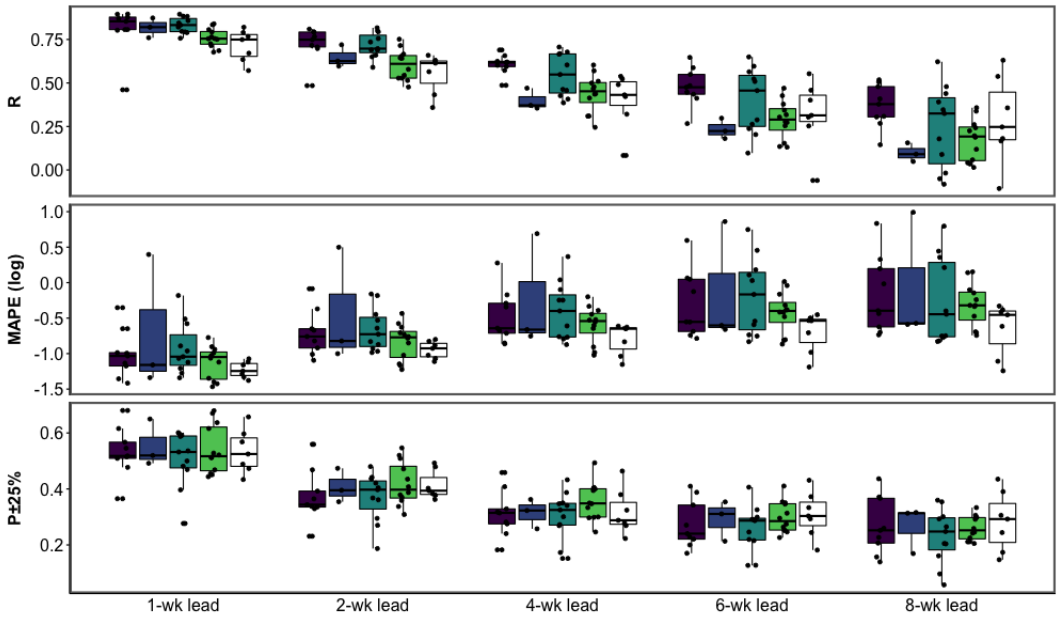

Figure 3. Performance of model-EAKF point forecasts over four years for the 42 local sites across Rwanda's five provinces. In the top panel are the site-level Pearson correlation estimate between dynamic predictions and observed malaria over the study period (R); in the middle panel are the MAPE values and in the bottom panel are the proportion of point forecasts for each site within 25% of observed incidence (P±25%). Each boxplot shows the median (thick line), interquartile range-IQR (box bounds), Q1 -1.5*IQR (lower whiskers) , Q1 +1.5*IQR (upper whiskers) of values for local sites within East (purple), Kigali City (blue), North (teal), South (green) and West (white) provinces. Actual site-level forecast performance values are indicated by jittered black dots.

The model-EAKF probabilistic forecasts typically were more precise in capturing future malaria outcomes than baseline historical predictions (Fig. 4). This performance was readily apparent across Rwanda for near-term forecasts (1 to 2 weeks). At longer lead times this advantage was less uniform geographically. For example, for sites in the North and West however, dynamic forecast distributions remained more precise than baseline forecasts regardless of forecast horizon. But in Kigali City and South provinces, precision dipped below baseline predictions with increasing forecast horizon. In terms of point forecast accuracy, the dynamic system outperformed the historical model (Fig. 5). Even with increasing lead times,

model-EAKF point forecasts generally were more skillful than historical expectance point predictions throughout Rwanda.

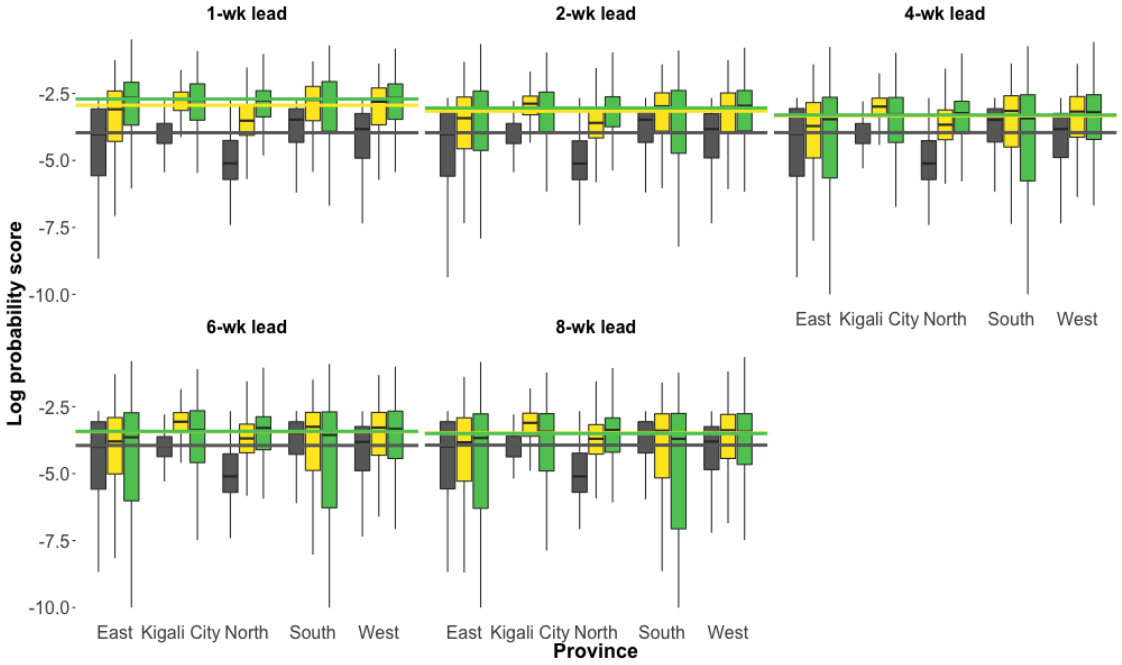

Figure 4. Boxplot of logarithmic score of local malaria forecasts generated by the various forecast systems. Each boxplot is showing the median (thick line), IQR (box bounds), Q1 -1.5*IQR (lower whiskers) , Q1 +1.5*IQR (upper whiskers) of forecast logarithmic scores for local sites in the provinces of Rwanda for model-EAKF system (green), historical probability model (grey) and top multi-model form (Multi-model V, yellow). Logarithmic scores are determined by the likelihood of local malaria data given the forecast distribution. A higher logarithmic score is better. Median country-wide logarithmic scores over various lead week predictions are indicated by corresponding colored solid lines.

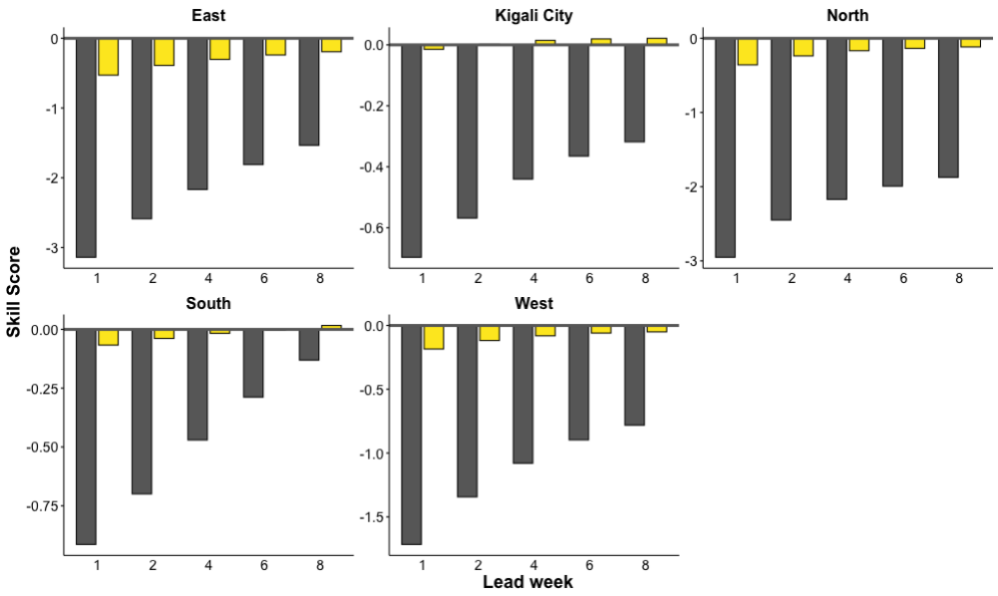

Figure 5. Relative forecast skill of historical probability and top multi-model compared to model-EAKF forecasts. Grey and yellow bars indicate the skill scores based on MAPE of historical expectance and multi-model V predictions respectively. Skill scores range from -∞ to 1, with 1 indicating perfect skill. Forecasts that are more accurate than model-EAKF forecasts will have a skill score greater than 0. And conversely, forecasts that are less accurate than model-EAKF predictions will have a skill score less than 0.

Several multi-model prediction systems comprised of different weight combinations of dynamic simulation and historical expectance forecasts were created. Among the multi-model ensembles considered, multi-model V produced the largest improvement to the model-EAKF system, by logarithmic scores (Table 1). Within this top multi-model, forecast score rises above the model-EAKF forecasts for the Kigali City and South regions at longer lead times (4-8 weeks) (Fig. 4); however, this increase of logarithmic score was not large. For point predictions, improvements over the model-EAKF forecasts were also observed for the South and Kigali City regions. Improvements to Kigali City point forecasts by the multi-model system were more highly pronounced and sustained at all forecast leads. Across the remaining three regions, however, the model-EAKF system provided the most skillful point prediction, although the gain in skill increasingly dropped as forecast horizon lengthened.

Table 1. Proportion of multi-model forecasts with higher logarithmic scores than model-EAKF predictions. Largest improvement to model-EAKF system is seen in multi-model V, the top weighted-averaged model.

Lead time	1-week lead	2-week lead	4-week lead	6-week lead	8-week lead
Multimodel I	36.85%	42.57%	46.85%	48.93%	50.72%
Multimodel II	38.61%	44.17%	48.25%	50.36%	52.04%
Multimodel III	40.69%	45.94%	49.83%	51.83%	53.33%
Multimodel IV	43.09%	47.96%	51.53%	53.26%	54.61%
Multimodel V	45.89%	50.12%	53.21%	54.70%	55.70%

More conclusively, the multi-model system improved forecast reliability. As shown in Fig. 6, model-EAKF forecasts are generally less reliable compared to weighted-average forecasts. Probabilistic model-EAKF forecasts showed a tendency towards overconfident predictions, particularly with increasing forecast horizon; however, multi-model averaging improved the forecast uncertainty. In the top multi-model (model V), with most weight (90%) given to the dynamic simulation and only a small fraction (10%) due to the historical probability model, forecasts retain the high accuracy of the dynamic prediction but are better calibrated, producing probabilistic forecasts that should be more useful for decision making.

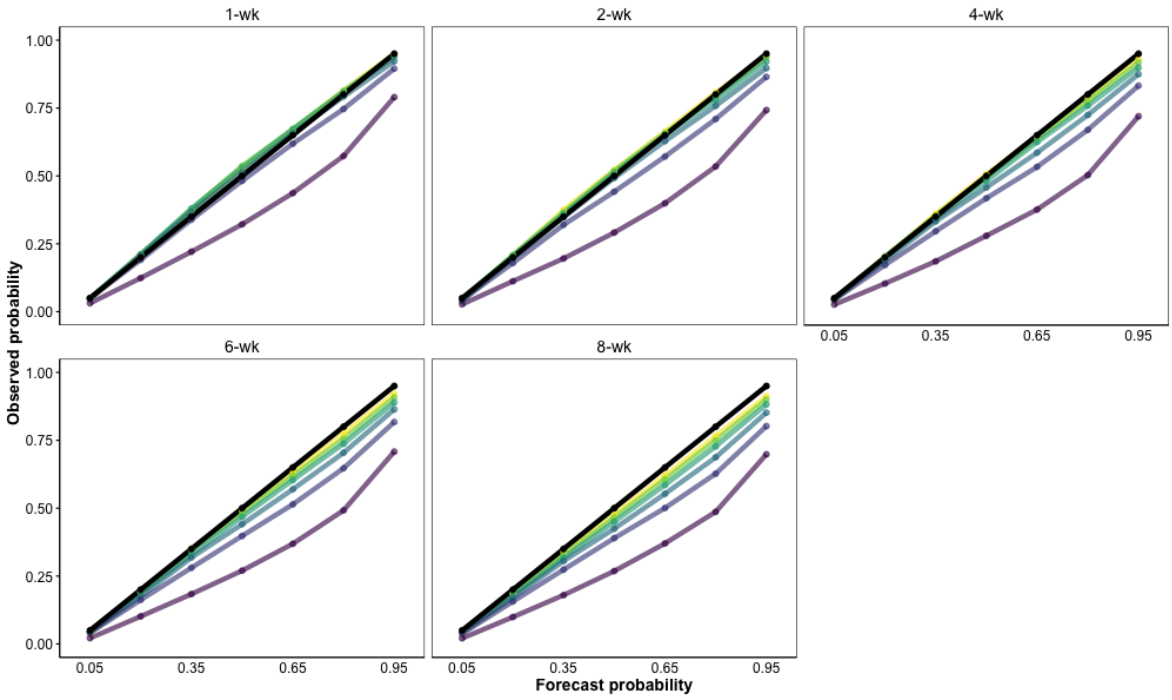

Figure 6. Forecast reliability of the model-EAKF and multi-model forecast systems. Solid lines show the observed forecast probabilities of model-EAKF predictions (purple), multi-model I (yellow), multi-model II (light green), multi-models III (teal), multi-models IV (dark green), and multi-model V (blue) – the top weighted-average forecast model. Black solid lines indicate a perfectly reliable forecast.

3.4 Conclusion

This study developed and assessed the utility of a forecasting system designed for probabilistic prediction of local malaria incidence. The system consists of a malaria transmission model and a data assimilation algorithm, which were used to forecast malaria incidence for 42 local sites and five larger provinces in Rwanda. Findings indicate that the malaria forecasting system is capable of skillful and accurate predictions at the local and regional scale, which are made more reliable when combined with historical expectance.

By using a mathematical model, vector-host population interactions that underpin malaria transmission and potentially determine future disease outcomes can be better represented. However, utilization of such nonlinear dynamic systems for prediction of outcomes can, without

proper constraint of the system, be subject to system divergence and rapid error accumulation (Lighthill et al. 1986). The data assimilation approach employed here has demonstrated ability to improve disease forecast outcomes for a number of infectious diseases (Yamana, Kandula, and Shaman 2016; DeFelice et al. 2017; 2018; Shaman and Karspeck 2012; Shaman et al. 2013b; 2017; W. Yang, Olson, and Shaman 2016; W. Yang, Karspeck, and Shaman 2014; Heaney, Alexander, and Shaman 2020). Within the dynamical forecasting system, the inference informs the evolving model state of observed change in malaria activity. This iterative data assimilation limits error growth within the model system and supports the more accurate near-term forecasts reported here. This benefit, however, diminishes at longer lead times at local and regional levels and is evident from the increasingly large prediction errors observed with increasing forecast leads.

The dynamical forecasting system was markedly more accurate and precise than the historical probability model. Malaria in Rwanda has clearly defined hyper-endemic seasonality; however, transmission intensity can vary temporally and regionally (National Institute of Statistics of Rwanda 2015a; Ministry of Health, Rwanda 2017), which may weaken the predictive strength of baseline forecasts. High burden regions throughout the country, especially in the East and South provinces, have been a major target in recent years for intensified control and intervention efforts (Ministry of Health, Rwanda 2017; U.S. President's Malaria Initiative 2018a; 2019a), such as blanket indoor residual spraying and wide insecticide treated bed net coverage, in order to approach national elimination goals. To achieve widespread success, these exogenous factors disrupt vector-host population interactions and shift entomological exposure away from *de facto* outcomes arising from the seasonal and ecological determinants of local transmission (U.S. President's Malaria Initiative 2018a; 2019a). The resulting deviations

increase the inherent variability of local malaria incidence, and without tracking of the concurrent changes to the disease system, historical probability predictions are more likely to be increasingly divergent depending on the degree of deviation of ongoing malaria activity from the norm. However, the model-EAKF framework is a more flexible, dynamic system. Even in the absence of exogenous actors, it is capable of reflecting the necessary changes to model state conditions to correspond with concurrent malaria activity.

Though the dynamic forecasting system alone is the best system for predicting weekly malaria variability, inclusion of historical probability weights could benefit the performance of long-range forecasts. Nonetheless, the relative gain from the multi-model approach was not conclusive. Contribution of historical expectance to forecast accuracy was largely deprecative in three regions, fairly appreciative in one region and only conclusively in one. Therefore, its use within multi-model prediction framework requires careful consultation on regional and forecast lead bases. Additionally, though the multi-model system combined the dynamical system and historical expectance, results denote that impact from model-EAKF were higher and critical for forecast skill and precision.

In the future, combining the dynamical model with statistical models capable of representing malaria variability and describing recent incidence, such as ARIMA models (Abeku et al. 2002; Midekisa et al. 2012), could contribute more informatively than historical expectance. Additionally, calibration techniques designed to address inherent bias and uncertainty of ensemble forecasts such as model output statistics and Nonhomogeneous Gaussian regression (Gebetsberger et al. 2018; Jewson, Brix, and Ziehmann 2004; Gneiting et al. 2005; D. S. Wilks and Hamill 2007; Veenhuis 2013) might also contribute to the development of a more robust and accurate system for forecasting malaria. Furthermore, due to the regulating effects of

local climate conditions on malaria mosquito entomology, future work should assess the impact of climate modulation within the malaria model on overall forecast quality of the multi-model system.

The malaria forecasting system developed here demonstrates that skillful and accurate probabilistic malaria forecasts can be generated using a mathematical transmission model and data assimilation techniques. As a forecaster for the region of study, the system showed superior predictive power over baseline historical probability predictions at both regional and local scales. However, a multi-model ensemble prediction system comprising of dynamic predictions and historical probability forecasts formed a more statistically reliable forecasting system although slightly less skillful than the dynamic forecasting system.

Conclusion

This dissertation focuses on leveraging the processes through which ambient conditions affect mosquito and parasite dynamics in order to develop lower-dimension process-based models of malaria capable of accurate simulation, inference and forecasting. The concluding sections here explore areas for future exploration and further consideration that could be pursued to improve model specification and the inference of malaria transmission dynamics. Additionally, this section explores measures for facilitating more accurate malaria forecasts and recommends approaches for effective use of the forecasting system in support of local malaria control efforts.

Summary of findings

Simple mathematical models of malaria transmission that implicitly represent the malaria force of transmission have previously represented the influence of meteorological variability on mosquito and parasite dynamics in an indirect manner. In Chapter one of this dissertation, an alternate model framework is delineated that leverages a simplified description of the force of transmission, the EIR, but includes direct climate regulation of vector and parasite ecology. Important climate-regulated facets of vector activity and entomological exposure, such as parasite sporogony, biting rate, mosquito development and survivorship specify transmission pressures within this novel model construct. Free-simulations using this climate-driven dynamic model, forced with seasonal rainfall and temperature conditions from select sites across Rwanda, are able to capture the seasonal variability of malaria.

In Chapter two, the model framework is coupled with data assimilation methods and used to more precisely reproduce retrospective malaria incidence in Rwanda. Malaria simulations with this combined model-inference system are able to capture the variability of malaria incidence at regional geographic scales, but at more resolved local scales, model accuracy was less consistent. For years with limited antimalaria control, the model-inference framework is able to reproduce malaria transmission more accurately than for periods of intensified control efforts. This discrepancy highlights the need to represent exogenous factors affecting malaria transmission in order to properly reflect changes in local risk within the model. Furthermore, counter to the historical pattern of malaria intensity in Rwanda, entomological exposure is estimated to be higher in the West and North regions than in the East and South regions. However, in spite of these differences, model-inferred parameters of malaria transmission are highly comparable to existing studies of malaria epidemiology, which externally validates the transmission model. Additionally, the model-inference system identifies moisture-regulated sub-adult mosquito survival, among the climate variables, as crucial for defining seasonal malaria dynamics, supporting the well-elucidated role of rainfall in determining seasonal malaria risk in the region.

In Chapter three, a dynamic forecasting system for accurate, probabilistic prediction of malaria incidence is successfully tested throughout Rwanda using four years of historical data. This system is comprised of the climate-driven mathematical transmission model, concurrent weekly malaria incidence data and the EAKF data assimilation algorithm. Skill and accuracy of retrospective 300-member ensemble forecasts are high for near-term predictions (predictions made 1-2 weeks in advance) of malaria incidence. However, over longer forecast horizons (lead times of 4 or more weeks), the probabilistic forecast error increases, indicating accumulating error within the forecasting system – an outcome expected for nonlinear model systems.

Combining the transmission model forecasts with conservative predictions derived from historical expectance in a multi-model forecasting system causes only a negligible decrease in overall predictive power. The joint system generally results in better calibrated probabilistic forecasts of malaria incidence at longer lead times throughout the country. However, improvements to forecast accuracy are variable and region dependent. These findings indicate accurate forecasts of local malaria incidence are possible; however, further work on forecast calibration and specification is needed to improve model performance for real-time prediction.

Improvements to model accuracy and forecast needed

Malaria surveillance and climate data

High quality data are key for proper inference in any model structure and particularly for systems that rely on complex and dynamic processes. In Rwanda, where the study is focused, malaria surveillance is strong and consists of mandatory parasitological diagnosis of all suspected malaria cases and timely reporting of confirmed cases (National Institute of Statistics of Rwanda 2015b). However, more buy-in and participation from private health facilities is needed to improve reporting of users of private healthcare options (Ministry of Health, Rwanda 2017). While malaria surveillance in Rwanda is fairly robust, unfortunately, in many other malaria endemic countries, particularly for populations in sub-Saharan Africa, routine malaria surveillance in both public and private health care sectors is often scarce and of poor quality (World Health Organization 2017b), limiting model inference capability and public health application.

To reproduce the inferential and predictive performance demonstrated in this work throughout Rwanda, more malaria regions, particularly high transmission settings, must consider

a cross-cutting transition to accurate methods of frequent surveillance of malaria activity. According to WHO recommendations accurate diagnosis of malaria for surveillance include microscopic confirmation, rapid diagnostics tests (RDTs), and polymerase chain reaction (PCR) techniques (World Health Organization 2018a).

In many malaria endemic countries, high infrastructure cost and low supply of highly skilled personnel are potential barriers to achieving this wider, comprehensive surveillance as recommended by WHO (World Health Organization 2018a). However, the advent of RDTs for malaria is levelling the field and enabling more accurate surveillance in resource-limited settings. RDTs are cheaper, portable alternatives to microscopy and PCR and they require limited training and skill to operationalize. These tests have increasingly been adopted for use by some surveillance systems, particularly those in many LMICs malaria regions (World Health Organization 2019). The technology for RDTs has also advanced (Cunningham et al. 2019; World Health Organization 2011), leading to sensitivity and specificity comparable to laboratory microscopy (Ogunfowokan, Ogunfowokan, and Nwajei 2020; Berzosa et al. 2018). By making RDTs more available at facilities such as health dispensaries and health posts, a strategy that has recently been shown to improve malaria testing quality (Maloney et al. 2017), many malaria LMICs regions could enrich their malaria surveillance without requiring extensive health and medical training for existing personnel. In addition to providing a more comprehensive estimate of current and recent malaria incidence, these data could support public health response efforts, as well as the modeling and forecasting efforts described in this dissertation.

Another surveillance approach that holds potential for improving malaria data for model inference and monitoring in malaria endemic regions is active case surveillance (World Health Organization 2018a). Given the low accessibility to healthcare systems and variable treatment-

seeking behavior noted for many endemic regions, including Rwanda, active surveillance, such as intermittent active case detection programs, could provide a more representative estimate of parasite circulation. These intermittent surveys can also document levels of asymptomatic and mild infections, which are usually not captured by passive systems. The infrequent but more comprehensive data could inform understanding of rates of non-clinical and subpatent infections, and enable better fine-tuning of malaria transmission models and projections of malaria transmission risk.

Incorporating anti-malaria control efforts to improve local prediction

Malaria control efforts disrupt malaria transmission dynamics such that transmission pressures are not solely a result of freely evolving disease processes within vector and host populations. Rather, the force of infection is instead a function of those disease processes plus the exogenous forcing from control efforts acting upon the disease transmission state. These exogenous effects can be immense, altering rates of vector-host contact and resulting in substantive shifts in model states. As a result, simple inference structures may be inadequately designed to capture trends introduced within the system or to reliably estimate the change of parameters for the current state of transmission.

In addition to climate and malaria incidence data, information on malaria control efforts needs to be documented. Anti-malaria measures such as insecticide treated nets (ITNs), indoor residual spraying (IRS), larvicide and seasonal chemoprophylaxis (SMC), and are typically planned to cover regions, high-risk populations, and regimentally implemented site-by-site throughout administrative units. The level of coverage achieved during campaigns could readily

inform the proportion of populations protected from vector exposure or contributing to parasite circulation within the transmission model.

In addition to coverage data, information on the effectiveness of these anti-malaria tools is also essential for accurately portraying transmission. Estimates of these potential effects could be acquired from preliminary efficacy assays, clinical trials, and ongoing field experiments. Anti-vector measures, like IRS, could inform the constraint on malaria transmisssion pressures through adjustment of the parameters controlling mosquito survivorship. Similarly, ITN coverage level and effectiveness could inform the proportion of susceptible and infected individuals available for mosquito bloodfeeding and able to circulate the parasite. The resulting effect of fewer available blood hosts in limiting mosquito oviposition could be reflected in the parameter controlling the length of gonotrophy. Furthermore, the timing of control activities could inform separate periods of inference when malaria control is not present, allowing precise and clear indication of the net forcing on the transmission system. Under this enhanced construct, the malaria model framework might be better positioned to reproduce changes during periods of malaria control, while enabling more reliable parameter estimation by the model-inference system. Similarly, because disease state variables and trends in transmission could be better reflected, model predictions of future local malaria activity might also see improvement.

Impact of remotely sensed climate data on model accuracy

Remote-sensing is an excellent, accessible source of environmental exposure data that has been used for investigating numerous natural and human health issues (Beck, Lobitz, and Wood 2000; Viana et al. 2017; Zhijie Zhang et al. 2013; Sorek-Hamer, Just, and Kloog 2016; Dlamini et al. 2019). The CHIRPS and CHIRTS data (Funk et al. 2015; 2019) used in this

dissertation is partially derived from satellite estimates of precipitation and temperature. However, even extensively validated remote datasets can possess discrepancies between ground observations and the magnitude and variability of satellite estimates (Luo et al. 2003; Duan et al. 2019; Siebert et al. 2019). Forcing malaria transmission with such data, as done in this work, propagates uncertainty within mosquito and parasite dynamics, further introducing potential systemic bias and error to parameter estimates and model predictions.

Especially for rainfall, because of its high spatial and temporal variation, disagreements among satellite and ground estimates can be pronounced. For malaria regions with historically less-frequent or unpredictable rainfall, such as the Sahel or mountainous regions (T. Dinku et al. 2007; T Dinku et al. 2018; Lebel and Amani 1999), data quality could introduce a significant uncertainty into model simulations of transmission potential and mosquito activity. Similarly, discrepancies in air temperature estimates, though often less pronounced, can induce exposure ascertainment issues particularly in barren areas, arid regions, or high elevation regions (Kambi, Wang, and Gulemvuga 2018; Mildrexler, Zhao, and Running 2011; Wan et al. 2002), adding further uncertainty to model simulations, inference and forecasting.

It is not readily apparent what the impact of biased remotely-sensed conditions will be on modeled malaria outcomes and forecast performance. Therefore, comparative entomological assessments with more reflective sources of environmental exposure such as ground observations or gridded station data must be made to highlight areas of disagreement and potential calibration. Furthermore, where available, in-situ based meteorological observations could be incorporated within the dynamic model to better portray the true vectorial capacity underpinning malaria transmission for local populations.

Better resolved denominator population

In developed malaria model system, the denominator population represents the number of people at disease risk in an area with ongoing disease transmission. This population includes individuals who are susceptible, recovering, and those contributing to the transmission pressures. Malaria transmission is typically localized around hotspots (Greenwood 1989). Certain features, such as the state of environment, proximity to water bodies and agricultural lands, and occupation, can combine to raise the local suitability of malaria transmission in one community above neighboring communities (Bousema et al. 2010; Kreuels et al. 2008; Ernst et al. 2006). These differences introduce spatial heterogeneity in the risk and level of transmission in communities within a region (Bousema et al. 2010; T. D. Clark et al. 2008; Woolhouse et al. 1997). As a result of these heterogeneities, estimation of the true population at risk for a particular region is challenging.

In Rwanda, malaria incidence data are reported at a regional level. Regional health catchment sites aggregate incidence data from health facilities from multiple lower administrative units. Aggregation at this geographic resolution obscures differences in sub-regional malaria risk and confounds estimation of entomological exposure for high-risk populations. Furthermore, an inability of the model-inference system to properly account for sub-regional sources of variability could negatively impact model identification of malaria and entomological parameters responsible for transmission in these more localized sub-communities. Similarly, malaria control efforts and future malaria predictions could be differentially effective or exhibit a decline in performance.

Increasing the spatial granularity of malaria surveillance data could provide the resolution needed to better approximate malaria denominator populations. In Rwanda, health catchment

sites consist of several lower administrative units called sectors, which are further broken down into cells and villages (National Institute of Statistics of Rwanda 2015b). The number of individuals with confirmed malaria incidence at the health facilities found in each sector are collated at a regional health catchment center, and an aggregate incidence is reported. However, reporting information on confirmed cases at the sector, cell or village level could improve model capture of the sub-regional population differences affecting malaria variability.

Opportunity for multi-model ensemble forecasting

No one model fully captures the true conditions of a given transmission system; model assumptions often engender biased estimates of the system. In some situations, the uncertainties of a single model construct can grow (Lighthill et al. 1986), making accurate predictions increasingly ineffective for public health control efforts. For this reason, many systems for predicting future outcomes of infectious diseases (Yamana, Kandula, and Shaman 2016), including malaria (Ruiz et al. 2014; Caminade et al. 2014; Laneri et al. 2015), have combined multiple models to create an ensemble system to address model uncertainty. Indeed, multi-model systems for infectious disease forecasts have demonstrated improved model accuracy over the individual models comprising the ensemble (Yamana, Kandula, and Shaman 2017; Reich et al. 2019; Johansson et al. 2019; McGowan et al. 2019). In these multi-model constructs, the uncertainties and inherent errors of each component model can offset one another, thus improving overall predictive performance when used together in an ensemble.

However, careful consideration must be given to the selection and combination of the composite models of the ensemble in order to avoid model redundancy, while highlighting the strengths of member models. Although the multi-model forecasting system developed in Chapter

3 of this dissertation improved forecast reliability, the historical expectance model used within the ensemble could become less predictive of transmission as shifts and disruption in seasonality arise from increased control efforts. Therefore, the built multi-model forecasting system requires further consideration.

In particular, a number of additional forecasting models could be developed and included in a future multi-model ensemble forecasting system. Potentially promising models include statistical or mathematical forms utilizing alternate environmental exposure data such as humidity, vegetative indices or hydrological model estimates. These ambient conditions have previously shown to describe malaria activity (Patz 1998; Craig et al. 1999; Wayant et al. 2010; Baeza et al. 2011) and explain vector dynamics (Yamana and Eltahir 2013; Kashiwada and Ohta 2010). Similarly, dynamical transmission models that emphasize competing hypotheses of transmission such as age-related susceptibility (Griffin, Ferguson, and Ghani 2014), human movement (Wesolowski et al. 2012; Ruktanonchai et al. 2016) and control measures are promising candidates that could further enrich the variety of model forms utilized.

Candidate models that demonstrate an ability to reasonably capture variability in historical malaria activity can subsequently be combined with the malaria transmission model developed here. Model weights such as Logarithmic score and Continuous Ranked Probability Score (Bröcker 2012) that assess the reliability and sharpness of probabilistic projections could measure the ability of individual models in capturing the distribution of malaria. To combine the top models, Bayesian methods, or weighted averages could readily generate multi-model predictions using model weights indicative of past performance of individual model predictions relative to observations.

Model application for malaria control

Planning of anti-malaria products

The simulation and forecasting capabilities of the malaria model developed in this dissertation can be used to support information systems for malaria control planning and strategy. Indeed, systems capable of accurately simulating and forecasting the intensity and timing of seasonal outbreaks are necessary for effective allocation of control resources. Especially in high-burden regions where economic and logistic support for malaria control are limited and largely depend on international aid (World Health Organization 2019), such systems could aid the judicious targeting of limited resources.

Currently, insecticide treated bednets (ITNs), indoor residual spraying (IRS), and antimalaria drugs are the most effective options for controlling malaria incidence. Annual projections of the demand level for these malaria commodities must be made well in advance of campaigns to secure funding, raw materials, manufacture (World Health Organization 2015a; 2012a; 2017a), and ensure timely disbursement of these products to end users, such as health centers, retailers and local consumers. With further validation of its abilities to simulate and forecast malaria variability, the malaria forecasting system combined with malaria data from a more strengthened malaria surveillance system could inform procurement estimates of antimalarial products. Outputs of the model include malaria incidence in human hosts and the entomological inoculation rate (EIR), which are indicators of the burden of malaria and the intensity of transmission respectively. With proper calibration to most recent malaria activity, projections of malaria incidence or EIR could be obtained based on the latest modeled conditions of malaria. Average values of these model outputs and their uncertainties can in turn serve as

inputs in market demand analyses for anti-malaria commodities at regional or national levels (World Health Organization 2017a).

Real-time forecast for ongoing control

Another benefit of using a dynamical model framework driven by observed climate data is the ability to evaluate the effects of unprecedent climate events on future malaria transmission. The El Niño Southern Oscillation (ENSO) is a dominant irregular weather phenomenon that has been connected to changes in ecosystems and outbreaks of various infectious diseases, including malaria (Plisnier, Serneels, and Lambin 2000; Moore et al. 2017; Heaney, Shaman, and Alexander 2019; Anyamba et al. 2019; R. Sari Kovats et al. 2003; R. S. Kovats 2000). ENSO events occur as the result of abnormal variation in sea surface temperatures (SST) and winds over the Pacific Ocean that impact global atmospheric conditions (Rasmusson and Wallace 1983; Ropelewski and Halpert 1987). The effect of ENSO on rainfall activity varies across the globe. In many parts of sub-Saharan Africa where malaria endemicity is widespread, above average warming over the eastern Pacific Ocean (i.e. an El Niño event) is typically associated with anomalous wet conditions in East Africa and below-average rainfall in southern Africa (Fig. 1). However, during La Niña episodes (i.e. below average SSTs over the western Pacific), a contrary relationship with rainfall is typically observed in the same regions. With malaria, an anomalous change in surface moisture conditions is likely to significantly impact the availability and persistence of the temporary pools used by *Anopheles* mosquitoes for breeding– hence, the strong association between ENSO events and malaria (R. S. Kovats 2000). A weak but abnormal association between regional surface air temperature conditions and ENSO occurrence is also

thought to exist (Lin and Qian 2019; Z. Zhang and Krishnamurti 1996; Hoskins and Karoly 1981; Kushnir et al. 2002).

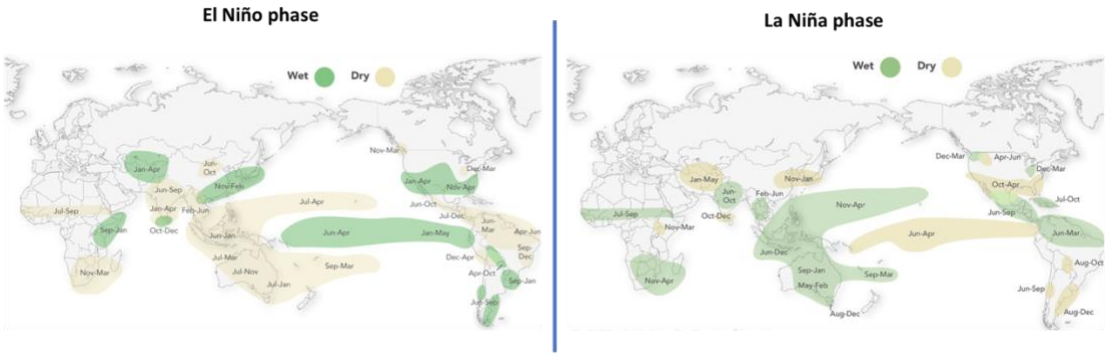

Figure 1. El Niño and global rainfall anomaly. Regions historically experiencing below average rainfall during El Niño/La Niña episodes are represented by yellow shadings and regions typically experiencing above normal wet conditions are indicated in green shading. Image credit: Lenssen, Nathan J. L., Lisa Goddard, and Simon Mason. 2020. "Seasonal Forecast Skill of ENSO Teleconnection Maps." Weather and Forecasting 35 (6): 2387–2406. https://doi.org/10.1175/WAF-D-19-0235.1.

In the malaria transmission model developed in this dissertation, surface moisture conditions regulate survivorship of aquatic-stage mosquitoes, while temperature conditions influence mosquito development, parasite sporogony and blood seeking behavior. These environmental effects combine with model time-evolving states of susceptibility and infection within host populations to dictate future disease trajectories. Although the ENSO phenomenon irregularly occurs, it is highly predictable as sea surface temperatures change very slowly, enabling forecast leads of 3-9 months (Cane, Zebiak, and Dolan 1986; Barnett et al. 1988). ENSO rainfall and temperature predictions (Kumar et al. 1996; Rowell 1998; Saha et al. 2014; S. Yang and Jiang 2014) coupled with the malaria forecasting system could enable more accurate probabilistic forecasts of malaria transmission and longer lead warnings of the anticipated effects of anomalous weather.

Characterizing local entomological profile for malaria control

Although malaria is a ubiquitous problem in communities around the globe, particularly in sub-Saharan Africa, the environmental and ecological conditions that govern local malaria dynamics can vary even for communities in the same region. For example, in the Rwanda study region, although moisture-regulated subadult development is a major determinant of seasonal risk, as shown in Chapter 1 of this dissertation, the magnitude of this effect varied within subpopulations. Like surface moisture, the relative importance of temperature can also differ within subregions. Rwanda has a varying mountainous geography, with arid lowlands in the south and east, and wet and humid highlands in the north and west. As a result, differences in thermal effects on vector and parasite exist between such communities across the regions.

For more effective and targeted malaria control, administered programs must account for differences in vector suitability and malaria susceptibility across localities. The climate-driven malaria transmission framework, paired more resolved climate data, can enable clearer investigation of the effects of ambient conditions on mosquito and parasite ecology at sub-regional scales, where control measures are typically implemented. Also, validating the climate-driven model against historical malaria activity could identify variables of major importance to entomological exposure, enabling emphasis on specific anti-malaria tools, such as source reduction (SR), larvicidal application, IRS, and ITN, to target relevant entomological pathways of malaria transmission.

Improving evaluation of the impact of malaria interventions

Although, climate plays a large role influencing the malaria dynamics of a region, it is seldom accounted for while assessing the impact of interventions. Though climate conditions play a large role in the seasonality of malaria, variability in climate conditions can cause unexpected outcomes during a season. Depending on timing and duration, climate events such as droughts (Kent et al. 2007; Poveda et al. 2001) or increased rainfall activity (Hashizume, Terao, and Minakawa 2009; K. A. Lindblade et al. 1999) (e.g. during ENSO) could cause a rise or fall in vector population dynamics and thereafter affect ongoing transmission. As a result, concurrent intervention efforts may experience enhanced impacts or counter-effects due to the influence of climate events. Failure to acknowledge possible climate effects during impact evaluation might misrepresent the true impact of control efforts (Yazoume Yé et al. 2017; Thomson et al. 2017). Indeed, future campaigns relying on such inadequately evaluated interventions could experience major reversals and inconsistency in outcomes should the prevailing variability in climate conditions differ.

Recently, several climate tools have been proposed to accompany impact evaluation of malaria interventions, some of which involve free parameters and covariance relationships (Thomson et al. 2017; Bhattarai et al. 2007; Aregawi et al. 2011). However, it is worth noting that ambient conditions influence malaria transmission by directly acting on vector and parasite ecology, through processes that are nonlinear and complex. Accounting for their impact on malaria incidence under time-evolving dynamical constructs could limit spurious associations and strengthen robustness of estimated effect sizes. The developed climate-driven malaria model provides a more realistic approach that simultaneously incorporates both climate and epidemiological factors of transmission. Within the model, anti-malaria measures could be

integrated as exogenous forces alongside climate modulation of vector and parasite activity in order to retrospectively assess the effects of climate on intervention outcomes. For example, data on timing and coverage of IRS could inform malaria entomological exposure within the dynamical model by altering the parameters controlling adult mortality rate, gonotrophy and oviposition frequency. Similarly, the proportion of susceptible and infected individuals available for vector contact could be adjusted by current ITN coverage data. This jointly-forced model can then be optimized by the model-inference system developed in Chapter 2. As the transmission model evolves over time host populations experience a net forcing effect resulting from climate conditions and from control measures dampening the force of infection. The contribution made by climate variability in the presence of control measures during a given period can subsequently be estimated by comparing the malaria outcomes predicted while using current and referent climate conditions (e.g. historical climate conditions) (Fig 2).

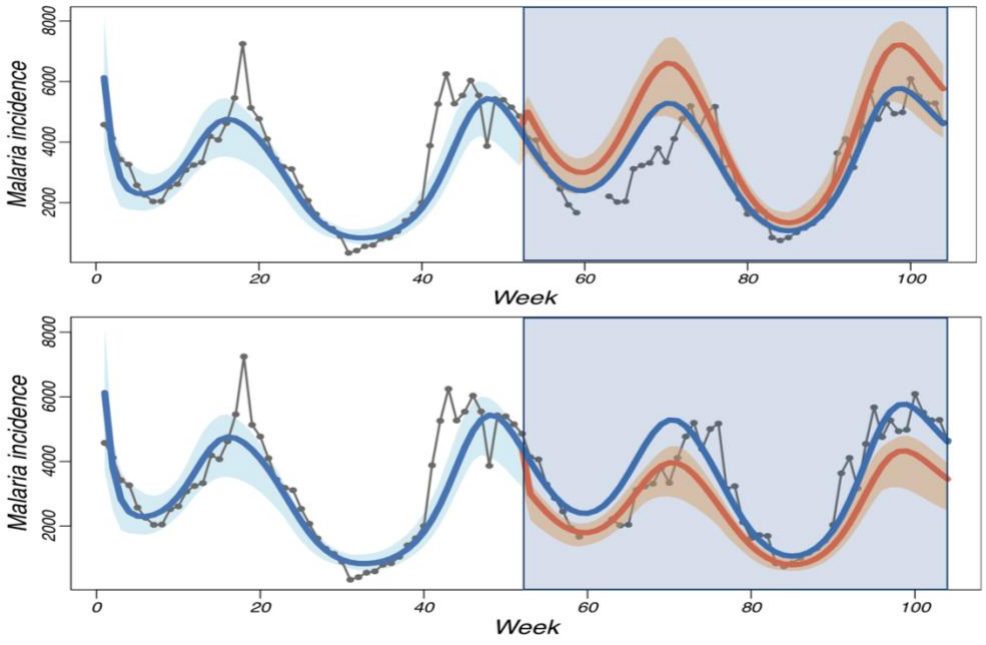

Figure 2. Counterfactual effects of climate variability while assessing the impact of concurrent control measures on malaria incidence. Model predicted malaria incidence under a hypothetical, jointly forced system using current climate and historical climate coupling are shown in

solid blue and orange lines respectively. The orange and blue shadings represent the 95% credible interval of the model incidence predictions. Solid lines and black dots indicate the observed malaria incidence, and the light blue shading highlights the window of interest for impact evaluation. The top panel indicates that climate variability may cause an overestimation of the impact of control efforts, given that current climate conditions, in the presence of current control measures, predicted a decrease in transmission (blue solid line) compared to historical climate variability (solid orange line). The bottom panel, on the other hand, suggests an underestimation of the impact of control efforts. A more impactful effect from control measures could have been observed had current climate conditions not been highly favorable to transmission (solid blue line) compared to historical conditions (solid orange line).

Importance to other vector-borne diseases

Although the modeling framework developed in this study is built for malaria, its implicit representation of transmission dynamics and direct representation of climate forcing could be transferred or applied to other vector-borne diseases such as dengue, filariasis or even Lyme disease. In such implicitly-forced model constructs, the force of transmission–the most relevant aspect of transmission– would be the focus. As shown here for malaria, simplifying assumptions around the force of transmission would allow adaptation to other disease systems in a biologically meaningful way without need for explicit or more complex representation of vector-host interactions. The transmission pressure experienced by the host population readily relates to pathogen transmissibility to host and the rate of vector-host contacts that are infective– the former being unique to the disease causative agent and the latter surmisable from the entomology of the disease vector.

Within the malaria framework, infective interactions between vector and host populations are captured through the Entomological Inoculation Rate (EIR), which describes the number of infective bites received per person per unit time. The EIR is an indicator of the transmission intensity and directly relates to the force of transmission (Smith and Ellis McKenzie 2004). It can be measured through sampling and field surveying of vector density, rates of pathogen infection in vector populations, and vector biting behavior, or estimated using mathematical derivations

informed by understanding of the entomology of the disease vector. These latter mathematical formulations, which indicate transmission intensity through the EIR or other measures, such as the reproductive number (R_0) and vectorial capacity (VC), convey the pressures experienced by hosts and have been used for malaria (Smith and Ellis McKenzie 2004), as employed in this study, and for other vector-borne diseases such as dengue, filariasis, and arboviruses (Smith et al. 2014; Kramer and Ciota 2015; Macdonald 1961; Zhu et al. 2016).

As observed in malaria, ambient conditions, including temperature and moisture conditions, can be a strong determinant of the transmission potential of many vector-borne diseases through ecological and biological processes, such as host-seeking, development rates, longevity, and pathogen transmissibility (Reisen, Fang, and Martinez 2006; Mordecai et al. 2019; Tesla et al. 2018; Delatte et al. 2009). And as acknowledged in this work, the use of these recognized relationships among climate, vector and pathogen, rather than indirect associations, could enhance the ecological grounding and utility of implicit model constructs of other vector-host dynamics influenced by climate.

Conclusion

Malaria imposes substantial public health and economic burden on many communities around the globe, particularly those in sub-Saharan Africa. Climate conditions play a large role in the seasonal variability, intensity and timing of malaria outbreaks due to multiple climate-regulated aspects of the malaria parasite and vector ecology. As the global gains made against malaria face continual threats from growing resistance to insecticide and anti-malaria drugs, closer attention to the roles of climate, ecology and the local environment in promoting transmission is warranted. In this regard, dynamical transmission models of malaria that account

for climate-mediated ecology and entomology of the malaria vector and parasite can help malaria control efforts to stay ahead of local malaria dynamics. This dissertation has focused on developing and validating an implicitly-forced transmission model framework capable of reproducing malaria transmission and leveraging the direct involvement of climate in the ecology of the malaria parasite and vector. The developed model framework advances the sophistication and abilities of implicitly-forced climate-based mathematical models of malaria transmission by improving their grounding in malaria entomology and imposes a more compelling, biologically-motivated environmental constraint. Without need for elaborate or more complex model representations, the model framework relatively accurately reproduces malaria transmission at various temporal and spatial scales while highlighting important vector and parasite connections to climate. This achievement demonstrates that lower dimension malaria transmission models can reproduce malaria activity, in a parsimonious manner, without compromising on relevant ecological variables that indicate potentially informative interactions between malaria and local conditions. Additionally, this study also developed a forecasting system comprised of the dynamical model and an iterative inference algorithm, similar to approaches used in numerical weather prediction (NWP) systems, which likewise demonstrated accurate prediction of future local malaria incidence. The descriptive capabilities and state-of-the-art forecasting capacity of the developed model framework doubly illustrate an important achievement for lower dimension process-based models of malaria transmission and highlight a key area of untapped potential in malaria forecasting. Efforts to monitor and control future risks of malaria could benefit from this parsimonious and powerful modeling form.

References

Abeku, Tarekegn A., Sake J. de Vlas, Gerard Borsboom, Awash Teklehaimanot, Asnakew Kebede, Dereje Olana, Gerrit J. van Oortmarssen, and J. D. F. Habbema. 2002. "Forecasting Malaria Incidence from Historical Morbidity Patterns in Epidemic-Prone Areas of Ethiopia: A Simple Seasonal Adjustment Method Performs Best." *Tropical Medicine & International Health: TM & IH* 7 (10): 851–57. https://doi.org/10.1046/j.1365-3156.2002.00924.x.

Abiodun, Gbenga J., Kevin Y. Njabo, Peter J. Witbooi, Abiodun M. Adeola, Trevon L. Fuller, Kazeem O. Okosun, Olusola S. Makinde, and Joel O. Botai. 2018. "Exploring the Influence of Daily Climate Variables on Malaria Transmission and Abundance of Anopheles Arabiensis over Nkomazi Local Municipality, Mpumalanga Province, South Africa." Research Article. Journal of Environmental and Public Health. Hindawi. October 9, 2018. https://doi.org/10.1155/2018/3143950.

Abiodun, Gbenga J., Peter J. Witbooi, Kazeem O. Okosun, and Rajendra Maharaj. 2018. "Exploring the Impact of Climate Variability on Malaria Transmission Using a Dynamic Mosquito-Human Malaria Model." *The Open Infectious Diseases Journal* 10 (1). https://doi.org/10.2174/1874279301810010088.

Adeola, Abiodun Morakinyo, Joel Ondego Botai, Jane Mukarugwiza Olwoch, Hannes C. J. De W Rautenbach, Omolola Mayowa Adisa, Christiaan De Jager, Christina M. Botai, and Mabuza Aaron. 2019. "Predicting Malaria Cases Using Remotely Sensed Environmental Variables in Nkomazi, South Africa." *Geospatial Health* 14 (1). https://doi.org/10.4081/gh.2019.676.

Agyapong, Jeffrey, Joseph Chabi, Aikins Ablorde, Worlasi D. Kartey, Joseph H.N. Osei, Dziedzom K. de Souza, Samuel Dadzie, et al. 2014. "Ovipositional Behavior of Anopheles Gambiae Mosquitoes." *Tropical Medicine and Health* 42 (4): 187–90. https://doi.org/10.2149/tmh.2014-13.

Alonso, David, Menno J. Bouma, and Mercedes Pascual. 2011. "Epidemic Malaria and Warmer Temperatures in Recent Decades in an East African Highland." *Proceedings of the Royal Society B: Biological Sciences* 278 (1712): 1661–69. https://doi.org/10.1098/rspb.2010.2020.

Alves, Fabiana Piovesan, Luiz Herman S. Gil, Mauro T. Marrelli, Paulo E. M. Ribolla, Erney P. Camargo, and Luiz Hildebrando Pereira Da Silva. 2005a. "Asymptomatic Carriers of Plasmodium Spp. as Infection Source for Malaria Vector Mosquitoes in the Brazilian Amazon." *Journal of Medical Entomology* 42 (5): 777–79. https://doi.org/10.1093/jmedent/42.5.777.

———. 2005b. "Asymptomatic Carriers of Plasmodium Spp. as Infection Source for Malaria Vector Mosquitoes in the Brazilian Amazon." *Journal of Medical Entomology* 42 (5): 777–79. https://doi.org/10.1093/jmedent/42.5.777.

A.N. Clements. 1992. *The Biology of Mosquitoes*. Chapman & Hall.

Anderson, Jeffrey L. 2001. “An Ensemble Adjustment Kalman Filter for Data Assimilation.” *Monthly Weather Review* 129 (12): 2884–2903. https://doi.org/10.1175/1520-0493(2001)129<2884:AEAKFF>2.0.CO;2.

Antonio-Nkondjio, Christophe, Clément Hinzoumbe Kerah, Frédéric Simard, Parfait Awono-Ambene, Mohamadou Chouaibou, Timoléon Tchuinkam, and Didier Fontenille. 2006. “Complexity of the Malaria Vectorial System in Cameroon: Contribution of Secondary Vectors to Malaria Transmission.” *Journal of Medical Entomology* 43 (6): 1215–21. https://doi.org/10.1603/0022-2585(2006)43[1215:cotmvs]2.0.co;2.

Anyamba, Assaf, Jean-Paul Chretien, Seth C. Britch, Radina P. Soebiyanto, Jennifer L. Small, Rikke Jepsen, Brett M. Forshey, et al. 2019. “Global Disease Outbreaks Associated with the 2015–2016 El Niño Event.” *Scientific Reports* 9 (1): 1930. https://doi.org/10.1038/s41598-018-38034-z.

Aregawi, Maru, Michael Lynch, Worku Bekele, Henok Kebede, Daddi Jima, Hiwot Solomon Taffese, Meseret Aseffa Yenehun, et al. 2014. “Time Series Analysis of Trends in Malaria Cases and Deaths at Hospitals and the Effect of Antimalarial Interventions, 2001–2011, Ethiopia.” *PLOS ONE* 9 (11): e106359. https://doi.org/10.1371/journal.pone.0106359.

Aregawi, Maru W, Abdullah S Ali, Abdul-wahiyd Al-mafazy, Fabrizio Molteni, Samson Katikiti, Marian Warsame, Ritha JA Njau, et al. 2011. “Reductions in Malaria and Anaemia Case and Death Burden at Hospitals Following Scale-up of Malaria Control in Zanzibar, 1999-2008.” *Malaria Journal* 10 (February): 46. https://doi.org/10.1186/1475-2875-10-46.

Asale, Abebe, Luc Duchateau, Brecht Devleesschauwer, Gerdien Huisman, and Delenasaw Yewhalaw. 2017. “Zooprophylaxis as a Control Strategy for Malaria Caused by the Vector Anopheles Arabiensis (Diptera: Culicidae): A Systematic Review.” *Infectious Diseases of Poverty* 6 (1): 160. https://doi.org/10.1186/s40249-017-0366-3.

Awolola, T. S., I. O. Oyewole, L. L. Koekemoer, and M. Coetzee. 2005. “Identification of Three Members of the Anopheles Funestus (Diptera: Culicidae) Group and Their Role in Malaria Transmission in Two Ecological Zones in Nigeria.” *Transactions of the Royal Society of Tropical Medicine and Hygiene* 99 (7): 525–31. https://doi.org/10.1016/j.trstmh.2004.12.003.

Baeza, Andres, Menno J. Bouma, Andy P. Dobson, Ramesh Dhiman, Harish C. Srivastava, and Mercedes Pascual. 2011. “Climate Forcing and Desert Malaria: The Effect of Irrigation.” *Malaria Journal* 10 (July): 190. https://doi.org/10.1186/1475-2875-10-190.

Baidjoe, Amrish Y., Jennifer Stevenson, Philip Knight, William Stone, Gillian Stresman, Victor Osoti, Euniah Makori, et al. 2016. “Factors Associated with High Heterogeneity of

Malaria at Fine Spatial Scale in the Western Kenyan Highlands." *Malaria Journal* 15 (1): 307. https://doi.org/10.1186/s12936-016-1362-y.

Baird, J. K. 1998. "Age-Dependent Characteristics of Protection v. Susceptibility to Plasmodium Falciparum." *Annals of Tropical Medicine and Parasitology* 92 (4): 367–90. https://doi.org/10.1080/00034989859366.

Barnett, T., N. Graham, M. Cane, S. Zebiak, S. Dolan, J. O'brien, and D. Legler. 1988. "On the Prediction of the El Niño of 1986-1987." *Science* 241 (4862): 192–96. https://doi.org/10.1126/science.241.4862.192.

Baton, Luke A., and Lisa C. Ranford-Cartwright. 2005. "Spreading the Seeds of Million-Murdering Death." *Trends in Parasitology* 21 (12): 573–80. https://doi.org/10.1016/j.pt.2005.09.012.

Battle, Katherine E., Donal Bisanzio, Harry S. Gibson, Samir Bhatt, Ewan Cameron, Daniel J. Weiss, Bonnie Mappin, et al. 2016. "Treatment-Seeking Rates in Malaria Endemic Countries." *Malaria Journal* 15 (1): 20. https://doi.org/10.1186/s12936-015-1048-x.

Bayoh, M. N., and S. W. Lindsay. 2003. "Effect of Temperature on the Development of the Aquatic Stages of Anopheles Gambiae Sensu Stricto (Diptera: Culicidae)." *Bulletin of Entomological Research* 93 (5): 375–81. https://doi.org/10.1079/BER2003259.

———. 2004. "Temperature-Related Duration of Aquatic Stages of the Afrotropical Malaria Vector Mosquito Anopheles Gambiae in the Laboratory." *Medical and Veterinary Entomology* 18 (2): 174–79. https://doi.org/10.1111/j.0269-283X.2004.00495.x.

Bayoh, Mohamed Nabie. 2001. "Studies on the Development and Survival of Anopheles Gambiae Sensu Stricto at Various Temperatures and Relative Humidities." Doctoral, Durham University. http://etheses.dur.ac.uk/4952/.

Beck, Louisa R., Bradley M. Lobitz, and Byron L. Wood. 2000. "Remote Sensing and Human Health: New Sensors and New Opportunities." *Emerg Infect Dis.* 3 (6): 217–27. https://doi.org/10.3201/eid0603.000301.

Becker, Norbert, Dusan Petric, Marija Zgomba, Clive Boase, Minoo Madon, Christine Dahl, and Achim Kaiser. 2010. *Mosquitoes and Their Control*. Berlin, Heidelberg: Springer Berlin Heidelberg. http://link.springer.com/10.1007/978-3-540-92874-4.

Beier, J. C., R. Copeland, C. Oyaro, A. Masinya, W. O. Odago, S. Oduor, D. K. Koech, and C. R. Roberts. 1990. "Anopheles Gambiae Complex Egg-Stage Survival in Dry Soil from Larval Development Sites in Western Kenya." *Journal of the American Mosquito Control Association* 6 (1): 105–9.

Berzosa, Pedro, Aida de Lucio, María Romay-Barja, Zaida Herrador, Vicenta González, Luz García, Amalia Fernández-Martínez, et al. 2018. "Comparison of Three Diagnostic Methods (Microscopy, RDT, and PCR) for the Detection of Malaria Parasites in

Representative Samples from Equatorial Guinea." *Malaria Journal* 17 (September). https://doi.org/10.1186/s12936-018-2481-4.

Bhadra, Anindya, Edward L. Ionides, Karina Laneri, Mercedes Pascual, Menno Bouma, and Ramesh C. Dhiman. 2011. "Malaria in Northwest India: Data Analysis via Partially Observed Stochastic Differential Equation Models Driven by Lévy Noise." *Journal of the American Statistical Association* 106 (494): 440–51. https://doi.org/10.1198/jasa.2011.ap10323.

Bhattarai, Achuyt, Abdullah S Ali, S. Patrick Kachur, Andreas Mårtensson, Ali K Abbas, Rashid Khatib, Abdul-wahiyd Al-mafazy, et al. 2007. "Impact of Artemisinin-Based Combination Therapy and Insecticide-Treated Nets on Malaria Burden in Zanzibar." *PLoS Medicine* 4 (11). https://doi.org/10.1371/journal.pmed.0040309.

Bigoga, Jude D., Lucien Manga, Vincent PK Titanji, Maureen Coetzee, and Rose GF Leke. 2007. "Malaria Vectors and Transmission Dynamics in Coastal South-Western Cameroon." *Malaria Journal* 6 (1): 5. https://doi.org/10.1186/1475-2875-6-5.

Bloland, PB, and HA Williams. 2002. "Epidemiology of Malaria." In *Malaria Control during Mass Population Movements and Natural Disasters.* Washington (DC): National Academies Press (US).

Bødker, R., J. Akida, D. Shayo, W. Kisinza, H. A. Msangeni, E. M. Pedersen, and S. W. Lindsay. 2003. "Relationship between Altitude and Intensity of Malaria Transmission in the Usambara Mountains, Tanzania." *Journal of Medical Entomology* 40 (5): 706–17. https://doi.org/10.1603/0022-2585-40.5.706.

Bomblies, Arne, Jean-Bernard Duchemin, and EAB Eltahir. 2008. "Hydrology of Malaria: Model Development and Application to a Sahelian Village." *Water Resources Research* 44 (12). https://doi.org/10.1029/2008WR006917.

Boudin, C., M. Olivier, J. F. Molez, J. P. Chiron, and P. Ambroise-Thomas. 1993. "High Human Malarial Infectivity to Laboratory-Bred Anopheles Gambiae in a Village in Burkina Faso." *The American Journal of Tropical Medicine and Hygiene* 48 (5): 700–706. https://doi.org/10.4269/ajtmh.1993.48.700.

Bousema, Teun, Chris Drakeley, Samwel Gesase, Ramadhan Hashim, Stephen Magesa, Frank Mosha, Silas Otieno, et al. 2010. "Identification of Hot Spots of Malaria Transmission for Targeted Malaria Control." *The Journal of Infectious Diseases* 201 (11): 1764–74. https://doi.org/10.1086/652456.

Boyd, Mark F., and S. F. Kitchen. 1937. "The Duration of the Intrinsic Incubation Period in Falciparum Malaria in Relation to Certain Factors Affecting the Parasites1." *The American Journal of Tropical Medicine and Hygiene* s1-17 (6): 845–48. https://doi.org/10.4269/ajtmh.1937.s1-17.845.

Brabin, B. J. 1983. “An Analysis of Malaria in Pregnancy in Africa.” *Bulletin of the World Health Organization* 61 (6): 1005–16.

Brady, Oliver J., H. Charles J. Godfray, Andrew J. Tatem, Peter W. Gething, Justin M. Cohen, F. Ellis McKenzie, T. Alex Perkins, et al. 2015. “Adult Vector Control, Mosquito Ecology and Malaria Transmission.” *International Health* 7 (2): 121–29. https://doi.org/10.1093/inthealth/ihv010.

Brady, Oliver J., H. Charles J. Godfray, Andrew J. Tatem, Peter W. Gething, Justin M. Cohen, F. Ellis McKenzie, T. Alex Perkins, et al. 2016. “Vectorial Capacity and Vector Control: Reconsidering Sensitivity to Parameters for Malaria Elimination.” *Transactions of The Royal Society of Tropical Medicine and Hygiene* 110 (2): 107–17. https://doi.org/10.1093/trstmh/trv113.

Bretscher, Michael T., Nicolas Maire, Nakul Chitnis, Ingrid Felger, Seth Owusu-Agyei, and Tom Smith. 2011. “The Distribution of Plasmodium Falciparum Infection Durations.” *Epidemics* 3 (2): 109–18. https://doi.org/10.1016/j.epidem.2011.03.002.

Briere, Jean-Francois, Pascale Pracros, Alain-Yves Le Roux, and Jean-Sebastien Pierre. 1999. “A Novel Rate Model of Temperature-Dependent Development for Arthropods.” *Environmental Entomology* 28 (1): 22–29. https://doi.org/10.1093/ee/28.1.22.

Bröcker, Jochen. 2012. “Evaluating Raw Ensembles with the Continuous Ranked Probability Score.” *Quarterly Journal of the Royal Meteorological Society* 138 (667): 1611–17. https://doi.org/10.1002/qj.1891.

Brooker, Simon, Siân Clarke, Joseph Kiambo Njagi, Sarah Polack, Benbolt Mugo, Benson Estambale, Eric Muchiri, Pascal Magnussen, and Jonathan Cox. 2004. “Spatial Clustering of Malaria and Associated Risk Factors during an Epidemic in a Highland Area of Western Kenya.” *Tropical Medicine & International Health* 9 (7): 757–66. https://doi.org/10.1111/j.1365-3156.2004.01272.x.

Bruce-Chwatt, LJ. 1988. “History of Malaria from Prehistory to Eradication.” In *Wernsdorfer W, Editor; , McGregor I, Editor. , Eds. Malaria: Principles and Practice of Microbiology.*, 1st ed. Edinburgh, United Kingdom: Churchill Livingstone. http://www.ncbi.nlm.nih.gov/books/NBK234333/.

Caminade, Cyril, Sari Kovats, Joacim Rocklov, Adrian M. Tompkins, Andrew P. Morse, Felipe J. Colón-González, Hans Stenlund, Pim Martens, and Simon J. Lloyd. 2014. “Impact of Climate Change on Global Malaria Distribution.” *Proceedings of the National Academy of Sciences of the United States of America* 111 (9): 3286–91. https://doi.org/10.1073/pnas.1302089111.

Cane, Mark A., Stephen E. Zebiak, and Sean C. Dolan. 1986. “Experimental Forecasts of El Niño.” *Nature* 321 (6073): 827–32. https://doi.org/10.1038/321827a0.

Caputo, Beniamino, Davis Nwakanma, Musa Jawara, Majidah Adiamoh, Ibrahima Dia, Lassana Konate, Vincenzo Petrarca, David J. Conway, and Alessandra della Torre. 2008. "Anopheles Gambiae Complex along The Gambia River, with Particular Reference to the Molecular Forms of An. Gambiae s.s." *Malaria Journal* 7 (1): 182. https://doi.org/10.1186/1475-2875-7-182.

Ceccato, Pietro, Christelle Vancutsem, Robert Klaver, James Rowland, and Stephen J. Connor. 2012. "A Vectorial Capacity Product to Monitor Changing Malaria Transmission Potential in Epidemic Regions of Africa, A Vectorial Capacity Product to Monitor Changing Malaria Transmission Potential in Epidemic Regions of Africa." *Journal of Tropical Medicine, Journal of Tropical Medicine* 2012, 2012 (January): e595948. https://doi.org/10.1155/2012/595948, 10.1155/2012/595948.

Charlwood, J. D., and P. M. Graves. 1987. "The Effect of Permethrin-Impregnated Bednets on a Population of Anopheles Farauti in Coastal Papua New Guinea." *Medical and Veterinary Entomology* 1 (3): 319–27. https://doi.org/10.1111/j.1365-2915.1987.tb00361.x.

Church, L. W. Preston, Thong P. Le, Joe P. Bryan, Daniel M. Gordon, Robert Edelman, Louis Fries, Jonathan R. Davis, et al. 1997. "Clinical Manifestations of Plasmodium Falciparum Malaria Experimentally Induced by Mosquito Challenge." *The Journal of Infectious Diseases* 175 (4): 915–20. https://doi.org/10.1086/513990.

Churcher, Thomas S., Robert E. Sinden, Nick J. Edwards, Ian D. Poulton, Thomas W. Rampling, Patrick M. Brock, Jamie T. Griffin, et al. 2017a. "Probability of Transmission of Malaria from Mosquito to Human Is Regulated by Mosquito Parasite Density in Naïve and Vaccinated Hosts." *PLoS Pathogens* 13 (1). https://doi.org/10.1371/journal.ppat.1006108.

———. 2017b. "Probability of Transmission of Malaria from Mosquito to Human Is Regulated by Mosquito Parasite Density in Naïve and Vaccinated Hosts." *PLoS Pathogens* 13 (1). https://doi.org/10.1371/journal.ppat.1006108.

Cisse, Badara, Matthew Cairns, Ernest Faye, Ousmane NDiaye, Babacar Faye, Cecile Cames, Yue Cheng, et al. 2009. "Randomized Trial of Piperaquine with Sulfadoxine-Pyrimethamine or Dihydroartemisinin for Malaria Intermittent Preventive Treatment in Children." *PloS One* 4 (9): e7164. https://doi.org/10.1371/journal.pone.0007164.

Clark, Robert L. 2009. "Embryotoxicity of the Artemisinin Antimalarials and Potential Consequences for Use in Women in the First Trimester." *Reproductive Toxicology (Elmsford, N.Y.)* 28 (3): 285–96. https://doi.org/10.1016/j.reprotox.2009.05.002.

Clark, Tamara D., Bryan Greenhouse, Denise Njama-Meya, Bridget Nzarubara, Catherine Maiteki-Sebuguzi, Sarah G. Staedke, Edmund Seto, Moses R. Kamya, Philip J. Rosenthal, and Grant Dorsey. 2008. "Factors Determining the Heterogeneity of Malaria Incidence in Children in Kampala, Uganda." *The Journal of Infectious Diseases* 198 (3): 393–400. https://doi.org/10.1086/589778.

Coetzee, M., and D. Fontenille. 2004. “Advances in the Study of Anopheles Funestus, a Major Vector of Malaria in Africa.” *Insect Biochemistry and Molecular Biology* 34 (7): 599–605. https://doi.org/10.1016/j.ibmb.2004.03.012.

Collins, William E., and Geoffrey M. Jeffery. 2003. “A Retrospective Examination of Mosquito Infection on Humans Infected with Plasmodium Falciparum.” *The American Journal of Tropical Medicine and Hygiene* 68 (3): 366–71.

Coluzzi, M. 1999. “The Clay Feet of the Malaria Giant and Its African Roots: Hypotheses and Inferences about Origin, Spread and Control of Plasmodium Falciparum.” *Parassitologia* 41 (1–3): 277–83.

Constable A & Co. 1824. “Essays Descriptive and Moral on Scenes in Italy, Switzerland, and France. By an American.” *The North American Review* 18 (42): 192–204.

Craig, M. H., R. W. Snow, D. le Sueur, M. H. Craig, R. W. Snow, D. le Sueur, M. H. Craig, R. W. Snow, and D. le Sueur. 1999. “A Climate-Based Distribution Model of Malaria Transmission in Sub-Saharan Africa.” *Parasitology Today* 15 (3): 105–11. https://doi.org/10.1016/S0169-4758(99)01396-4.

Cunningham, Jane, Sophie Jones, Michelle L. Gatton, John W. Barnwell, Qin Cheng, Peter L. Chiodini, Jeffrey Glenn, et al. 2019. “A Review of the WHO Malaria Rapid Diagnostic Test Product Testing Programme (2008–2018): Performance, Procurement and Policy.” *Malaria Journal* 18 (1): 387. https://doi.org/10.1186/s12936-019-3028-z.

DeFelice, Nicholas B., Eliza Little, Scott R. Campbell, and Jeffrey Shaman. 2017. “Ensemble Forecast of Human West Nile Virus Cases and Mosquito Infection Rates.” *Nature Communications* 8 (February): 14592. https://doi.org/10.1038/ncomms14592.

DeFelice, Nicholas B., Zachary D. Schneider, Eliza Little, Christopher Barker, Kevin A. Caillouet, Scott R. Campbell, Dan Damian, et al. 2018. “Use of Temperature to Improve West Nile Virus Forecasts.” *PLOS Computational Biology* 14 (3): e1006047. https://doi.org/10.1371/journal.pcbi.1006047.

Delatte, H., G. Gimonneau, A. Triboire, and D. Fontenille. 2009. “Influence of Temperature on Immature Development, Survival, Longevity, Fecundity, and Gonotrophic Cycles of Aedes Albopictus, Vector of Chikungunya and Dengue in the Indian Ocean.” *Journal of Medical Entomology* 46 (1): 33–41. https://doi.org/10.1603/033.046.0105.

Dhiman, Sunil. 2019. “Are Malaria Elimination Efforts on Right Track? An Analysis of Gains Achieved and Challenges Ahead.” *Infectious Diseases of Poverty* 8 (1): 14. https://doi.org/10.1186/s40249-019-0524-x.

Diabaté, Abdoulaye, Roch K. Dabiré, Kyle Heidenberger, Jacob Crawford, William O. Lamp, Lauren E. Culler, and Tovi Lehmann. 2008. “Evidence for Divergent Selection between

the Molecular Forms of Anopheles Gambiae: Role of Predation." *BMC Evolutionary Biology* 8 (1): 5. https://doi.org/10.1186/1471-2148-8-5.

Diabaté, Abdoulaye, Roch K. Dabire, Eun H. Kim, Ryan Dalton, Niama Millogo, Thierry Baldet, Frederic Simard, John E. Gimnig, William A. Hawley, and Tovi Lehmann. 2005. "Larval Development of the Molecular Forms of Anopheles Gambiae (Diptera: Culicidae) in Different Habitats: A Transplantation Experiment." *Journal of Medical Entomology* 42 (4): 548–53. https://doi.org/10.1093/jmedent/42.4.548.

Dinku, T., P. Ceccato, E. Grover-Kopec, M. Lemma, S. J. Connor, and C. F. Ropelewski. 2007. "Validation of Satellite Rainfall Products over East Africa's Complex Topography." *International Journal of Remote Sensing* 28 (7): 1503–26. https://doi.org/10.1080/01431160600954688.

Dinku, T, Chris Funk, Pete Peterson, Ross Maidment, Tsegaye Tadesse, Hussein Gadain, and Pietro Ceccato. 2018. "Validation of the CHIRPS Satellite Rainfall Estimates over Eastern Africa." *Quarterly Journal of the Royal Meteorological Society* 144 (S1): 292–312. https://doi.org/10.1002/qj.3244.

Dlamini, Sabelo Nick, Anton Beloconi, Sizwe Mabaso, Penelope Vounatsou, Benido Impouma, and Ibrahima Socé Fall. 2019. "Review of Remotely Sensed Data Products for Disease Mapping and Epidemiology." *Remote Sensing Applications: Society and Environment* 14 (April): 108–18. https://doi.org/10.1016/j.rsase.2019.02.005.

Donnelly, Blánaid, Lea Berrang-Ford, Nancy A. Ross, and Pascal Michel. 2015. "A Systematic, Realist Review of Zooprophylaxis for Malaria Control." *Malaria Journal* 14 (1): 313. https://doi.org/10.1186/s12936-015-0822-0.

Doolan, Denise L., Carlota Dobaño, and J. Kevin Baird. 2009. "Acquired Immunity to Malaria." *Clinical Microbiology Reviews* 22 (1): 13–36. https://doi.org/10.1128/CMR.00025-08.

Drakeley, Chris, Colin Sutherland, J. Teun Bousema, Robert W. Sauerwein, and Geoffrey A. T. Targett. 2006. "The Epidemiology of Plasmodium Falciparum Gametocytes: Weapons of Mass Dispersion." *Trends in Parasitology* 22 (9): 424–30. https://doi.org/10.1016/j.pt.2006.07.001.

Duan, Si-Bo, Zhao-Liang Li, Hua Li, Frank-M. Göttsche, Hua Wu, Wei Zhao, Pei Leng, Xia Zhang, and César Coll. 2019. "Validation of Collection 6 MODIS Land Surface Temperature Product Using in Situ Measurements." *Remote Sensing of Environment* 225 (May): 16–29. https://doi.org/10.1016/j.rse.2019.02.020.

Duffy, P. E., and M. Fried. 2005. "Malaria in the Pregnant Woman." *Current Topics in Microbiology and Immunology* 295: 169–200. https://doi.org/10.1007/3-540-29088-5_7.

Ebhuoma, Osadolor, and Michael Gebreslasie. 2016. "Remote Sensing-Driven Climatic/Environmental Variables for Modelling Malaria Transmission in Sub-Saharan

Africa." *International Journal of Environmental Research and Public Health* 13 (6). https://doi.org/10.3390/ijerph13060584.

Eling, W., J. Hooghof, M. G. van de Vegte-Bolmer, and Robert W. Sauerwein. 2001a. "Tropical Temperatures Can Inhibit Development of the Human Malaria Parasite Plasmodium Falciparum in the Mosquito." In .

———. 2001b. "Tropical Temperatures Can Inhibit Development of the Human Malaria Parasite Plasmodium Falciparum in the Mosquito." In .

Ermert, Volker, Andreas H. Fink, Anne E. Jones, and Andrew P. Morse. 2011. "Development of a New Version of the Liverpool Malaria Model. II. Calibration and Validation for West Africa." *Malaria Journal* 10 (1): 62. https://doi.org/10.1186/1475-2875-10-62.

Ernst, Kacey C., Samson O. Adoka, Dickens O. Kowuor, Mark L. Wilson, and Chandy C. John. 2006. "Malaria Hotspot Areas in a Highland Kenya Site Are Consistent in Epidemic and Non-Epidemic Years and Are Associated with Ecological Factors." *Malaria Journal* 5 (September): 78. https://doi.org/10.1186/1475-2875-5-78.

Faye, O., L. Konate, J. Mouchet, D. Fontenille, N. Sy, G. Hebrard, and J. P. Herve. 1997. "Indoor Resting by Outdoor Biting Females of Anopheles Gambiae Complex (Diptera:Culicidae) in the Sahel of Northern Senegal." *Journal of Medical Entomology* 34 (3): 285–89. https://doi.org/10.1093/jmedent/34.3.285.

Felger, Ingrid, Martin Maire, Michael T. Bretscher, Nicole Falk, André Tiaden, Wilson Sama, Hans-Peter Beck, Seth Owusu-Agyei, and Thomas A. Smith. 2012. "The Dynamics of Natural Plasmodium Falciparum Infections." *PLOS ONE* 7 (9): e45542. https://doi.org/10.1371/journal.pone.0045542.

Fernandes, Luís, and Hans Briegel. 2005. "Reproductive Physiology of Anopheles Gambiae and Anopheles Atroparvus." *Journal of Vector Ecology : Journal of the Society for Vector Ecology*.

Filipe, João A. N., Eleanor M. Riley, Christopher J. Drakeley, Colin J. Sutherland, and Azra C. Ghani. 2007. "Determination of the Processes Driving the Acquisition of Immunity to Malaria Using a Mathematical Transmission Model." *PLOS Computational Biology* 3 (12): e255. https://doi.org/10.1371/journal.pcbi.0030255.

Funk, Chris, Pete Peterson, Martin Landsfeld, Diego Pedreros, James Verdin, Shraddhanand Shukla, Gregory Husak, et al. 2015. "The Climate Hazards Infrared Precipitation with Stations—a New Environmental Record for Monitoring Extremes." *Scientific Data* 2 (1): 1–21. https://doi.org/10.1038/sdata.2015.66.

Funk, Chris, Pete Peterson, Seth Peterson, Shraddhanand Shukla, Frank Davenport, Joel Michaelsen, Kenneth R. Knapp, et al. 2019. "A High-Resolution 1983–2016 Tmax Climate Data Record Based on Infrared Temperatures and Stations by the Climate

Hazard Center." *Journal of Climate* 32 (17): 5639–58. https://doi.org/10.1175/JCLI-D-18-0698.1.

Gagnon, Alexandre S., Karen E. Smoyer-Tomic, and Andrew B. G. Bush. 2002. "The El Niño Southern Oscillation and Malaria Epidemics in South America." *International Journal of Biometeorology* 46 (2): 81–89. https://doi.org/10.1007/s00484-001-0119-6.

Gallup, John Luke, and Jeffrey D. Sachs. 2001. *The Economic Burden of Malaria*. *The Intolerable Burden of Malaria: A New Look at the Numbers: Supplement to Volume 64(1) of the American Journal of Tropical Medicine and Hygiene*. American Society of Tropical Medicine and Hygiene. http://www.ncbi.nlm.nih.gov/books/NBK2624/.

Gaudart, Jean, Ousmane Touré, Nadine Dessay, A. Lassane Dicko, Stéphane Ranque, Loic Forest, Jacques Demongeot, and Ogobara K. Doumbo. 2009. "Modelling Malaria Incidence with Environmental Dependency in a Locality of Sudanese Savannah Area, Mali." *Malaria Journal* 8 (April): 61. https://doi.org/10.1186/1475-2875-8-61.

Gebetsberger, Manuel, Jakob W. Messner, Georg J. Mayr, and Achim Zeileis. 2018. "Estimation Methods for Nonhomogeneous Regression Models: Minimum Continuous Ranked Probability Score versus Maximum Likelihood." *Monthly Weather Review* 146 (12): 4323–38. https://doi.org/10.1175/MWR-D-17-0364.1.

Gething, Peter W., Anand P. Patil, David L. Smith, Carlos A. Guerra, Iqbal RF Elyazar, Geoffrey L. Johnston, Andrew J. Tatem, and Simon I. Hay. 2011. "A New World Malaria Map: Plasmodium Falciparum Endemicity in 2010." *Malaria Journal* 10 (1): 378. https://doi.org/10.1186/1475-2875-10-378.

Gething, Peter W, Thomas P Van Boeckel, David L Smith, Carlos A Guerra, Anand P Patil, Robert W Snow, and Simon I Hay. 2011. "Modelling the Global Constraints of Temperature on Transmission of Plasmodium Falciparum and P. Vivax." *Parasites & Vectors* 4 (May): 92. https://doi.org/10.1186/1756-3305-4-92.

Ghani, Azra C., Colin J. Sutherland, Eleanor M. Riley, Chris J. Drakeley, Jamie T. Griffin, Roly D. Gosling, and Joao A. N. Filipe. 2009. "Loss of Population Levels of Immunity to Malaria as a Result of Exposure-Reducing Interventions: Consequences for Interpretation of Disease Trends." *PLoS ONE* 4 (2). https://doi.org/10.1371/journal.pone.0004383.

Gillies, M. T. 1953. "The Duration of the Gonotrophic Cycle in Anopheles Gambiae and Anopheles Funestus, with a Note on the Efficiency of Hand Catching." *East African Medical Journal* 30 (4): 129–35.

Gillies, M. T., and B. De Meillon. 1968. "The Anophelinae of Africa south of the Sahara (Ethiopian Zoogeographical Region)." *The Anophelinae of Africa south of the Sahara (Ethiopian Zoogeographical Region).* https://www.cabdirect.org/cabdirect/abstract/19692900946.

Gimnig, J. E., M. Ombok, L. Kamau, and W. A. Hawley. 2001. "Characteristics of Larval Anopheline (Diptera: Culicidae) Habitats in Western Kenya." *Journal of Medical Entomology* 38 (2): 282–88. https://doi.org/10.1603/0022-2585-38.2.282.

Gneiting, Tilmann, Adrian E. Raftery, Anton H. Westveld, and Tom Goldman. 2005. "Calibrated Probabilistic Forecasting Using Ensemble Model Output Statistics and Minimum CRPS Estimation." *Monthly Weather Review* 133 (5): 1098–1118. https://doi.org/10.1175/MWR2904.1.

Gomez-Elipe, Alberto, Angel Otero, Michel van Herp, and Armando Aguirre-Jaime. 2007. "Forecasting Malaria Incidence Based on Monthly Case Reports and Environmental Factors in Karuzi, Burundi, 1997–2003." *Malaria Journal* 6 (1): 129. https://doi.org/10.1186/1475-2875-6-129.

Greenwood, B. M. 1989. "The Microepidemiology of Malaria and Its Importance to Malaria Control." *Transactions of the Royal Society of Tropical Medicine and Hygiene* 83 Suppl: 25–29. https://doi.org/10.1016/0035-9203(89)90599-3.

Griffin, Jamie T., Neil M. Ferguson, and Azra C. Ghani. 2014. "Estimates of the Changing Age-Burden of Plasmodium Falciparum Malaria Disease in Sub-Saharan Africa." *Nature Communications* 5: 3136. https://doi.org/10.1038/ncomms4136.

Gupta, Sunetra, Robert W. Snow, Christl A. Donnelly, Kevin Marsh, and Chris Newbold. 1999. "Immunity to Non-Cerebral Severe Malaria Is Acquired after One or Two Infections." *Nature Medicine* 5 (3): 340–43. https://doi.org/10.1038/6560.

Hakizimana, Emmanuel, Corine Karema, Dunia Munyakanage, John Githure, Jean Baptiste Mazarati, Jon Eric Tongren, Willem Takken, Agnes Binagwaho, and Constantianus J. M. Koenraadt. 2018. "Spatio-Temporal Distribution of Mosquitoes and Risk of Malaria Infection in Rwanda." *Acta Tropica* 182 (June): 149–57. https://doi.org/10.1016/j.actatropica.2018.02.012.

Hashizume, Masahiro, Toru Terao, and Noboru Minakawa. 2009. "The Indian Ocean Dipole and Malaria Risk in the Highlands of Western Kenya." *Proceedings of the National Academy of Sciences of the United States of America* 106 (6): 1857–62. https://doi.org/10.1073/pnas.0806544106.

Hauser, Gaël, Kevin Thiévent, and J. Koella. 2019. "The Ability of Anopheles Gambiae Mosquitoes to Bite through a Permethrin-Treated Net and the Consequences for Their Fitness." *Undefined*. /paper/The-ability-of-Anopheles-gambiae-mosquitoes-to-bite-Hauser-Thi%C3%A9vent/549352dfd46064fdeefa4858023d905d71f581b9.

Hay, Simon I., David J. Rogers, Jonathan F. Toomer, and Robert W. Snow. 2000. "Annual Plasmodium Falciparum Entomological Inoculation Rates (EIR) across Africa: Literature Survey, Internet Access and Review." *Transactions of The Royal Society of Tropical Medicine and Hygiene* 94 (2): 113–27. https://doi.org/10.1016/S0035-9203(00)90246-3.

Hay, Simon I., Marianne E. Sinka, Robi M. Okara, Caroline W. Kabaria, Philip M. Mbithi, Carolynn C. Tago, David Benz, et al. 2010. "Developing Global Maps of the Dominant Anopheles Vectors of Human Malaria." *PLOS Medicine* 7 (2): e1000209. https://doi.org/10.1371/journal.pmed.1000209.

Heaney, Alexandra K., Kathleen A. Alexander, and Jeffrey Shaman. 2020. "Ensemble Forecast and Parameter Inference of Childhood Diarrhea in Chobe District, Botswana." *Epidemics* 30 (March): 100372. https://doi.org/10.1016/j.epidem.2019.100372.

Heaney, Alexandra K., Jeffrey Shaman, and Kathleen A. Alexander. 2019. "El Niño-Southern Oscillation and under-5 Diarrhea in Botswana." *Nature Communications* 10 (1): 5798. https://doi.org/10.1038/s41467-019-13584-6.

Henninger, Sascha M. 2013. "Does the Global Warming Modify the Local Rwandan Climate?" *Natural Science* 5 (1): 124–29. https://doi.org/10.4236/ns.2013.51A019.

Hogg, J. C., and H. Hurd. 1997. "The Effects of Natural Plasmodium Falciparum Infection on the Fecundity and Mortality of Anopheles Gambiae s. l. in North East Tanzania." *Parasitology* 114 (Pt 4) (April): 325–31.

Hogg, J. C., M. C. Thomson, and H. Hurd. 1996. "Comparative Fecundity and Associated Factors for Two Sibling Species of the Anopheles Gambiae Complex Occurring Sympatrically in The Gambia." *Medical and Veterinary Entomology* 10 (4): 385–91.

Holstein, M. H. 1954. "Biology of Anopheles Gambiae. Research in French West Africa." World Health Organization. /paper/Biology-of-Anopheles-gambiae.-Research-in-French-Holstein/dae2a67bf4c02efffbf32b48dbecd2f1802115a6.

Hoshen, Moshe B., and Andrew P. Morse. 2004. "A Weather-Driven Model of Malaria Transmission." *Malaria Journal* 3: 32. https://doi.org/10.1186/1475-2875-3-32.

Hoskins, Brian J., and David J. Karoly. 1981. "The Steady Linear Response of a Spherical Atmosphere to Thermal and Orographic Forcing." *Journal of Atmospheric Sciences* 38 (June): 1179–96. https://doi.org/10.1175/1520-0469(1981)038<1179:TSLROA>2.0.CO;2.

Institute of Medicine. 2004a. "Malaria Control." In *Arrow KJ, Panosian C, Gelband H, Editors. Saving Lives, Buying Time: Economics of Malaria Drugs in an Age of Resistance.* Washington, DC.: National Academies Press (US). http://www.ncbi.nlm.nih.gov/books/NBK215634/.

———. 2004b. "The Human and Economic Burden of Malaria." In *Arrow KJ, Panosian C, Gelband H, Editors. Saving Lives, Buying Time: Economics of Malaria Drugs in an Age of Resistance.* Washington, DC.: National Academies Press (US). http://www.ncbi.nlm.nih.gov/books/NBK215634/.

———. 2004c. “The Parasite, the Mosquito, and the Disease.” In *Arrow KJ, Panosian C, Gelband H, Editors. Saving Lives, Buying Time: Economics of Malaria Drugs in an Age of Resistance.* Washington, DC.: National Academies Press (US). http://www.ncbi.nlm.nih.gov/books/NBK215634/.

Jacobs, A. F. G., B. G. Heusinkveld, and J. P. Nieveen. 1998. “Temperature Behavior of a Natural Shallow Water Body during a Summer Period.” *Theoretical and Applied Climatology* 59 (1): 121–27. https://doi.org/10.1007/s007040050017.

Jacobs, Adrie F. G., Bert G. Heusinkveld, Aline Kraai, and Krijn P. Paaijmans. 2008. “Diurnal Temperature Fluctuations in an Artificial Small Shallow Water Body.” *International Journal of Biometeorology* 52 (4): 271–80. https://doi.org/10.1007/s00484-007-0121-8.

Jeffery, Geoffrey M., and Don E. Eyles. 1955. “Infectivity to Mosquitoes of Plasmodium Falciparum as Related to Gametocyte Density and Duration of Infection1.” *The American Journal of Tropical Medicine and Hygiene* 4 (5): 781–89. https://doi.org/10.4269/ajtmh.1955.4.781.

Jewson, Stephen, Anders Brix, and Christine Ziehmann. 2004. “A New Parametric Model for the Assessment and Calibration of Medium-Range Ensemble Temperature Forecasts.” *Atmospheric Science Letters* 5 (5): 96–102. https://doi.org/10.1002/asl.69.

Johansson, Michael A., Karyn M. Apfeldorf, Scott Dobson, Jason Devita, Anna L. Buczak, Benjamin Baugher, Linda J. Moniz, et al. 2019. “An Open Challenge to Advance Probabilistic Forecasting for Dengue Epidemics.” *Proceedings of the National Academy of Sciences* 116 (48): 24268–74. https://doi.org/10.1073/pnas.1909865116.

Jones, Anne E., and Andrew P. Morse. 2010. “Application and Validation of a Seasonal Ensemble Prediction System Using a Dynamic Malaria Model.” *Journal of Climate* 23 (15): 4202–15. https://doi.org/10.1175/2010JCLI3208.1.

Kabbale, Fredrick G., Anne M. Akol, John B. Kaddu, and Ambrose W. Onapa. 2013. “Biting Patterns and Seasonality of Anopheles Gambiae Sensu Lato and Anopheles Funestus Mosquitoes in Kamuli District, Uganda.” *Parasites & Vectors* 6 (December): 340. https://doi.org/10.1186/1756-3305-6-340.

Kakuru, Abel, Prasanna Jagannathan, Emmanuel Arinaitwe, Humphrey Wanzira, Mary Muhindo, Victor Bigira, Emmanuel Osilo, et al. 2013. “The Effects of ACT Treatment and TS Prophylaxis on Plasmodium Falciparum Gametocytemia in a Cohort of Young Ugandan Children.” *The American Journal of Tropical Medicine and Hygiene* 88 (4): 736–43. https://doi.org/10.4269/ajtmh.12-0654.

Kambi, Maixent Olivier C., Zhenhui Wang, and Georges Gulemvuga. 2018. “Determination of the Correlation between the Air Temperature Measured in Situ and Remotely Sensed Data from MODIS and SEVIRI in Congo-Brazzaville.” *Atmospheric and Climate Sciences* 8 (2): 192–211. https://doi.org/10.4236/acs.2018.82013.

Kamya, Moses R., Adoke Yeka, Hasifa Bukirwa, Myers Lugemwa, John B. Rwakimari, Sarah G. Staedke, Ambrose O. Talisuna, et al. 2007. "Artemether-Lumefantrine versus Dihydroartemisinin-Piperaquine for Treatment of Malaria: A Randomized Trial." *PLoS Clinical Trials* 2 (5): e20. https://doi.org/10.1371/journal.pctr.0020020.

Karema, Corine, Shawn Wen, Abigail Sidibe, Jennifer L. Smith, Roly Gosling, Emmanuel Hakizimana, Marcel Tanner, Abdisalan M. Noor, and Allison Tatarsky. 2020. "History of Malaria Control in Rwanda: Implications for Future Elimination in Rwanda and Other Malaria-Endemic Countries." *Malaria Journal* 19 (October). https://doi.org/10.1186/s12936-020-03407-1.

Karspeck, Alicia R., and Jeffrey L. Anderson. 2007. "Experimental Implementation of an Ensemble Adjustment Filter for an Intermediate ENSO Model." *Journal of Climate* 20 (18): 4638–58. https://doi.org/10.1175/JCLI4245.1.

Kashiwada, Momoyo, and Shunji Ohta. 2010. "Modeling the Spatio-Temporal Distribution of the Anopheles Mosquito Based on Life History and Surface Water Conditions." *The Open Ecology Journal* 3 (1). https://benthamopen.com/ABSTRACT/TOECOLJ-3-1-29.

Kawada, Hitoshi, Kazunori Ohashi, Gabriel O. Dida, George Sonye, Sammy M. Njenga, Charles Mwandawiro, and Noboru Minakawa. 2014. "Preventive Effect of Permethrin-Impregnated Long-Lasting Insecticidal Nets on the Blood Feeding of Three Major Pyrethroid-Resistant Malaria Vectors in Western Kenya." *Parasites & Vectors* 7 (1): 383. https://doi.org/10.1186/1756-3305-7-383.

Keegan, Lindsay T., and Jonathan Dushoff. 2013. "Population-Level Effects of Clinical Immunity to Malaria." *BMC Infectious Diseases* 13 (1): 428. https://doi.org/10.1186/1471-2334-13-428.

Kent, Rebekah J., Philip E. Thuma, Sungano Mharakurwa, and Douglas E. Norris. 2007. "Seasonality, Blood Feeding Behavior, and Transmission of Plasmodium Falciparum by Anopheles Arabiensis after an Extended Drought in Southern Zambia." *The American Journal of Tropical Medicine and Hygiene* 76 (2): 267–74.

Kinyanjui, Samson M., David J. Conway, David E. Lanar, and Kevin Marsh. 2007. "IgG Antibody Responses to Plasmodium Falciparum Merozoite Antigens in Kenyan Children Have a Short Half-Life." *Malaria Journal* 6 (1): 82. https://doi.org/10.1186/1475-2875-6-82.

Koenraadt, Constantianus JM, Krijn P. Paaijmans, Andrew K. Githeko, Bart GJ Knols, and Willem Takken. 2003. "Egg Hatching, Larval Movement and Larval Survival of the Malaria Vector Anopheles Gambiae in Desiccating Habitats." *Malaria Journal* 2 (July): 20. https://doi.org/10.1186/1475-2875-2-20.

Kovats, R. S. 2000. “El Niño and Human Health.” *Bulletin of the World Health Organization* 78 (9): 1127–35.

Kovats, R. Sari, Menno J. Bouma, Shakoor Hajat, Eve Worrall, and Andy Haines. 2003. “El Niño and Health.” *Lancet (London, England)* 362 (9394): 1481–89. https://doi.org/10.1016/S0140-6736(03)14695-8.

Kramer, Laura D., and Alexander T. Ciota. 2015. “Dissecting Vectorial Capacity for Mosquito-Borne Viruses.” *Current Opinion in Virology* 15 (December): 112–18. https://doi.org/10.1016/j.coviro.2015.10.003.

Kreuels, Benno, Robin Kobbe, Samuel Adjei, Christina Kreuzberg, Claudia von Reden, Kathrin Bäter, Stefan Klug, Wibke Busch, Ohene Adjei, and Jürgen May. 2008. “Spatial Variation of Malaria Incidence in Young Children from a Geographically Homogeneous Area with High Endemicity.” *The Journal of Infectious Diseases* 197 (1): 85–93. https://doi.org/10.1086/524066.

Krishnamurti, T. N., C. M. Kishtawal, Timothy E. LaRow, David R. Bachiochi, Zhan Zhang, C. Eric Williford, Sulochana Gadgil, and Sajani Surendran. 1999. “Improved Weather and Seasonal Climate Forecasts from Multimodel Superensemble.” *Science* 285 (5433): 1548–50. https://doi.org/10.1126/science.285.5433.1548.

Kulkarni, M. A., E. Kweka, E. Nyale, E. Lyatuu, F. W. Mosha, D. Chandramohan, M. E. Rau, and C. Drakeley. 2006. “Entomological Evaluation of Malaria Vectors at Different Altitudes in Hai District, Northeastern Tanzania.” *Journal of Medical Entomology* 43 (3): 580–88. https://doi.org/10.1603/0022-2585(2006)43[580:eeomva]2.0.co;2.

Kumar, A., M. Hoerling, M. Ji, A. Leetmaa, and P. Sardeshmukh. 1996. “Assessing a GCM’s Suitability for Making Seasonal Predictions.” *Journal of Climate* 9 (1): 115–29. https://doi.org/10.1175/1520-0442(1996)009<0115:AAGSFM>2.0.CO;2.

Kushnir, Y., W. A. Robinson, I. Bladé, N. M. J. Hall, S. Peng, and R. Sutton. 2002. “Atmospheric GCM Response to Extratropical SST Anomalies: Synthesis and Evaluation.” *Journal of Climate* 15 (16): 2233–56. https://doi.org/10.1175/1520-0442(2002)015<2233:AGRTES>2.0.CO;2.

Laneri, Karina, Anindya Bhadra, Edward L. Ionides, Menno Bouma, Ramesh C. Dhiman, Rajpal S. Yadav, and Mercedes Pascual. 2010a. “Forcing versus Feedback: Epidemic Malaria and Monsoon Rains in Northwest India.” *PLoS Computational Biology* 6 (9): e1000898. https://doi.org/10.1371/journal.pcbi.1000898.

———. 2010b. “Forcing Versus Feedback: Epidemic Malaria and Monsoon Rains in Northwest India.” *PLOS Computational Biology* 6 (9): e1000898. https://doi.org/10.1371/journal.pcbi.1000898.

Laneri, Karina, Richard E. Paul, Adama Tall, Joseph Faye, Fatoumata Diene-Sarr, Cheikh Sokhna, Jean-François Trape, and Xavier Rodó. 2015. “Dynamical Malaria Models

Reveal How Immunity Buffers Effect of Climate Variability." *Proceedings of the National Academy of Sciences* 112 (28): 8786–91. https://doi.org/10.1073/pnas.1419047112.

Langhorne, Jean, Francis M. Ndungu, Anne-Marit Sponaas, and Kevin Marsh. 2008. "Immunity to Malaria: More Questions than Answers." *Nature Immunology* 9 (7): 725–32. https://doi.org/10.1038/ni.f.205.

Lardeux, Frédéric J., Rosenka H. Tejerina, Vicente Quispe, and Tamara K. Chavez. 2008. "A Physiological Time Analysis of the Duration of the Gonotrophic Cycle of Anopheles Pseudopunctipennis and Its Implications for Malaria Transmission in Bolivia." *Malaria Journal* 7: 141. https://doi.org/10.1186/1475-2875-7-141.

Lebel, Thierry, and Abou Amani. 1999. "Rainfall Estimation in the Sahel: What Is the Ground Truth?" *Journal of Applied Meteorology and Climatology* 38 (5): 555–68. https://doi.org/10.1175/1520-0450(1999)038<0555:REITSW>2.0.CO;2.

Lengeler, Christian. 2004. "Insecticide-treated Bed Nets and Curtains for Preventing Malaria." *Cochrane Database of Systematic Reviews*, no. 2. https://doi.org/10.1002/14651858.CD000363.pub2.

Li, Ruiyun, Lei Xu, Ottar N. Bjørnstad, Keke Liu, Tie Song, Aifang Chen, Bing Xu, Qiyong Liu, and Nils C. Stenseth. 2019. "Climate-Driven Variation in Mosquito Density Predicts the Spatiotemporal Dynamics of Dengue." *Proceedings of the National Academy of Sciences* 116 (9): 3624–29. https://doi.org/10.1073/pnas.1806094116.

Lighthill, Michael James, John Michael Tutill Thompson, A. K. Sen, A. G. M. Last, D. J. Tritton, Basil John Mason, P. Mathias, and John Hugh - Na3923 Westcott. 1986. "The Recently Recognized Failure of Predictability in Newtonian Dynamics." *Proceedings of the Royal Society of London. A. Mathematical and Physical Sciences* 407 (1832): 35–50. https://doi.org/10.1098/rspa.1986.0082.

Lin, Jialin, and Taotao Qian. 2019. "A New Picture of the Global Impacts of El Nino-Southern Oscillation." *Scientific Reports* 9 (1): 17543. https://doi.org/10.1038/s41598-019-54090-5.

Lindblade, K. A., E. D. Walker, A. W. Onapa, J. Katungu, and M. L. Wilson. 1999. "Highland Malaria in Uganda: Prospective Analysis of an Epidemic Associated with El Niño." *Transactions of the Royal Society of Tropical Medicine and Hygiene* 93 (5): 480–87. https://doi.org/10.1016/s0035-9203(99)90344-9.

Lindblade, Kim A., Laura Steinhardt, Aaron Samuels, S. Patrick Kachur, and Laurence Slutsker. 2013. "The Silent Threat: Asymptomatic Parasitemia and Malaria Transmission." *Expert Review of Anti-Infective Therapy* 11 (6): 623–39. https://doi.org/10.1586/eri.13.45.

Lindsay, S. W., and W. J. Martens. 1998. “Malaria in the African Highlands: Past, Present and Future.” *Bulletin of the World Health Organization* 76 (1): 33–45.

Lindsay, S W, L Parson, and C J Thomas. 1998. “Mapping the Ranges and Relative Abundance of the Two Principal African Malaria Vectors, Anopheles Gambiae Sensu Stricto and An. Arabiensis, Using Climate Data.” *Proceedings of the Royal Society B: Biological Sciences* 265 (1399): 847–54.

Lou, Yijun, and Xiao-Qiang Zhao. 2010. “A Climate-Based Malaria Transmission Model with Structured Vector Population.” *SIAM Journal on Applied Mathematics* 70 (6): 2023–44. https://doi.org/10.1137/080744438.

Luo, Lifeng, Alan Robock, Kenneth E. Mitchell, Paul R. Houser, Eric F. Wood, John C. Schaake, Dag Lohmann, et al. 2003. “Validation of the North American Land Data Assimilation System (NLDAS) Retrospective Forcing over the Southern Great Plains.” *Journal of Geophysical Research: Atmospheres* 108 (D22): 8843. https://doi.org/10.1029/2002JD003246.

Lyimo, Edith O., and W. Takken. 1993. “Effects of Adult Body Size on Fecundity and the Pre-Gravid Rate of Anopheles Gambiae Females in Tanzania.” *Medical and Veterinary Entomology* 7 (4): 328–32. https://doi.org/10.1111/j.1365-2915.1993.tb00700.x.

Lyon, Bradfield, Tufa Dinku, Anita Raman, and Madeleine C. Thomson. 2017. “Temperature Suitability for Malaria Climbing the Ethiopian Highlands.” *Environmental Research Letters* 12 (6): 064015. https://doi.org/10.1088/1748-9326/aa64e6.

Macdonald, G. 1956. “Epidemiological Basis of Malaria Control.” *Bulletin of the World Health Organization* 15 (3–5): 613–26.

Macdonald, George. 1957. *The Epidemiology and Control of Malaria.* Oxford University Press.

———. 1961. “Epidemiologic Models in Studies of Vetor-Borne Diseases.” *Public Health Reports* 76 (9): 753–64.

Mahande, Aneth, Franklin Mosha, Johnson Mahande, and Eliningaya Kweka. 2007. “Feeding and Resting Behaviour of Malaria Vector, Anopheles Arabiensis with Reference to Zooprophylaxis.” *Malaria Journal* 6 (July): 100. https://doi.org/10.1186/1475-2875-6-100.

Mahmoudi, Shima, and Hossein Keshavarz. 2017. “Efficacy of Phase 3 Trial of RTS, S/AS01 Malaria Vaccine: The Need for an Alternative Development Plan.” *Human Vaccines & Immunotherapeutics* 13 (9): 2098–2101. https://doi.org/10.1080/21645515.2017.1295906.

Maloney, Kathleen, Abigail Ward, Bonnie Krenz, Nora Petty, Lindsay Bryson, Caitlin Dolkart, Theodoor Visser, et al. 2017. “Expanding Access to Parasite-Based Malaria Diagnosis through Retail Drug Shops in Tanzania: Evidence from a Randomized Trial and

Implications for Treatment." *Malaria Journal* 16 (1): 6. https://doi.org/10.1186/s12936-016-1658-y.

Mandal, Sandip, Ram Rup Sarkar, and Somdatta Sinha. 2011. "Mathematical Models of Malaria - a Review." *Malaria Journal* 10: 202. https://doi.org/10.1186/1475-2875-10-202.

Matuschewski, Kai. 2006. "Getting Infectious: Formation and Maturation of Plasmodium Sporozoites in the Anopheles Vector." *Cellular Microbiology* 8 (10): 1547–56. https://doi.org/10.1111/j.1462-5822.2006.00778.x.

Mayne, Bruce. 1926. "Notes on the Influence of Temperature and Humidity on Oviposition and Early Life of Anopheles." *Public Health Reports (1896-1970)* 41 (21): 986–90. https://doi.org/10.2307/4577885.

McCann, Robert S., Joseph P. Messina, David W. MacFarlane, M. Nabie Bayoh, John M. Vulule, John E. Gimnig, and Edward D. Walker. 2014. "Modeling Larval Malaria Vector Habitat Locations Using Landscape Features and Cumulative Precipitation Measures." *International Journal of Health Geographics* 13 (1): 17. https://doi.org/10.1186/1476-072X-13-17.

McGowan, Craig J., Matthew Biggerstaff, Michael Johansson, Karyn M. Apfeldorf, Michal Ben-Nun, Logan Brooks, Matteo Convertino, et al. 2019. "Collaborative Efforts to Forecast Seasonal Influenza in the United States, 2015–2016." *Scientific Reports* 9 (1): 683. https://doi.org/10.1038/s41598-018-36361-9.

Menendez, C. 1995. "Malaria during Pregnancy: A Priority Area of Malaria Research and Control." *Parasitology Today (Personal Ed.)* 11 (5): 178–83. https://doi.org/10.1016/0169-4758(95)80151-0.

———. 2006. "Malaria during Pregnancy." *Current Molecular Medicine* 6 (2): 269–73. https://doi.org/10.2174/156652406776055186.

Meremikwu, Martin M., Sarah Donegan, David Sinclair, Ekpereonne Esu, and Chioma Oringanje. 2012. "Intermittent Preventive Treatment for Malaria in Children Living in Areas with Seasonal Transmission." *The Cochrane Database of Systematic Reviews*, no. 2 (February): CD003756. https://doi.org/10.1002/14651858.CD003756.pub4.

Midekisa, Alemayehu, Gabriel Senay, Geoffrey M Henebry, Paulos Semuniguse, and Michael C Wimberly. 2012. "Remote Sensing-Based Time Series Models for Malaria Early Warning in the Highlands of Ethiopia." *Malaria Journal* 11 (May): 165. https://doi.org/10.1186/1475-2875-11-165.

Mildrexler, David J., Maosheng Zhao, and Steven W. Running. 2011. "A Global Comparison between Station Air Temperatures and MODIS Land Surface Temperatures Reveals the Cooling Role of Forests." *Journal of Geophysical Research: Biogeosciences* 116 (G3). https://doi.org/10.1029/2010JG001486.

Miller, Max J. 1958. “Observations on the Natural History of Malaria in the Semi-Resistant West African.” *Transactions of The Royal Society of Tropical Medicine and Hygiene* 52 (2): 152–68. https://doi.org/10.1016/0035-9203(58)90036-1.

Minakawa, N., C. M. Mutero, J. I. Githure, J. C. Beier, and G. Yan. 1999. “Spatial Distribution and Habitat Characterization of Anopheline Mosquito Larvae in Western Kenya.” *The American Journal of Tropical Medicine and Hygiene* 61 (6): 1010–16. https://doi.org/10.4269/ajtmh.1999.61.1010.

Minakawa, Noboru, George Sonye, Motoyoshi Mogi, Andre Githeko, and Guiyun Yan. 2002. “The Effects of Climatic Factors on the Distribution and Abundance of Malaria Vectors in Kenya.” *Journal of Medical Entomology* 39 (6): 833–41. https://doi.org/10.1603/0022-2585-39.6.833.

Ministry of Health (MoH). 2016. “Health Surveillance & Emergency Preparedness & Response.” Rwanda Biomedical Centre. 2016. https://rbc.gov.rw/index.php?id=697.

Ministry of Health, Rwanda. 2017. “Rwanda Malaria Indicator Survey (RMIS) 2017.” Rwanda Biomedical Center. Kigali, Rwanda, and Rockville, Maryland, USA: MOPDD and ICF.

M.J. Lehane. 2005. *The Biology of Blood-Sucking Insects.* Cambridge University Press.

Moore, Sean M., Andrew S. Azman, Benjamin F. Zaitchik, Eric D. Mintz, Joan Brunkard, Dominique Legros, Alexandra Hill, et al. 2017. “El Niño and the Shifting Geography of Cholera in Africa.” *Proceedings of the National Academy of Sciences* 114 (17): 4436–41. https://doi.org/10.1073/pnas.1617218114.

Mordecai, Erin A., Jamie M. Caldwell, Marissa K. Grossman, Catherine A. Lippi, Leah R. Johnson, Marco Neira, Jason R. Rohr, et al. 2019. “Thermal Biology of Mosquito-Borne Disease.” *Ecology Letters* 22 (10): 1690–1708. https://doi.org/10.1111/ele.13335.

Mordecai, Erin A., Krijn P. Paaijmans, Leah R. Johnson, Christian Balzer, Tal Ben-Horin, Emily de Moor, Amy McNally, et al. 2013. “Optimal Temperature for Malaria Transmission Is Dramatically Lower than Previously Predicted.” *Ecology Letters* 16 (1): 22–30. https://doi.org/10.1111/ele.12015.

Murindahabi, Marilyn Milumbu, Willem Takken, Xavier Misago, Elias Niyituma, Jackie Umupfasoni, Emmanuel Hakizimana, Arnold J. H. van Vliet, et al. 2021. “Monitoring Mosquito Nuisance for the Development of a Citizen Science Approach for Malaria Vector Surveillance in Rwanda.” *Malaria Journal* 20 (1): 36. https://doi.org/10.1186/s12936-020-03579-w.

Mutuku, Francis M., Jane A. Alaii, M. Nabie Bayoh, John E. Gimnig, John M. Vulule, Edward D. Walker, Ephantus Kabiru, and William A. Hawley. 2006. “Distribution, Description, and Local Knowledge of Larval Habitats of Anopheles Gambiae s.l. in a Village in

Western Kenya." *The American Journal of Tropical Medicine and Hygiene* 74 (1): 44–53.

National Institute of Statistics of Rwanda. 2012. "Rwanda Demographic and Health Survey 2010." NISR, MOH, ICF International, Calverton, Maryland, USA.
———. 2015a. "Rwanda Demographic and Health Survey 2014-15."
———. 2015b. "Rwanda Demographic and Health Survey 2014-15." National Institute of Statistics of Rwanda (NISR) [Rwanda].

Noden, B. H., M. D. Kent, and J. C. Beier. 1995. "The Impact of Variations in Temperature on Early Plasmodium Falciparum Development in Anopheles Stephensi." *Parasitology* 111 (Pt 5) (December): 539–45. https://doi.org/10.1017/s0031182000077003.

Norris, Laura C., Christen M. Fornadel, Wei-Chien Hung, Fernando J. Pineda, and Douglas E. Norris. 2010. "Frequency of Multiple Blood Meals Taken in a Single Gonotrophic Cycle by Anopheles Arabiensis Mosquitoes in Macha, Zambia." *The American Journal of Tropical Medicine and Hygiene* 83 (1): 33–37. https://doi.org/10.4269/ajtmh.2010.09-0296.

Nyirakanani, Chantal, Raymond Chibvongodze, Lenson Kariuki, Michael Habtu, Moses Masika, Dunstan Mukoko, and Kato J. Njunwa. 2017. "Characterization of Malaria Vectors in Huye District, Southern Rwanda." *Tanzania Journal of Health Research* 19 (3). https://doi.org/10.4314/thrb.v19i3.

Ogunfowokan, Oluwagbenga, Bamidele A. Ogunfowokan, and Anthony I. Nwajei. 2020. "Sensitivity and Specificity of Malaria Rapid Diagnostic Test (MRDT CareStatTM) Compared with Microscopy amongst under Five Children Attending a Primary Care Clinic in Southern Nigeria." *African Journal of Primary Health Care & Family Medicine* 12 (1). https://doi.org/10.4102/phcfm.v12i1.2212.

Okal, Michael N., Benjamin Francis, Manuela Herrera-Varela, Ulrike Fillinger, and Steven W. Lindsay. 2013. "Water Vapour Is a Pre-Oviposition Attractant for the Malaria Vector Anopheles Gambiae Sensu Stricto." *Malaria Journal* 12 (1): 365. https://doi.org/10.1186/1475-2875-12-365.

Olayemi, I. K., A. T. Ande, A. V. Ayanwale, A. Z. Mohammed, I. M. Bello, B. Idris, B. Isah, V. Chukwuemeka, and A. C. Ukubuiwe. 2011. "Seasonal Trends in Epidemiological and Entomological Profiles of Malaria Transmission in North Central Nigeria." *Pakistan Journal of Biological Sciences: PJBS* 14 (4): 293–99. https://doi.org/10.3923/pjbs.2011.293.299.

O'Meara, Wendy Prudhomme, Judith Nekesa Mangeni, Rick Steketee, and Brian Greenwood. 2010. "Changes in the Burden of Malaria in Sub-Saharan Africa." *The Lancet. Infectious Diseases* 10 (8): 545–55. https://doi.org/10.1016/S1473-3099(10)70096-7.

Omumbo, Judith A., Bradfield Lyon, Samuel M. Waweru, Stephen J. Connor, and Madeleine C. Thomson. 2011. "Raised Temperatures over the Kericho Tea Estates: Revisiting the Climate in the East African Highlands Malaria Debate." *Malaria Journal* 10: 12. https://doi.org/10.1186/1475-2875-10-12.

Paaijmans, K. P., A. F. G. Jacobs, W. Takken, B. G. Heusinkveld, A. K. Githeko, M. Dicke, and A. A. M. Holtslag. 2008. "Observations and Model Estimates of Diurnal Water Temperature Dynamics in Mosquito Breeding Sites in Western Kenya." *Hydrological Processes* 22 (November): 4789–4801. https://doi.org/10.1002/hyp.7099.

Paaijmans, Krijn P, Susan S Imbahale, Matthew B Thomas, and Willem Takken. 2010. "Relevant Microclimate for Determining the Development Rate of Malaria Mosquitoes and Possible Implications of Climate Change." *Malaria Journal* 9 (July): 196. https://doi.org/10.1186/1475-2875-9-196.

Paaijmans, Krijn P., Andrew F. Read, and Matthew B. Thomas. 2009. "Understanding the Link between Malaria Risk and Climate." *Proceedings of the National Academy of Sciences* 106 (33): 13844–49. https://doi.org/10.1073/pnas.0903423106.

Paaijmans, Krijn P., Moses O. Wandago, Andrew K. Githeko, and Willem Takken. 2007. "Unexpected High Losses of Anopheles Gambiae Larvae Due to Rainfall." *PLoS ONE* 2 (11). https://doi.org/10.1371/journal.pone.0001146.

Parham, Paul Edward, and Edwin Michael. 2010. "Modeling the Effects of Weather and Climate Change on Malaria Transmission." *Environmental Health Perspectives* 118 (5): 620–26. https://doi.org/10.1289/ehp.0901256.

Pates, Helen, and Christopher Curtis. 2005. "Mosquito Behavior and Vector Control." *Annual Review of Entomology* 50: 53–70. https://doi.org/10.1146/annurev.ento.50.071803.130439.

Patz, Jonathan A. 1998. "Predicting Key Malaria Transmission Factors, Biting and Entomological Inoculation Rates, Using Modelled Soil Moisture in Kenya." *Tropical Medicine & International Health* 3 (10): 818–27. https://doi.org/10.1046/j.1365-3156.1998.00309.x.

Pei, Sen, Flaviano Morone, Fredrik Liljeros, Hernán Makse, and Jeffrey L Shaman. 2018. "Inference and Control of the Nosocomial Transmission of Methicillin-Resistant Staphylococcus Aureus." *ELife* 7. https://doi.org/10.7554/eLife.40977.

Penny, Melissa A., Nicolas Maire, Caitlin A. Bever, Peter Pemberton-Ross, Olivier J. T. Briët, David L. Smith, Peter W. Gething, and Thomas A. Smith. 2015. "Distribution of Malaria Exposure in Endemic Countries in Africa Considering Country Levels of Effective Treatment." *Malaria Journal* 14 (1): 384. https://doi.org/10.1186/s12936-015-0864-3.

Piegorsch, W. W. 1990. “Maximum Likelihood Estimation for the Negative Binomial Dispersion Parameter.” *Biometrics* 46 (3): 863–67.

Plisnier, P. D., S. Serneels, and E. F. Lambin. 2000. “Impact of ENSO on East African Ecosystems: A Multivariate Analysis Based on Climate and Remote Sensing Data.” *Global Ecology and Biogeography* 9 (6): 481–97.

Pluess, Bianca, Frank C. Tanser, Christian Lengeler, and Brian L. Sharp. 2010. “Indoor Residual Spraying for Preventing Malaria.” *The Cochrane Database of Systematic Reviews*, no. 4 (April): CD006657. https://doi.org/10.1002/14651858.CD006657.pub2.

Poveda, G., W. Rojas, M. L. Quiñones, I. D. Vélez, R. I. Mantilla, D. Ruiz, J. S. Zuluaga, and G. L. Rua. 2001. “Coupling between Annual and ENSO Timescales in the Malaria-Climate Association in Colombia.” *Environmental Health Perspectives* 109 (5): 489–93. https://doi.org/10.1289/ehp.01109489.

R Core Team. 2019. *R: A Language and Environment for Statistical Computing.* Vienna, Austria.: R Foundation for Statistical Computing. https://www.R-project.org/.

Rasmusson, Eugene M., and John M. Wallace. 1983. “Meteorological Aspects of the El Niño/Southern Oscillation.” *Science* 222 (4629): 1195–1202. https://doi.org/10.1126/science.222.4629.1195.

Reich, Nicholas G., Craig J. McGowan, Teresa K. Yamana, Abhinav Tushar, Evan L. Ray, Dave Osthus, Sasikiran Kandula, et al. 2019. “Accuracy of Real-Time Multi-Model Ensemble Forecasts for Seasonal Influenza in the U.S.” *PLOS Computational Biology* 15 (11): e1007486. https://doi.org/10.1371/journal.pcbi.1007486.

Reisen, William K., Ying Fang, and Vincent M. Martinez. 2006. “Effects of Temperature on the Transmission of West Nile Virus by Culex Tarsalis (Diptera: Culicidae).” *Journal of Medical Entomology* 43 (2): 309–17. https://doi.org/10.1603/0022-2585(2006)043[0309:EOTOTT]2.0.CO;2.

Ropelewski, C. F., and M. S. Halpert. 1987. “Global and Regional Scale Precipitation Patterns Associated with the El Niño/Southern Oscillation.” *Monthly Weather Review* 115 (8): 1606–26. https://doi.org/10.1175/1520-0493(1987)115<1606:GARSPP>2.0.CO;2.

Ross, Ronald. 1899. “Mosquitos and Malaria: The Infection of Birds by Mosquitos.” *British Medical Journal* 1 (1990): 432–33.
———. 1915. “Some a Priori Pathometric Equations.” *British Medical Journal* 1 (2830): 546–47.

Rowell, David P. 1998. “Assessing Potential Seasonal Predictability with an Ensemble of Multidecadal GCM Simulations.” *Journal of Climate* 11 (2): 109–20. https://doi.org/10.1175/1520-0442(1998)011<0109:APSPWA>2.0.CO;2.

Ruiz, Daniel, Cyrille Brun, Stephen J Connor, Judith A Omumbo, Bradfield Lyon, and Madeleine C Thomson. 2014. “Testing a Multi-Malaria-Model Ensemble against 30 Years of Data in the Kenyan Highlands.” *Malaria Journal* 13 (May): 206. https://doi.org/10.1186/1475-2875-13-206.

Ruktanonchai, Nick W., Patrick DeLeenheer, Andrew J. Tatem, Victor A. Alegana, T. Trevor Caughlin, Elisabeth zu Erbach-Schoenberg, Christopher Lourenço, Corrine W. Ruktanonchai, and David L. Smith. 2016. “Identifying Malaria Transmission Foci for Elimination Using Human Mobility Data.” *PLOS Computational Biology* 12 (4): e1004846. https://doi.org/10.1371/journal.pcbi.1004846.

Saha, Suranjana, Shrinivas Moorthi, Xingren Wu, Jiande Wang, Sudhir Nadiga, Patrick Tripp, David Behringer, et al. 2014. “The NCEP Climate Forecast System Version 2.” *Journal of Climate* 27 (6): 2185–2208. https://doi.org/10.1175/JCLI-D-12-00823.1.

Sama, W., K. Dietz, and T. Smith. 2006. “Distribution of Survival Times of Deliberate Plasmodium Falciparum Infections in Tertiary Syphilis Patients.” *Transactions of the Royal Society of Tropical Medicine and Hygiene* 100 (9): 811–16. https://doi.org/10.1016/j.trstmh.2005.11.001.

Sama, Wilson, Gerry Killeen, and Tom Smith. 2004. “Estimating the Duration of Plasmodium Falciparum Infection from Trials of Indoor Residual Spraying.” *The American Journal of Tropical Medicine and Hygiene* 70 (6): 625–34.

Sato, Yuko, Georgina N. Montagna, and Kai Matuschewski. 2014. “Plasmodium Berghei Sporozoites Acquire Virulence and Immunogenicity during Mosquito Hemocoel Transit.” *Infection and Immunity* 82 (3): 1164–72. https://doi.org/10.1128/IAI.00758-13.

Schellenberg, J. R., T. Smith, P. L. Alonso, and R. J. Hayes. 1994. “What Is Clinical Malaria? Finding Case Definitions for Field Research in Highly Endemic Areas.” *Parasitology Today (Personal Ed.)* 10 (11): 439–42. https://doi.org/10.1016/0169-4758(94)90179-1.

Scott, Thomas W., and Willem Takken. 2012. “Feeding Strategies of Anthropophilic Mosquitoes Result in Increased Risk of Pathogen Transmission.” *Trends in Parasitology* 28 (3): 114–21. https://doi.org/10.1016/j.pt.2012.01.001.

Shaman, Jeffrey, Sasikiran Kandula, Wan Yang, and Alicia Karspeck. 2017. “The Use of Ambient Humidity Conditions to Improve Influenza Forecast.” *PLOS Computational Biology* 13 (11): e1005844. https://doi.org/10.1371/journal.pcbi.1005844.

Shaman, Jeffrey, and Alicia Karspeck. 2012. “Forecasting Seasonal Outbreaks of Influenza.” *Proceedings of the National Academy of Sciences* 109 (50): 20425–30. https://doi.org/10.1073/pnas.1208772109.

Shaman, Jeffrey, Alicia Karspeck, Wan Yang, James Tamerius, and Marc Lipsitch. 2013a. "Real-Time Influenza Forecasts during the 2012–2013 Season." *Nature Communications* 4: 2837. https://doi.org/10.1038/ncomms3837.

———. 2013b. "Real-Time Influenza Forecasts during the 2012–2013 Season." *Nature Communications* 4 (December): 2837. https://doi.org/10.1038/ncomms3837.

Shanks, G. Dennis, Simon I. Hay, Judy A. Omumbo, and Robert W. Snow. 2005. "Malaria in Kenya's Western Highlands." *Emerging Infectious Diseases* 11 (9): 1425–32. https://doi.org/10.3201/eid1109.041131.

Shapiro, Lillian L. M., Shelley A. Whitehead, and Matthew B. Thomas. 2017. "Quantifying the Effects of Temperature on Mosquito and Parasite Traits That Determine the Transmission Potential of Human Malaria." *PLoS Biology* 15 (10): e2003489. https://doi.org/10.1371/journal.pbio.2003489.

Sherman, Irwin W. 1998. "A Brief History of Malaria and Discovery of the Parasite's Life Cycle." In *In: Sherman IW, Editor. , Ed. Malaria: Parasite Biology, Pathogenesis, and Protection*. Washington, DC: ASM Press.

Shiff, Clive. 2002. "Integrated Approach to Malaria Control." *Clinical Microbiology Reviews* 15 (2): 278–93. https://doi.org/10.1128/CMR.15.2.278-293.2002.

Shililu, J. I., W. B. Grueber, C. M. Mbogo, J. I. Githure, L. M. Riddiford, and J. C. Beier. 2004. "Development and Survival of Anopheles Gambiae Eggs in Drying Soil: Influence of the Rate of Drying, Egg Age, and Soil Type." *Journal of the American Mosquito Control Association* 20 (3): 243–47.

Shililu, Josephat, Tewolde Ghebremeskel, Fessahaye Seulu, Solomon Mengistu, Helen Fekadu, Mehari Zerom, G. E. Asmelash, et al. 2004. "Seasonal Abundance, Vector Behavior, and Malaria Parasite Transmission in Eritrea." *Journal of the American Mosquito Control Association* 20 (2): 155–64.

Siebert, Asher, Tufa Dinku, Floribert Vuguziga, Anthony Twahirwa, Desire M. Kagabo, John delCorral, and Andrew W. Robertson. 2019. "Evaluation of ENACTS-Rwanda: A New Multi-Decade, High-Resolution Rainfall and Temperature Data Set—Climatology." *International Journal of Climatology* 39 (6): 3104–20. https://doi.org/10.1002/joc.6010.

Sinka, Marianne E., Michael J. Bangs, Sylvie Manguin, Maureen Coetzee, Charles M. Mbogo, Janet Hemingway, Anand P. Patil, et al. 2010. "The Dominant Anopheles Vectors of Human Malaria in Africa, Europe and the Middle East: Occurrence Data, Distribution Maps and Bionomic Précis." *Parasites & Vectors* 3 (December): 117. https://doi.org/10.1186/1756-3305-3-117.

Sinka, Marianne E., Michael J. Bangs, Sylvie Manguin, Yasmin Rubio-Palis, Theeraphap Chareonviriyaphap, Maureen Coetzee, Charles M. Mbogo, et al. 2012. "A Global Map of

Dominant Malaria Vectors." *Parasites & Vectors* 5 (1): 69. https://doi.org/10.1186/1756-3305-5-69.

Siraj, A. S., M. Santos-Vega, M. J. Bouma, D. Yadeta, D. Ruiz Carrascal, and M. Pascual. 2014. "Altitudinal Changes in Malaria Incidence in Highlands of Ethiopia and Colombia." *Science* 343 (6175): 1154–58. https://doi.org/10.1126/science.1244325.

Slater, Hannah C., Amanda Ross, Ingrid Felger, Natalie E. Hofmann, Leanne Robinson, Jackie Cook, Bronner P. Gonçalves, et al. 2019. "The Temporal Dynamics and Infectiousness of Subpatent Plasmodium Falciparum Infections in Relation to Parasite Density." *Nature Communications* 10 (1): 1433. https://doi.org/10.1038/s41467-019-09441-1.

Smith, D. L., J. Dushoff, R. W. Snow, and S. I. Hay. 2005. "The Entomological Inoculation Rate and Plasmodium Falciparum Infection in African Children." *Nature* 438 (7067): 492–95. https://doi.org/10.1038/nature04024.

Smith, David L., Katherine E. Battle, Simon I. Hay, Christopher M. Barker, Thomas W. Scott, and F. Ellis McKenzie. 2012. "Ross, Macdonald, and a Theory for the Dynamics and Control of Mosquito-Transmitted Pathogens." *PLOS Pathogens* 8 (4): e1002588. https://doi.org/10.1371/journal.ppat.1002588.

Smith, David L., Chris J. Drakeley, Christinah Chiyaka, and Simon I. Hay. 2010. "A Quantitative Analysis of Transmission Efficiency versus Intensity for Malaria." *Nature Communications* 1 (1): 108. https://doi.org/10.1038/ncomms1107.

Smith, David L., and F. Ellis McKenzie. 2004. "Statics and Dynamics of Malaria Infection in Anopheles Mosquitoes." *Malaria Journal* 3 (1): 13. https://doi.org/10.1186/1475-2875-3-13.

Smith, David L., F. Ellis McKenzie, Robert W. Snow, and Simon I. Hay. 2007. "Revisiting the Basic Reproductive Number for Malaria and Its Implications for Malaria Control." *PLOS Biology* 5 (3): e42. https://doi.org/10.1371/journal.pbio.0050042.

Smith, David L., T. Alex Perkins, Robert C. Reiner Jr., Christopher M. Barker, Tianchan Niu, Luis Fernando Chaves, Alicia M. Ellis, et al. 2014. "Recasting the Theory of Mosquito-Borne Pathogen Transmission Dynamics and Control." *Transactions of The Royal Society of Tropical Medicine and Hygiene* 108 (4): 185–97. https://doi.org/10.1093/trstmh/tru026.

Smith, T., G. Killeen, C. Lengeler, and M. Tanner. 2004. "Relationships between the Outcome of Plasmodium Falciparum Infection and the Intensity of Transmission in Africa." *The American Journal of Tropical Medicine and Hygiene* 71 (2 Suppl): 80–86.

Smith, Thomas A. 2008. "Estimation of Heterogeneity in Malaria Transmission by Stochastic Modelling of Apparent Deviations from Mass Action Kinetics." *Malaria Journal* 7 (1): 12. https://doi.org/10.1186/1475-2875-7-12.

Smith, Thomas, Gerry F. Killeen, Nicolas Maire, Amanda Ross, Louis Molineaux, Fabrizio Tediosi, Guy Hutton, Jürg Utzinger, Klaus Dietz, and Marcel Tanner. 2006. "Mathematical Modeling of the Impact of Malaria Vaccines on the Clinical Epidemiology and Natural History of Plasmodium Falciparum Malaria: Overview." *The American Journal of Tropical Medicine and Hygiene* 75 (2 Suppl): 1–10. https://doi.org/10.4269/ajtmh.2006.75.2_suppl.0750001.

Sogoba, Nafomon, Seydou Doumbia, Penelope Vounatsou, Magaran Monzon Bagayoko, Guimogo Dolo, Sékou Fantamady Traoré, Hamidou Moussa Maïga, Yéya Tiémoko Touré, and Thomas Smith. 2007. "Malaria Transmission Dynamics in Niono, Mali: The Effect of the Irrigation Systems." *Acta Tropica* 101 (3): 232–40. https://doi.org/10.1016/j.actatropica.2007.02.005.

Sorek-Hamer, Meytar, Allan C. Just, and Itai Kloog. 2016. "Satellite Remote Sensing in Epidemiological Studies." *Current Opinion in Pediatrics* 28 (2): 228–34. https://doi.org/10.1097/MOP.0000000000000326.

Sumba, Leunita A, Kenneth Okoth, Arop L Deng, John Githure, Bart GJ Knols, John C Beier, and Ahmed Hassanali. 2004. "Daily Oviposition Patterns of the African Malaria Mosquito Anopheles Gambiae Giles (Diptera: Culicidae) on Different Types of Aqueous Substrates." *Journal of Circadian Rhythms* 2 (December): 6. https://doi.org/10.1186/1740-3391-2-6.

Tadesse, Fitsum G., Hannah C. Slater, Wakweya Chali, Karina Teelen, Kjerstin Lanke, Mulualem Belachew, Temesgen Menberu, et al. 2018. "The Relative Contribution of Symptomatic and Asymptomatic Plasmodium Vivax and Plasmodium Falciparum Infections to the Infectious Reservoir in a Low-Endemic Setting in Ethiopia." *Clinical Infectious Diseases: An Official Publication of the Infectious Diseases Society of America* 66 (12): 1883–91. https://doi.org/10.1093/cid/cix1123.

Takken, W., B. G. J. Knols, and H. Otten. 1997. "Interactions between Physical and Olfactory Cues in the Host-Seeking Behaviour of Mosquitoes: The Role of Relative Humidity." *Annals of Tropical Medicine & Parasitology* 91 (sup1): S119–20. https://doi.org/10.1080/00034983.1997.11813251.

Targett, G., C. Drakeley, M. Jawara, L. von Seidlein, R. Coleman, J. Deen, M. Pinder, et al. 2001. "Artesunate Reduces but Does Not Prevent Posttreatment Transmission of Plasmodium Falciparum to Anopheles Gambiae." *The Journal of Infectious Diseases* 183 (8): 1254–59. https://doi.org/10.1086/319689.

Taylor, Terrie, and Tsiri Agbenyenga. 2013. "Malaria." In *Alan J. Magill, David R Hill, Tom Solomon, Edward T Ryan, Editors. Hunter's Tropical Medicine and Emerging Infectious Disease (Ninth Edition)*, 695–717. London: W.B. Saunders. https://doi.org/10.1016/B978-1-4160-4390-4.00096-5.

Teklehaimanot, Hailay D, Joel Schwartz, Awash Teklehaimanot, and Marc Lipsitch. 2004. "Weather-Based Prediction of Plasmodium Falciparum Malaria in Epidemic-Prone Regions of Ethiopia II. Weather-Based Prediction Systems Perform Comparably to Early Detection Systems in Identifying Times for Interventions." *Malaria Journal* 3 (November): 44. https://doi.org/10.1186/1475-2875-3-44.

Tesla, Blanka, Leah R. Demakovsky, Erin A. Mordecai, Sadie J. Ryan, Matthew H. Bonds, Calistus N. Ngonghala, Melinda A. Brindley, and Courtney C. Murdock. 2018. "Temperature Drives Zika Virus Transmission: Evidence from Empirical and Mathematical Models." *Proceedings of the Royal Society B: Biological Sciences* 285 (1884): 20180795. https://doi.org/10.1098/rspb.2018.0795.

Thomson, Madeleine C., Simon J. Mason, Thandie Phindela, and Stephen J. Connor. 2005. "Use of Rainfall and Sea Surface Temperature Monitoring for Malaria Early Warning in Botswana." *The American Journal of Tropical Medicine and Hygiene* 73 (1): 214–21. https://doi.org/10.4269/ajtmh.2005.73.214.

Thomson, Madeleine C., Israel Ukawuba, Christine L. Hershey, Adam Bennett, Pietro Ceccato, Bradfield Lyon, and Tufa Dinku. 2017. "Using Rainfall and Temperature Data in the Evaluation of National Malaria Control Programs in Africa." *The American Journal of Tropical Medicine and Hygiene* 97 (3_Suppl): 32–45. https://doi.org/10.4269/ajtmh.16-0696.

Tirados, I., C. Costantini, G. Gibson, and S. J. Torr. 2006. "Blood-Feeding Behaviour of the Malarial Mosquito Anopheles Arabiensis: Implications for Vector Control." *Medical and Veterinary Entomology* 20 (4): 425–37. https://doi.org/10.1111/j.1365-2915.2006.652.x.

Tompkins, Adrian M., Felipe J. Colón-González, Francesca Di Giuseppe, and Didacus B. Namanya. 2019. "Dynamical Malaria Forecasts Are Skillful at Regional and Local Scales in Uganda up to 4 Months Ahead." *GeoHealth* 3 (3): 58–66. https://doi.org/10.1029/2018GH000157.

Tompkins, Adrian M, and Volker Ermert. 2013. "A Regional-Scale, High Resolution Dynamical Malaria Model That Accounts for Population Density, Climate and Surface Hydrology." *Malaria Journal* 12 (February): 65. https://doi.org/10.1186/1475-2875-12-65.

Trampuz, Andrej, Matjaz Jereb, Igor Muzlovic, and Rajesh M. Prabhu. 2003. "Clinical Review: Severe Malaria." *Critical Care* 7 (4): 315. https://doi.org/10.1186/cc2183.

Trigg, J. K, H Mbwana, O Chambo, E Hills, W Watkins, and C. F Curtis. 1997. "Resistance to Pyrimethamine/Sulfadoxine in Plasmodium Falciparum in 12 Villages in North East Tanzania and a Test of Chlorproguanil/Dapsone." *Acta Tropica* 63 (2): 185–89. https://doi.org/10.1016/S0001-706X(96)00617-1.

U.S. President's Malaria Initiative. 2017. "Rwanda: 2017 Entomological Monitoring, July 2016–June 2017. Final Report." Kigali, Rwanda: VectorLink Project, Abt Associates Inc.

———. 2018a. “Rwanda Malaria Operational Plan FY 2018.” USAID. President’s Malaria Initiative.
———. 2018b. “Rwanda: 2018 Entomological Monitoring, July 2017–June 2018. Final Report.” Kigali, Rwanda: VectorLink Project, Abt Associates Inc.
———. 2019a. “Rwanda Malaria Operational Plan FY 2019.” USAID. President’s Malaria Initiative.
———. 2019b. “Rwanda: 2019 Entomological Monitoring, July 2018–June 2019. Final Report.” Kigali, Rwanda: VectorLink Project, Abt Associates Inc.

Vanderberg, J. P. 1975. “Development of Infectivity by the Plasmodium Berghei Sporozoite.” *The Journal of Parasitology* 61 (1): 43–50.

Veenhuis, Bruce A. 2013. “Spread Calibration of Ensemble MOS Forecasts.” *Monthly Weather Review* 141 (7): 2467–82. https://doi.org/10.1175/MWR-D-12-00191.1.

Vernick, K. D., F Oduol, B. P. Lazzaro, J. Glazebrook, J Xu, M Riehle, and J Li. 2005. “Molecular Genetics of Mosquito Resistance to Malaria Parasites.” In *D.J. Sullivan and S. Krishna (Eds.). Malaria: Drugs, Disease and Post-Genomic Biology*. Berlin Heidelberg: Springer-Verlag.

Viana, João, João Vasco Santos, Rui Manuel Neiva, Júlio Souza, Lia Duarte, Ana Cláudia Teodoro, and Alberto Freitas. 2017. “Remote Sensing in Human Health: A 10-Year Bibliometric Analysis.” *Remote Sensing* 9 (12): 1225. https://doi.org/10.3390/rs9121225.

Vleugels, M. P., W. M. Eling, R. Rolland, and R. de Graaf. 1987. “Cortisol and Loss of Malaria Immunity in Human Pregnancy.” *British Journal of Obstetrics and Gynaecology* 94 (8): 758–64. https://doi.org/10.1111/j.1471-0528.1987.tb03722.x.

Waite, Jessica L., Eunho Suh, Penelope A. Lynch, and Matthew B. Thomas. 2019. “Exploring the Lower Thermal Limits for Development of the Human Malaria Parasite, Plasmodium Falciparum.” *Biology Letters* 15 (6). https://doi.org/10.1098/rsbl.2019.0275.

Wan, Zhengming, Yulin Zhang, Qincheng Zhang, and Zhao-liang Li. 2002. “Validation of the Land-Surface Temperature Products Retrieved from Terra Moderate Resolution Imaging Spectroradiometer Data.” *Remote Sensing of Environment*, The Moderate Resolution Imaging Spectroradiometer (MODIS): a new generation of Land Surface Monitoring, 83 (1): 163–80. https://doi.org/10.1016/S0034-4257(02)00093-7.

Watkins, W. M., E. K. Mberu, P. A. Winstanley, and C. V. Plowe. 1997. “The Efficacy of Antifolate Antimalarial Combinations in Africa: A Predictive Model Based on Pharmacodynamic and Pharmacokinetic Analyses.” *Parasitology Today* 13 (12): 459–64. https://doi.org/10.1016/S0169-4758(97)01124-1.

Wayant, Nicole M., Diego Maldonado, Antonieta Rojas de Arias, Blanca Cousiño, and Douglas G. Goodin. 2010. “Correlation between Normalized Difference Vegetation Index and

Malaria in a Subtropical Rain Forest Undergoing Rapid Anthropogenic Alteration." *Geospatial Health* 4 (2): 179–90. https://doi.org/10.4081/gh.2010.199.

Wesolowski, Amy, Nathan Eagle, Andrew J. Tatem, David L. Smith, Abdisalan M. Noor, Robert W. Snow, and Caroline O. Buckee. 2012. "Quantifying the Impact of Human Mobility on Malaria." *Science (New York, N.Y.)* 338 (6104): 267–70. https://doi.org/10.1126/science.1223467.

White, Michael T., Jamie T. Griffin, Thomas S. Churcher, Neil M. Ferguson, María-Gloria Basáñez, and Azra C. Ghani. 2011. "Modelling the Impact of Vector Control Interventions on Anopheles Gambiae Population Dynamics." *Parasites & Vectors* 4 (July): 153. https://doi.org/10.1186/1756-3305-4-153.

Wilks, Daniel. 1995. "Forecast Verification." In *Statistical Methods in the Atmospheric Sciences*, 1st ed., 59:233–83. Academic Press.

Wilks, Daniel S., and Thomas M. Hamill. 2007. "Comparison of Ensemble-MOS Methods Using GFS Reforecasts." *Monthly Weather Review* 135 (6): 2379–90. https://doi.org/10.1175/MWR3402.1.

Wilson, Anne L. and IPTc Taskforce. 2011. "A Systematic Review and Meta-Analysis of the Efficacy and Safety of Intermittent Preventive Treatment of Malaria in Children (IPTc)." *PloS One* 6 (2): e16976. https://doi.org/10.1371/journal.pone.0016976.

Woolhouse, M. E., C. Dye, J. F. Etard, T. Smith, J. D. Charlwood, G. P. Garnett, P. Hagan, et al. 1997. "Heterogeneities in the Transmission of Infectious Agents: Implications for the Design of Control Programs." *Proceedings of the National Academy of Sciences of the United States of America* 94 (1): 338–42. https://doi.org/10.1073/pnas.94.1.338.

World Health Organization. 2000. "Severe Falciparum Malaria." *Transactions of The Royal Society of Tropical Medicine and Hygiene* 94 (Supplement_1): 1–90. https://doi.org/10.1016/S0035-9203(00)90300-6.

———. 2011. "Malaria Rapid Diagnostic Test Performance: Results of WHO Product Testing of Malaria RDTs: Round 3 (2010-2011)." World Health Organization on behalf of the Special Programme for Research and Training in Tropical Diseases 2011.

———. 2012a. "Demand Forecast for Artemisinin-Based Combination Therapies (ACTs) in 2012-2013 Q1-2012 Report." UNITAID Secretariat, ACT Forecasting Consortium.

———. 2012b. "International Travel and Health." International Health Regulations Coordination WHO press.

———. 2014. "WHO Preferred Product Characteristics (PPC) for Malaria Vaccines." Department of Immunization, Vaccines and Biologicals. WHO Press.

———. 2015a. "Global Technical Strategy for Malaria 2016–2030." global malaria Programme, World Health Organization(WHO) Press.

———. 2015b. "World Health Organization. Global Technical Strategy for Malaria 2016-2030." WHO press.

———. 2016a. “World Malaria Report 2016 Country Profiles.” https://www.who.int/malaria/publications/world-malaria-report-2016/en/.
———. 2016b. “Malaria Vaccine: WHO Position Paper-January 2016.” *Releve Epidemiologique Hebdomadaire* 91 (4): 33–51.
———. 2017a. “Global Malaria Diagnostic and Artemisinin Treatment Commodities Demand Forecast: 2017–2020.” World Health Organization(WHO),Secretariat of Unitaid.
———. 2017b. “World Malaria Report 2017.” WHO press.
———. 2017c. “World Malaria Report 2017 Country Profiles.” https://www.who.int/malaria/publications/world-malaria-report-2017/en/.
———. 2018a. “Malaria Surveillance, Monitoring & Evaluation: A Reference Manual.”
———. 2018b. “World Malaria Report 2018.” WHO press. https://www.who.int/malaria/publications/world-malaria-report-2018/en/.
———. 2018c. “World Malaria Report 2018 Country Profiles.” https://www.who.int/malaria/publications/world-malaria-report-2018/en/.
———. 2019. “World Malaria Report 2019.” WHO press. https://www.who.int/publications-detail-redirect/9789241565721.

Yamana, Teresa K., and Elfatih A. B. Eltahir. 2013. “Incorporating the Effects of Humidity in a Mechanistic Model of Anopheles Gambiae Mosquito Population Dynamics in the Sahel Region of Africa.” *Parasites & Vectors* 6 (1): 235. https://doi.org/10.1186/1756-3305-6-235.

Yamana, Teresa K., Sasikiran Kandula, and Jeffrey Shaman. 2016. “Superensemble Forecasts of Dengue Outbreaks.” *Journal of The Royal Society Interface* 13 (123): 20160410. https://doi.org/10.1098/rsif.2016.0410.
———. 2017. “Individual versus Superensemble Forecasts of Seasonal Influenza Outbreaks in the United States.” *PLOS Computational Biology* 13 (11): e1005801. https://doi.org/10.1371/journal.pcbi.1005801.

Yang, Song, and Xingwen Jiang. 2014. “Prediction of Eastern and Central Pacific ENSO Events and Their Impacts on East Asian Climate by the NCEP Climate Forecast System.” *Journal of Climate* 27 (12): 4451–72. https://doi.org/10.1175/JCLI-D-13-00471.1.

Yang, Wan, Alicia Karspeck, and Jeffrey Shaman. 2014. “Comparison of Filtering Methods for the Modeling and Retrospective Forecasting of Influenza Epidemics.” *PLOS Computational Biology* 10 (4): e1003583. https://doi.org/10.1371/journal.pcbi.1003583.

Yang, Wan, Donald R. Olson, and Jeffrey Shaman. 2016. “Forecasting Influenza Outbreaks in Boroughs and Neighborhoods of New York City.” *PLOS Computational Biology* 12 (11): e1005201. https://doi.org/10.1371/journal.pcbi.1005201.

Yé, Yazoume, Thomas P. Eisele, Erin Eckert, Eline Korenromp, Jui A. Shah, Christine L. Hershey, Elizabeth Ivanovich, et al. 2017. “Framework for Evaluating the Health Impact of the Scale-Up of Malaria Control Interventions on All-Cause Child Mortality in Sub-Saharan Africa.” *The American Journal of Tropical Medicine and Hygiene* 97 (3 Suppl): 9–19. https://doi.org/10.4269/ajtmh.15-0363.

Yé, Yazoumé, Moshe Hoshen, Catherine Kyobutungi, Valérie R. Louis, and Rainer Sauerborn. 2009. “Local Scale Prediction of Plasmodium Falciparum Malaria Transmission in an Endemic Region Using Temperature and Rainfall.” *Global Health Action* 2 (November). https://doi.org/10.3402/gha.v2i0.1923.

Yeka, Adoke, Grant Dorsey, Moses R. Kamya, Ambrose Talisuna, Myers Lugemwa, John Bosco Rwakimari, Sarah G. Staedke, Philip J. Rosenthal, Fred Wabwire-Mangen, and Hasifa Bukirwa. 2008. “Artemether-Lumefantrine versus Dihydroartemisinin-Piperaquine for Treating Uncomplicated Malaria: A Randomized Trial to Guide Policy in Uganda.” *PloS One* 3 (6): e2390. https://doi.org/10.1371/journal.pone.0002390.

Zhang, Z., and T. N. Krishnamurti. 1996. “A Generalization of Gill’s Heat-Induced Tropical Circulation.” *Journal of the Atmospheric Sciences* 53 (7): 1045–52. https://doi.org/10.1175/1520-0469(1996)053<1045:AGOGHI>2.0.CO;2.

Zhang, Zhijie, Michecal Ward, Jie Gao, Zengliang Wang, Baodong Yao, Tiejun Zhang, and Qingwu Jiang. 2013. “Remote Sensing and Disease Control in China: Past, Present and Future.” *Parasites & Vectors* 6 (1): 11. https://doi.org/10.1186/1756-3305-6-11.

Zhou, Guofa, Noboru Minakawa, Andrew K. Githeko, and Guiyun Yan. 2004. “Association between Climate Variability and Malaria Epidemics in the East African Highlands.” *Proceedings of the National Academy of Sciences of the United States of America* 101 (8): 2375–80. https://doi.org/10.1073/pnas.0308714100.

Zhu, Guanghu, Jiming Liu, Qi Tan, and Benyun Shi. 2016. “Inferring the Spatio-Temporal Patterns of Dengue Transmission from Surveillance Data in Guangzhou, China.” *PLOS Neglected Tropical Diseases* 10 (4): e0004633. https://doi.org/10.1371/journal.pntd.0004633.

Zwang, Julien, Elizabeth A. Ashley, Corine Karema, Umberto D’Alessandro, Frank Smithuis, Grant Dorsey, Bart Janssens, et al. 2009. “Safety and Efficacy of Dihydroartemisinin-Piperaquine in Falciparum Malaria: A Prospective Multi-Centre Individual Patient Data Analysis.” *PLoS ONE* 4 (7). https://doi.org/10.1371/journal.pone.0006358.